# COLD RESPONSE BIOMARKER IDENTIFICATION IN STRAWBERRY

by

**Zachary M. Deitch**

**A Thesis**

*Submitted to the Faculty of Purdue University*

*In Partial Fulfillment of the Requirements for the degree of*

**Master of Science**


Department of Biology

Indianapolis, Indiana

August 2018

# THE PURDUE UNIVERSITY GRADUATE SCHOOL
# STATEMENT OF COMMITTEE APPROVAL

Dr. Stephen Randall, Chair
Department of Biology
Dr. John Watson
Department of Biology
Dr. AJ Baucum
Department of Biology

**Approved by:**

Dr. Theodore Cummins
Head of the Graduate Program

# ACKNOWLEDGMENTS

First and foremost, I would like to acknowledge Dr. Stephen Randall for his unwavering patience, support, and guidance throughout this project. I would also like to recognize Dr. John Watson for his insightful input in lab meetings and Dr. AJ Baucum for his methodological advice. I would like to acknowledge Jahn Davik, Anne Langerud, and Muath Alsheikh for their gracious provision of research materials. Special thanks to the IUPUI Biology Department for the opportunity to earn my masters at IUPUI and by helping me stay on top of administrative deadlines. Finally, I would like to thank Jennifer Robison for being an outstanding mentor and an ever-present advisor to myself and the rest of the lab. More thanks go out to the rest of my lab mates Adib Behrouzi, Cecelia Chapin, Jacob Hamilton, Katarina Mazari, and Megan McVey for their friendship and support throughout my project.

# TABLE OF CONTENTS

# LIST OF TABLES

# LIST OF FIGURES

# LIST OF ABBREVIATIONS

> - Greater than
≥ - Greater than or equal to
% - Percent
°C – Degrees Celsius
aa – Amino Acid
ABA – Abscisic Acid
ADH – Alcohol Dehydrogenase
*ADH1* – Alcohol Dehydrogenase 1
AFP – Anti-Freeze Protein
bHLH – basic helix-loop-helix
BME – 2 - Mercaptoethanol
bp – Base pairs
BSA – Bovine Serum Albumin
$Ca^{2+}$ - Calcium
CBF – C-repeat binding factors
cDNA – Complement DNA
co-IP – Co-immunoprecipitation
COR – Cold Responsive Gene
CRT – C-repeat Element
Cys – Cysteine
DHN – Dehydrin
DI – De-ionized
DMSO – Dimethyl Sulfoxide
DNA – Deoxyribonucleic Acid
DRE – Drought Responsive Element
DREB – Drought Responsive Element Binding Factors
DTT – Dithiothreitol
EDTA - Ethylenediaminetetraacetic Acid
ELISA – Enzyme-linked Immunosorbant Assay
F1 – Filial 1 generation
gDNA – genomic DNA
g - gram
GRBP – Glycine Rich Binding Protein
HOS1 – High Expression of Osmotically Responsive Gene 1
Hr - Hour
HSC70 – Heat – Shock Cognate 70
ICE1 – Inducer of CBF Expression 1
IDPs – Intrinsically Disordered Proteins
JA – Jasmonic Acid
Kg - kilogram
LDH – Lactate Dehydrogenase
LEA – Late Embryogenesis Abundant
LOS4 – Low Expression of Osmotically Responsive Genes 4
$LT_{50}$ – Lethal Temperature at which 50% of the plants die
M – Molar
Mg – Milli-gram
Min – Minute(s)
mL – Milli-liter
mM – Milli molar
mRNA – Messenger RNA
miRNA – MicroRNA
ng - nanogram
nm - nanometers
OST1 – OPEN STOMATA 1
PBS – Protein Buffer Solution
PCR – Polymerase Chain Reaction
pH – Potential of Hydrogen
PIF3 – Phytochrome-Interacting Factor 3

PMSF – Phenylmethylsulfonyl Fluoride
PR – Pathogenesis Related
PVDF – Polyvinylidene Fluoride
PVPP - Polyvinylpolypyrrolidone
RNA – Ribonucleic Acid
RNA-SEQ – RNA Sequencing
ROS – Reactive Oxygen Species
RPIs – Complete Protease Inhibitor Cocktail Tablets (Roche Diagnostics)
rpm – revolutions per minute
RT-PCR – Reverse Transcription Polymerase Chain Reaction
RT-qPCR – Real-Time Quantitative Polymerase Chain Reaction
SA – Salicylic Acid
SDS – Sodium dodecyl sulfate
siRNA – Short Interfering RNA
SSB – SDS Page Sample Buffer (0.25 mM Tris pH 6.8, 50% glycerol, 10% (w/v) SDS, small amount of bromophenol blue) (Laemmli 1970)
STA1 – STABILIZED 1
SUMO – Small ubiquitin – related modifier
Trp – Tryptophan
uL – Micro liter
ug – Micro gram
Ver. - Version

# ABSTRACT

Author: Deitch, Zachary, M. MS
Institution: Purdue University
Degree Received: August 2018
Title: Cold Response Biomarker Identification in Strawberry
Major Professor: Stephen Randall

Strawberry (*Fragaria* spp.*)* is an agricultural crop grown often in temperate regions that has high variability in its susceptibility to freezing injury. To breed cultivars for frost and freezing tolerance, identification of molecular markers associated with low temperature tolerance is advantageous. In this work, I investigated a high-throughput method for protein assays and western blotting. Success in streamlining these processes saves an immense amount of time and allows for the processing of more samples and obtaining larger datasets. Thirty-three octoploid varieties were tested for their accumulation of five different potential biomarkers in response to cold exposure. It was found that total dehydrin content, has the strongest potential to be reliable biomarkers for breeding programs. Previous work identified seven putative dehydrins in *Fragaria,* where two were purified and positively identified by mass spectrometry and determined to be COR47-like (SKn) and XERO2-like (YnSKn). This work demonstrated that cold tolerance positively correlated with dehydrin protein expression levels. To understand the cold-regulated expression of dehydrins as a function of cold exposure time, the levels of transcripts and corresponding proteins were examined in strongly cold tolerant (Alta) and lesser cold tolerant (FDP817, NCGR1363) *Fragaria* diploid genotypes. The COR47-like (SKn) and XERO2-like (YnSKn) dehydrins both had higher transcript accumulation and protein levels in the more cold tolerant line in comparison to the two less cold tolerant lines. Lack of correlation between transcript and resulting COR47 protein level in Alta were observed at several different timepoints, where protein accumulation preceded an increase in RNA. This trend was not seen with XERO2. This initiated an investigation to discover at what level COR47 is being regulated. First, the COR47 coding region was sequenced for all the genotypes to confirm against the predicted sequence. In addition, since two isoforms of the COR47 gene exist, and could possibly explain the discrepancy in transcript counts, primers were designed for both isoforms and RT-qPCR was performed to examine the transcripts of COR47 more closely. Through examination

of the non-congruence of COR47 transcripts and protein, it was found that transcriptional mechanisms of regulation are not involved, and that post transcriptional and post-RNA splicing mechanisms are likely to be responsible for the observed trend in Alta. Conclusions from this work demonstrate that dehydrin transcripts and dehydrin protein accumulations are strong potential biomarkers for identifying low temperature tolerance in diploid strawberry.

# CHAPTER 1. INTRODUCTION

Crop plants worldwide are subjected to many stressors that affect their productivity and ability to thrive. Stresses, either abiotic or biotic, have been reported to negatively affect the biomass and yield of crops up to 70% (Parihar et al. 2015) with abiotic stresses contributing to an average >50% annual yield loss worldwide (Boyer 1982; Wang et al. 2003). With the pressure to feed a growing global population, crops with an improved ability to grow and tolerate abiotic stress is crucial.

Strawberries are one of the most variable of all crop plants, and for this reason it is one of the most widely adapted and widely raised of all crops (Darrow 1966). However in temperate climates, strawberry plants grown for agriculture are subject to up to 20% crop loss because of low and freezing temperatures (Davik et al. 2000). By increasing cold and winter hardiness for strawberries, an improved yield would increase productivity in these regions. Previous research using molecular and proteomic techniques has identified potential biomarkers that can be used to select for more cold tolerant genotypes in conventional breeding programs. Confirmation of these biomarkers as true indicators of a plant's cold tolerance would increase screening efficiency compared to field experiments. Understanding the biochemical and molecular changes that take place in strawberries under cold stress is vital for increasing production through increased overwintering hardiness, and in turn, expanding the growing season and geographical range for cultivation. Ultimately, indirect selection using a marker-assisted approach could enhance the efficiency for cultivar development for all *Rosaceae* crops (e.g., strawberry, apple, cherry, and apricot) (Davik et al. 2013).

## 1.1 Ploidy of Strawberry

*Fragaria vesca* is of great research interest because of its wide distribution, its aromatic, high-flavored berries, and its everbearing forms (Darrow 1966). The diploid strawberry or "wild strawberry" is an exceptionally good model organism because it has a relatively small, completely sequenced genome. In addition, biologically identical replicates can be easily obtained through vegetative structures (runners) avoiding a necessity for sexual propagation. Diploid varieties also have higher cold tolerance than most octoploid strains, but have relatively

small berries. Strawberry plants are perennial and overwinter with a specific structure referred to as the crown. Thus, studying the crown is very important for understanding overwintering survival. One process for defining the cold survival characteristics of a specific accession has been developed. The $LT_{50}$ (Lethal Temperature where 50% of the plants survive) is evaluated by subjecting the plants to lowering temperatures in increments. After a period of time the plants are placed back in normal temperatures to see which varieties continue to survive until half of the plants remain living. In addition to this evaluation, tissue browning, intensity of discoloration, and regrowth can also be measured and used to find correlations with other molecular components (Davik et al. 2013). Diploid vesca is known to display simple mendelian inheritance while octoploid varieties have a more complicated inheritance pattern (Darrow 1966). Therefore, research in diploids can then be utilized as a starting point and then later applied to commercial varieties where ploidy level adds a significant layer of complexity. Using these varieties can be directly applied to breeding programs with goals to improve overwintering hardiness.

Commercial strawberries are octoploid and produce much larger berries than diploid strains. They have a chromosome number of 56 and a ploidy of 8. Octoploid varieties are native to the Americas and the Hawaiian Islands and the modern commercial varieties are mainly descendants of *F. chiloensis* and *F. virginiana* (Darrow 1966). Since octoploids are sold in markets, the importance of discovering traits for cold and freezing tolerance is vital to directly breed a crop with higher yield potential via overwintering success.

## 1.2 Cold Signaling & Low Temperature Stress Response in Plants

Cold stress affects almost all aspects of cellular function in plants, which presents a complex cellular network of changes in global gene expression profiles (Gao et al. 2009). The ability of a plant to tolerate cold temperatures is not entirely constitutive (Zhou et al. 2011). Plants in temperate regions have increased freezing tolerance while plants of tropical and subtropical origins are generally sensitive to chilling stress and often lack the ability to cold acclimate (Miura and Furumoto 2013). Plants have evolved mechanisms to enhance tolerance to freezing during exposure to low, but non-freezing temperatures also known as cold acclimation (Miura and Furumoto 2013). During this time, plants respond to low temperature by regulating the expression of transcription factors and effector genes (Zhou et al. 2011). Soybean is known as a cold intolerant plant that was previously thought to lack the ability to cold acclimate. But

following short acclimation periods, soybean seedlings significantly increased freezing tolerance and indeed are capable of cold acclimation (Robison et al. 2017). Recent studies demonstrate that the signaling pathways include transcriptional, post-transcriptional, translational, and post-translational regulation of low temperature induced genes (Zhou et al. 2011).

### 1.2.1 Cold Sensing in Plants

The initial sensing of cold in plants involves changes in the physical properties of membranes, likely through the sensing of decreased membrane fluidity which is reduced during cold temperatures (Miura and Furumoto 2013). This is the first step to switch on molecular responses and to relay the information through a signal transduction pathway, ultimately resulting in the induction of COR (cold responsive) genes (Chinnusamy et al. 2007; Heidarvand and Maali Amiri 2010). These responses are mediated by phytohormones that regulate every aspect of plant growth and development, along with responses to stress (Peleg and Blumwald 2011). In pea plants, two genes related to the jasmonate (JA) pathway were associated with frost damage, suggesting the involvement of this pathway during the cold response (Legrand et al. 2013). These secondary signals such as ABA and reactive oxygen species (ROS) can also induce calcium signatures that impact cold signaling (Chinnusamy et al. 2007).

Within seconds of cold shock, a transient increase in cytosolic $Ca^{2+}$ is observed (Miura and Furumoto 2013). Calcium is a secondary messenger in plant cells and is an important component of the signaling network by which plant cells respond to stimuli. Each stimulus can elicit a characteristic $Ca^{2+}$ signature that is recognized by different calcium sensing or responsive elements (Heidarvand and Maali Amiri 2010). Calcium sensors then transduce the calcium signatures into downstream effects and different pathways work as positive and negative regulators of gene expression (Heidarvand and Maali Amiri 2010).

In addition to the plasma membrane, chloroplasts may also play a role in sensing ambient temperature via energy balance (Miura and Furumoto 2013). In *Thellungiella halophila*, which is more cold tolerant than *Arabidopsis*, nearly half of the identified cold-responsive proteins were associated with chloroplasts suggesting that cold stress tolerance is achieved at least in part by regulation of chloroplast function (Gao et al. 2009). It was shown that the photoreceptor phytochrome B regulates expression of DREB1 gene to enhance cold tolerance (Singh et al. 2017). In addition to this, the phosphorylation of proteins in response to cold and the suppression

of protein phosphatase activity may also provide a means for the plant to sense low temperatures (Miura and Furumoto 2013). Overall, multiple signaling pathways can be utilized to initiate production of COR proteins.

### 1.2.2 Promoter Region Elements

Plant cold acclimation responses are highly integrated into cellular functions at all levels (Chinnusamy et al. 2007). Cold signaling and cold responses seem to be regulated by factors such as $Ca^{2+}$ signaling, chloroplast status, and perception of membrane rigidification. The promoters of many cold responsive genes contain a *cis*-element called C-repeat element/dehydration-responsive elements (CRT/DRE) where C-repeat binding factors/Drought response element binding factors (CBF/DREB1) can bind, resulting in increased transcription and ultimately increased freezing tolerance (Zhou et al. 2011). This CBF/DREB – pathway plays a central role in the regulation of cold signaling and is the best characterized and key regulatory pathway for cold signaling (Miura and Furumoto 2013). The CBF3/DREB1A pathway is controlled by a MYC-type transcription factor called Inducer of CBF expression 1 (ICE1), an upstream positive regulator of CBF3 (Zhou et al. 2011). The ICE1 gene encodes a MYC basic helix-loop-helix (bHLH) transcription activator, which is localized in the nucleus and obtains functional activity by a low temperature induced post-translational modification, specifically phosphorylation, which is necessary for ICE1 to activate downstream genes (Zhou et al. 2011). ICE1 appears to negatively regulate MYB15, an upstream negative regulator of CBFs in addition to the direct induction of CBF expression (Chinnusamy et al. 2007). Fine-tuning of the ICE1 protein level and activity are regulated post-translationally by HOS1-mediated ubiquitination and proteolysis, and by SIZ1-mediated sumoylation (Chinnusamy et al. 2007). Approximately 40% of COR genes and 46% of cold-regulated transcription factor genes are regulated by ICE1 (Miura and Furumoto 2013). Further investigation into these areas will help develop an understanding of this complex network of cold stress response in plants.

### 1.2.3 Negative Regulators of the Cold Response

Negative regulators which act via feedback repression of transcription factors, regulate cold-responsive gene expression, and appear to be key to maintaining an optimal cold-induced transcriptome. In Arabidopsis, it was found that Phytochrome-Interacting Factor 3 (PIF3) was

acting as a negative regulator by directly repressing the expression of CBF genes, preventing runaway expression of the CBF pathway (Jiang et al. 2017). It is debated that CBF2 is a negative regulator of CBF1 and CBF3 expression during cold acclimation (Thomashow 2010). From overexpression of each of the CBF genes in Arabidopsis, it was concluded by Novillo et al. (2004) that the function of CBF2 is distinct from that of CBF1 and CBF3 (Thomashow 2010). But studies have come to opposite conclusions as to whether down-regulation of CBF2 increases or decreases freezing tolerance (Thomashow 2010). In addition, CBFs are negatively regulated by an upstream transcription factor, MYB15 (Chinnusamy et al. 2007). The cold-induced $C_2H_2$ zinc finger transcription factor, ZAT12 and ZAT10 gene, appear to function as negative regulators of CBFs as well by repressing expression of CBF-target genes (Chinnusamy et al. 2007). Therefore ZAT10 and ZAT12 might regulate a subset of genes involved in cold acclimation, and these transcription factors are induced by cold and other abiotic stresses, resulting in transgenic plants overexpressing these genes to exhibit enhanced osmotic and oxidative stress tolerance (Chinnusamy et al. 2007). Overall, CBFs regulate around 12% of the cold responsive genes in *Arabidopsis* (Chinnusamy et al. 2007). A known transcription repressor, High Expression of Osmotically Responsive Gene, HOS1, targets upstream the ICE1 transcription factor of the CBF-dependent signaling pathway. HOS1 ubiquitinates ICE1 to negatively regulate levels of ICE1 target genes (Chinnusamy et al. 2007). A recent study demonstrates that a protein kinase OST1 (OPEN STOMATA 1), a key component in ABA signaling, is also activated by cold stress. OST1 is a positive regulator of the CBF pathway, phosphorylating and stabilizing ICE1, thus suppressing the HOS1-mediated ICE1 degradation, and promoting the expression of downstream cold tolerance genes (Ding et al. 2015).

### 1.2.4 Plant hormones involved in the cold response

There is also a response in plants to cold stress with relation to plant hormones, metabolites and flavonoids. ABA levels increase in response to low temperatures and CBF genes are induced by exogenous ABA. ABA induces the expression of the cold-regulated gene, *ADH1* (Alcohol Dehydrogenase 1), further indicating the effect of ABA in the cold response. In addition to this, cold signaling and salicylic acid (SA) signaling are interrelated where it has been shown that an essential function of ICE1 is as a cold and SA signaling integrator (Miura and Furumoto 2013). In a recent study, evidence for a functional role of flavonoids in plant cold

acclimation has been proposed (Schulz et al. 2016). Low temperature strongly increases flavonoid content, the abundance of enzymes involved in flavonoid biosynthesis, and the expression of flavonoid biosynthesis genes in various plant species (Schulz et al. 2016). In strawberry, some varieties known to have a reduced cold tolerance in comparison to more winter hardy varieties utilize the flavonoid pathway response (Koehler et al. 2012). It was suggested that some varieties mount an alternative, perhaps lesser, but effective response to cold stress that utilizes alternative pathways that may be better suited for the environment in which they are typically grown (Koehler et al. 2012). Overall, comprehensive characterization of the flavonoid mutants with respect to their freezing tolerance, gene expression, and metabolite profiles indicates a role of flavonoids in freezing tolerance and cold acclimation and demonstrates that plants can mount a multiple pathway response to cold stress (Schulz et al. 2016).

## 1.3 Transcriptional, Post-Transcriptional, Translational, and Post-Translational Regulation in Plant Responses to Stress

Gene expression can be regulated via transcriptional, post-transcriptional, translational, and post-translational mechanisms. Identification of specific mechanisms at the different levels of regulation play an important role in characterizing how plants respond to abiotic stresses (Jensen et al. 2006; Floris et al. 2009; Yan et al. 2006). Post-transcriptional mechanisms comprised of alternative splicing, RNA processing, RNA turnover or stability, and RNA-mediated silencing define the actual transcriptome supporting the stress response (Mazzucotelli et al. 2008). Post-translational modifications like phosphorylation, ubiquitination, and sumoylation regulate the activation of pre-existing protein to ensure a quick response to stress (Mazzucotelli et al. 2008). The network of post-transcriptional and post-translational modifications ensures temporally and spatially appropriate patterns of downstream stress-related gene expression (Mazzucotelli et al. 2008).

### 1.3.1 Post-Transcriptional Regulation in the Cold Response

Post-transcriptional mechanisms based on alternative splicing, pre-mRNA processing, RNA stability, RNA silencing, and export from the nucleus play critical roles in cold acclimation and cold tolerance (Miura and Furumoto 2013). STA1, a nuclear pre-mRNA splicing factor is upregulated by cold stress in *Arabidopsis.* The *sta1* mutant is defective in splicing of the cold-

induced COR15A pre-mRNA and is hypersensitive to chilling, ABA, and salt stresses. Therefore STA1 is required for splicing and turnover of cold specific transcripts, and under cold stress there is an increased demand for this factor (Chinnusamy et al. 2007). RNA helicase LOS4 (low expression of osmotically responsive genes 4) is important for nuclear mRNA export, particularly in response to temperature stress. mRNA export is decreased in the *los4-1* mutation, leading to reduced expression of CBF and sensitivity to chilling stress (Miura and Furumoto 2013). Thus efficient mRNA export is important for the regulation of CBF expression. In *Arabidopsis*, an RNA-SEQ approach revealed that in normal conditions, approximately 42% of genes undergo alternative splicing to produce different proteins (Miura and Furumoto 2013). Cold-regulated alternative splicing of CCA1 was shown to contribute to freezing tolerance (Miura and Furumoto 2013). Gene expression can be altered through the action of miRNAs and siRNAs either by repressing translation, by direct cleavage of complementary target mRNAs, or by inducing transcriptional silencing of target genes (Chinnusamy et al. 2007). Abiotic stress-induced miRNAs and siRNAs have been proposed to down-regulate target genes that might encode negative regulators or determinants of stress response (Chinnusamy et al. 2007). Additionally, downregulation of miRNAs and siRNAs could result in the accumulation of their target mRNAs that encode positive regulators or determinants of stress tolerance (Chinnusamy et al. 2007). Therefore, it is plausible that post-transcriptional regulation might serve as a major mode of downregulation of genes during cold acclimation (Chinnusamy et al. 2007).

### 1.3.2 Post-Transcriptional Regulation and Alternative Splicing

Post-transcriptional regulation of gene expression occurs at the level of mRNA localization, mRNA processing (capping, splicing, and polyadenylation), mRNA stability, and mRNA translation (Floris et al. 2009). Alternative splicing is particularly important in the availability of different kinds of transcripts, and ultimately of proteins. Splicing results in the excision of introns sequences from the pre-mRNA and sometimes allows for the production of more than one mRNA from a single gene (Floris et al. 2009). Currently, four main types of alternative splicing are known and are called exon skipping, alternative 5’ and 3’ splice sites, and intron retention (Mazzucotelli et al. 2008). In Arabidopsis and rice, intron retention is the most common form of alternative splicing (>50%) and mRNAs with introns usually lead to truncated polypeptides from the introduction of premature stop codons (Ner-Gaon et al. 2004). In

*Medicago truncatula* (alfalfa), a jumonji C domain-containing demethylase that is involved with removal of methyl groups at lysine and arginine residues was found to undergo cold-induced alternative splicing (Shen et al. 2016). Under cold treatment, four alternative spliced RNA isoforms were revealed having alternative 3' splice sites at the first and second intron (Shen et al. 2016). In common wheat, the amount of WDREB2 transcription factors was found to be differentially controlled at the transcript accumulation level, while alternative splicing occurred based on cold and drought/salt conditions (Egawa et al. 2006). The accumulation of the three alternatively spliced forms was differentially regulated through two independent pathways (Egawa et al. 2006). One pathway for drought and salt stresses is abscisic acid (ABA)-dependent while the other pathway for cold stress is ABA-independent (Egawa et al. 2006). Thus, this strongly suggested that abiotic stress conditions affect the alternative splicing patterns of the *Wdreb2* transcripts (Egawa et al. 2006). ABA is a key hormone responsible for activation of different response genes and pathways related to drought signaling in plant cells as well as activation of dehydrative response genes (Charfeddine et al. 2017). It is also known to be a key regulator is stomatal closure (Charfeddine et al. 2017). In Arabidopsis, STA1 (STABILIZED 1) is a gene coding for a nuclear pre-mRNA splicing factor that is involved in regulating the splicing and turnover of transcripts, contributing to resistance to cold stress (Floris et al. 2009). These examples show that alternative splicing is a common step at which post-transcriptional regulation occurs in plants under stress.

### 1.3.3 Post-Transcriptional Regulation and RNA Silencing

A post-transcriptional regulation that can have a direct impact on stress response is RNA-mediated silencing, which can control the amount of specific transcripts via degradation (Mazzucotelli et al. 2008). A glycine-rich RNA binding protein (GR-RBPs) may stabilize mRNA either during the transfer from the nucleus to cytoplasm or directly in the cytoplasm, allowing efficient mRNA processing (Floris et al. 2009). miRNAs and siRNAs post-transcriptionally silence target genes either by guiding degradation or repressing translation of target mRNAs. In rice, analysis suggested that epigenetic and post-transcriptional regulatory mechanisms are involved in the differentiation of egg and synergid cells showing that these mechanisms can have a huge impact on the regulation and expression of genes (Ohnishi et al. 2011). In a study examining gene expression in oxygen deprived roots in maize, two factors were predicted to be

the driving force for the level of protein synthesis. First is that competition among mRNAs for limiting translation initiation factors appears to be a general mechanism regulating protein synthesis and the other is that these factors could also affect mRNA stability, impairing translation initiation in response to stress treatment (Fennoy et al. 1998).

### 1.3.4 Post-Translational Regulation

While it is known that protein synthesis is regulated primarily during the initiation phase, there are multiple post-translational mechanisms involved in regulating gene expression (Mazzucotelli et al. 2008). Ubiquitination is the covalent addition of the small protein ubiquitin to selected target proteins and marks the protein for degradation, which plays a fundamental role in ABA homeostasis and response (Mazzucotelli et al. 2008). Sumoylation alters protein function by masking and/or adding interaction surfaces, or by inducing conformational changes. The biological consequences of sumoylation include sub-cellular re-localization, changes in enzymatic activity, and protection from ubiquitin-mediated degradation. Ubiquitination and sumoylation often have antagonistic effects by acting on the same amino acid residues (Mazzucotelli et al. 2008). Phosphorylation is known to affect conformation, activity, localization, and stability of target proteins (Mazzucotelli et al. 2008). The gain or loss of transcriptional regulation of a gene is correlated with the gain or loss of phosphorylation of the gene product and has led to the idea that these levels of regulation have co-evolved for gene regulation homeostasis (Jensen et al. 2006). These regulations portray a complicated system based on a network of reciprocal interactions, for example sumoylation and phosphorylation interact on target proteins, with sumoylation only targeting phosphorylated proteins, or preventing phosphorylation (Mazzucotelli et al. 2008).

### 1.3.5 Post-Translational Regulation and the Cold Response

Post-translational regulation mechanisms deal with phosphorylation, ubiquitination, and sumoylation of proteins. Ubiquitination of a protein leads to its degradation while sumoylation often protects against proteasomal degradation by preventing ubiquitination (Chinnusamy et al. 2007). HOS1 is an ubiquitin E3 ligase that results in the degradation of ICE1, decreasing expression of ICE1 target genes and thus being critical for the de-sensitization of plant cells to cold stress. In contrast to HOS1, SIZ1, a SUMO (Small ubiquitin-related modifier) E3 ligase,

mediates conjugation of SUMO to ICE1 during cold acclimation, blocking its ubiquitination, facilitating ICE1 stability and activity, which is necessary for CBF expression and MYB15 repression to fine-tune the transcription of COR genes during cold acclimation (Chinnusamy et al. 2007).

### 1.3.6 Transcripts and Corresponding Protein to Identify Level of Regulation

Multiple levels of regulation act synergistically to enhance a cell's ability to respond effectively to the conditions it encounters (Koussounadis et al. 2015). Different events may uncouple transcription and translation continuously or under certain conditions, and it is estimated that about one third of expressed genes are translationally regulated in yeast (Maier et al. 2009). Often times, looking at mRNA and corresponding protein levels can indicate a regulatory mechanism that depends on various biological and technical factors (Pradet-Balade et al. 2001). In rice leaves, suppression as well as induction of gene expression as a result of cold stress alters the accumulation of mRNAs as well as the accumulation of Rubisco in chloroplasts; in a coordinated fashion (Hahn and Walbot 1989). Since the level of mRNA does not always correlate well with the level of protein, one has to be careful in predicting protein expression levels from quantitative mRNA data (Yan et al. 2006). Protein for a given mRNA expression level might vary by up to 30-fold (Pradet-Balade et al. 2001). When a difference in abundance of mRNA compared to its protein product occurs, an initial suspect would be post-transcriptional regulation. In addition, translational control is a common mechanism for regulating gene expression and the relevance of mRNA data might be improved if these regulations were considered (Pradet-Balade et al. 2001). Upstream molecular mechanisms are involved in the regulation of timings and amount of specific stress responses leaving many potential options for regulation (Mazzucotelli et al. 2008). Determining the specific experiment to give an unambiguous result due to a specific part of regulation is vital. One way to get a good measure of translational efficiency is ribosome fractionation. The number of ribosome-associated mRNA correlates significantly better with absolute protein levels than mRNA abundance alone (Maier et al. 2009). Polysomes generally represent actively translated transcripts, and thus the number of mRNA molecules engaged in polysomes should be a robust indicator of the synthesis rate of the corresponding protein. Hybridization of northern blots could then reveal the distribution profile of specific mRNAs (e.g., differing splicing variants) between ribosome-free and polysome-

bound fractions. The comparison between the total and polysome-bound mRNAs enables transcriptional and translational regulation to be distinguished (Pradet-Balade et al. 2001). These data can be further quantified by transcript-specific RT-qPCR.

## 1.4 Dehydrins

Dehydrins (DHN) belong to group 2 of late embryogenesis abundant (LEA) proteins and are characterized by the presence or absence of specific segments unique to dehydrins. The only required motif to classify dehydrins is their 15 amino acid lysine-rich consensus domain, EKKGIMDKIKEKLPG, referred to as the K-segment (Close 1996). All dehydrins are known to contain from one to eleven K-segments and play a role in protecting cellular macromolecules and lipid membranes (Close 1996). It is suggested that K-segments form an amphipathic alpha-helix responsible for its lipid-associating properties (Close 1997). The K-segment is essential to the protection of enzyme activity during oxidative stress conditions (Liu et al. 2017). It has also been suggested that the K-segment could play a role in establishing a dimerization interaction among dehydrins that would create a more effective molecular shield than one (Hernandez-Sanchez et al. 2017). This would give a combinatorial effect of multiple complexes with different affinities and specificities of their biological targets, giving the cell an instrument for fine-tuning its stress response (Hernandez-Sanchez et al. 2017). There is also evidence that K-segments are involved in membrane binding, and that the pair of Lys residues in the center of the K-segments have the strongest binding interactions, which would explain a functional importance for the conserved sequence (Atkinson et al. 2016). Since dehydrins prefer to bind to negatively charged lipids, negatively charged amino groups near the conserved Lysines may help orient hydrophobic residues toward membrane surfaces (Atkinson et al. 2016). Some dehydrins contain one to three repeats of the Y-segment (T/VDEYGNP) near their N-terminus and is suggested to play a role in nucleotide binding (Hughes et al. 2013). In addition to these motifs, the S-segment is a tract of five to seven serine residues, which can be phosphorylated and regulate ion binding (Alsheikh et al. 2005). It has been shown that phosphorylation-regulated ion binding activity is generally conserved in the acidic subfamily of DHNs and may have the capability to stabilize the cytoskeleton (Abu-Abied et al. 2006; Kovacs et al. 2008; Vaseva et al. 2014) It was also shown that these segments can bind to nuclear localization signal peptides of proteins and facilitate their transport to the nucleus (Charfeddine et al. 2017). The dehydrins can be found in the cytoplasm,

nucleus, plasma membranes, and mitochondria of various cell types and generally are deficient in the amino acids Cys and Trp (J. 1997; Atkinson et al. 2016). But they are known to accumulate in different sites depending on the development stage and tissue type (Vaseva et al. 2014).

### 1.4.1 Dehydrins are Intrinsically Disordered

Dehydrins constitute a group of intrinsically disordered proteins (IDPs) that accumulate in response to any environmental stimulus with a dehydrative component (Eriksson et al. 2011). This includes drought, low temperature, salinity, seed maturation, heavy-metal stress, and perhaps biotic stress as well. IDPs are known to participate in developmental control, light perception, transcriptional regulation, and response to abiotic stress and it is thought that dehydrins have evolved to stay disordered under cellular conditions and that disorder might be required to properly fulfill their function (Cuevas-Velazquez et al. 2016). This ability to perform multiple functions in the plant cell has been termed “moonlighting”, which is a characteristic feature of most IDPs (Banerjee and Roychoudhury 2016). Currently, the fundamental biochemical mode of action and molecular mechanisms behind their function is not clear, but many advances in deciphering their role have been made in recent years. The Arabidopsis COR15A is a cold-regulated, nuclear-encoded IDP that accumulates in the chloroplast stroma. It was found to fold into an alpha-helix and insert into a membrane parallel to the surface in dehydration conditions, likely functioning as a protective protein-membrane interaction (Bremer et al. 2017). In Arabidopsis, overexpression of *MtCAS31* reduced stomatal density to confer increased drought tolerance, a first report of a DHN affecting stomatal density. (Xie et al. 2012). Nonetheless dehydrins are a versatile group of proteins that exhibit a myriad of functions when exposed to various stress factors that suggest some dehydrins play a regulatory role in the stress response (Hanin et al. 2011).

### 1.4.2 Dehydrin Classification

A plant genome usually contains several dehydrin genes belonging to different structural sub-classes where expression differs based on tissue type and environmental conditions (Koehler et al. 2007; Kosova et al. 2011). The dehydrins are subdivided into several classes according to the amount and presence of these motifs (Koehler et al. 2007; Wang et al. 2014). The number (n)

and order of Y-, S-, and K- segments define five different DHN sub-classes: $Y_nSK_n$, $SK_n$, $K_n$, $Y_nK_n$, and $K_nS$. $Y_nSK_n$ is induced by drought, $SK_n$ are acidic DHNs responding to cold and drought, $K_n$ is usually related to cold tolerance, while $Y_nK_n$ is related to drought and cold tolerance (Vaseva et al. 2014). In maize, a KS-type dehydrin ZMDHN13, contained three conserved segments that exhibited a cooperative effect in response to environmental stresses *in vivo* (Liu et al. 2017). The expressions of $SK_n$-, $K_n$, and KS-type DHNs were induced by both low-temperature stress and drought stress (Wang et al. 2014). There are also less conserved regions rich in glycine and polar amino acids called ϕ – segments (Vaseva et al. 2014). These segments interact with macromolecules, to prevent structural damage and maintain enzyme activity (Charfeddine et al. 2017). These highly flexible regions interspersed with K-segments allow the latter to optimally orient with target ligands, maintaining a large hydrodynamic radius (Banerjee and Roychoudhury 2016). In *Vitis riparia,* the larger the hydrodynamic radius of the dehydrin, the more effective the cryoprotection (Hughes et al. 2013). Additionally, all parts of the protein, not just the K-segment were contributing, and that disorder and length were the most important factors for dehydrins to function as effective molecular shields (Hughes et al. 2013). It has also been suggested that dehydrins have antifreeze protein (AFP) activity, yet AFPs are very rigid, but natural dehydrins as well as synthesized K-segments were found unable to stop the growth of ice crystals (Hughes et al. 2013). They concluded that previous reports of antifreeze protein-like activity in dehydrins are likely due to contamination, and that dehydrins do not protect enzymes by inhibiting ice growth (Hughes et al. 2013).

### 1.4.3 Dehydrin Contribution to the Cold Response

Dehydrin levels strongly correlate with freezing tolerance, many are regulated by the CBF cold-responsive pathway, and when overexpressed increase cold tolerance (Houde et al. 2004). In addition they are suggested to be involved in the cryoprotection of the plasma membrane against freezing (Houde et al. 2004). In a study focused on identifying the importance of the K-segment, it was found that the K-segment is critical for stabilizing lactate dehydrogenase (LDH) activity and preventing protein aggregation during temperature stress in the wheat dehydrin WZY2 in *E. coli* (Yang et al. 2015). In a separate study on membrane binding of a dehydrin Lti30 (XERO2), it was concluded that the interaction between Lti30 and membranes consists of two components: a K-segment in combination with a pH-controlled affinity switch of flanking His residues, which

can be further fine-tuned by protein phosphorylation (Eriksson et al. 2011). This led them to demonstrate that the distinct phosphorylation profiles of the different classes of dehydrins show that their biological function can be regulated separately based on their acidic or basic nature (Eriksson et al. 2011). Upon further examination it was found that the K-segment of Lti30 had helical structure upon binding, hydrophobically to one vesicle and electrostatically to the other, possibly with the aid of the pH tuneable, flanking histidines (Eriksson et al. 2016). Interestingly, it was found that the phosphorylated forms of the acidic dehydrins COR47, ERD10, and ERD14 bind $Ca^{2+}$ much more efficiently than the dephosphorylated ones (Alsheikh et al. 2005). In Gentians, expression of *GtDHNs* enhanced freezing and dehydration tolerance, probably via activation of antioxidant mechanisms activated by ABA and dehydration stress (Imamura et al. 2013). In transgenic strawberry, expression of WCOR410, a wheat dehydrin, improved the freezing tolerance of strawberry leaves by preventing destabilization of the plasma membrane that occurs during the dehydrating conditions associated with freezing. The hydrophilic nature of WCOR410 means that it is well suited to replace water and stabilize membranes through polar interactions (Houde et al. 2004). Recent work in the Randall lab has identified seven putative dehydrins in diploid strawberry and identified two of them through mass spectrometry to be COR47-like and XERO2-like dehydrins (Koehler, Fattash, Osuagwu, Randall, Unpublished data). Overall, dehydrins play a fundamental role in the dehydration and cold response in plants and function to a range of environmental and developmental stimuli.

## 1.5 Biomarkers

### 1.5.1 Proteomic Potential Biomarkers from Octoploid Strawberries

From previous work in the lab (Koehler et al. 2012; Rohloff et al. 2012; Davik et al. 2013; Koehler et al. 2015; Koehler et al. 2010), several proteins were identified as being associated with cold tolerance. Other research has also been done looking at the expression profiles of genes (CBF4, COR47, F3H) strongly upregulated in strawberry as well (Badek et al. 2014). The most promising biomarkers are the dehydrins and ADH. In a proteomic study comparing crowns of octoploid cultivars done by Koehler et al. (2012), several proteins were identified as associated with cold tolerance. They suggested that the variability of cold hardiness observed for strawberry species is likely contributed by the proteins that accumulate in the

overwintering crown to mitigate adverse effects of freezing damage (Koehler et al. 2012). The cultivars could clearly be distinguished from each other in the cold, based on their protein expression profiles. The cold response of 'Frida' upregulated proteins largely to flavonoid biosynthesis, while 'Jonsok' had a wider array of cold-response proteins involved in a variety of associated responses including disease resistance, antioxidation, and detoxification. In addition, 'Jonsok' had a much higher constitutive level of cold tolerance-related protein expression that 'Frida' lacked, giving it an innate advantage for cold response. Thaumatin, β-1,3-glucanase, Alcohol Dehydrogenase (ADH), and dehydrins were the strongest contributing proteins for distinguishing the cold tolerant 'Jonsok' from lesser cold tolerant 'Frida' in the experiments. Thaumatin is a sweet tasting pathogenesis-related (PR) protein known to have membrane permeabilizing properties, but its biological function in cold stress is not yet clear (Rajam et al. 2007). The introduction of thaumatin into transgenic tobacco resulted in fungal pathogen resistance, as well as abiotic stress tolerance (Rajam et al. 2007). ADH is a protein upregulated by anaerobiosis, that catalyzes the reduction of pyruvate to ethanol, ensuring a constant supply of $NAD^+$ and its activity is considered essential for survival during anaerobic conditions (Chung and Ferl 1999). ADH has high expression in low oxygen levels and is known to increase in response to dehydration, low temperatures, and ABA while playing a functional role in food ripening, as well as seed and pollen development (Thompson et al. 2010). HSC70 is a chaperone protein that aids in the transport of proteins in the mitochondria and chloroplast, and is known to be expressed in response to environmental stress such as heat, cold, and drought (Wang et al. 2004). β-1,3-glucanase is a pathogenesis-related protein that is known to play a role in plant development, pathogen defense, and has been shown to be cold induced (Castresana et al. 1990). Koehler et al. (2012) also suggested that the COR47-like and XERO2-like transcripts (or protein) could have different temporal roles based on their varying dynamics of expression. In addition, they also state that it should be considered that changes in transcript and protein levels are often not concomitant, raising the idea that protein levels could be regulated post-transcriptionally and that an increase in mRNA does not always constitute an equal increase in subsequent protein.

### 1.5.2 Diploid Potential Biomarkers

In a study of diploid strawberry genotypes, Davik et al. (2013) examined correlations between tolerance to low-temperature stress and certain metabolites and proteins in order to

identify biomarkers related to cold tolerance. They compared 22 genotypes consisting of Alta, FDP817, NCGR1363, as well as other diploid varieties varying in cold tolerance. Davik et al. (2013) concluded that ADH, dehydrins, and galactinol showed the greatest potential to serve as biomarkers for cold tolerance in diploid strawberry because of their high correlation with the $LT_{50}$ of the genotypes. One interesting observation was that the amount of time spent acclimating the plants in the cold could have a huge impact for deep cold hardiness. An acclimation time of six weeks may have been too short of a time frame to attain the full level of cold hardiness, potentially missing the full extent of cold acclimation changes.

### 1.5.3 Proposed Biomarker Evaluation Strategies

In this project, I focused on three main avenues for confirming biomarkers in strawberry. The first was developing a high throughput method for protein assays and subsequent western blotting (Appendix). The second was analyzing octoploid F1 leaves and crowns in 0 and 42 day cold treatment for 5 different proposed biomarkers, further confirmation of these biomarkers in a segregating F1 population will increase the confidence that these are true biomarkers for cold tolerance. The third was analyzing diploid leaf and crown tissue at 9 different timepoints during cold exposure. Comparison of transcripts and resulting protein for XERO2 and COR47 dehydrins will determine if transcript accumulation is a sufficient parameter reflecting cold tolerance. Finally, investigation into the discrepancy (where protein increase precedes RNA increases) between transcript and protein for COR47 to identify the level of regulation or mechanism involved for expression of this dehydrin protein.

# CHAPTER 2. METHODS

## 2.1 Plant Material and Experimental Design for Freezing Experiments

The plant runners of three *Fragaria vesca* genotypes, ALTA, FDP817 and NCGR1363 were planted in a peat-based potting compost (90% peat, 10% clay) containing 1:5 (v/v) granulated perlite in a 10 cm plastic container. The diploid strawberry material; propagation and cold treatments, were prepared by Jahn Davik and Anne Langerud, at The Norwegian Institute of Bioeconony Research (NIBIO), Kvithamar, Norway. Plants were watered via flow-irrigation twice a week with a solution containing 7.8 mmol nitrogen, 1 mmol phosphorus, and 4.6 mmol potassium per liter. The plantlets were propagated in a greenhouse with supplementary light (temperature 18 ± 2°C and 20 hours photoperiod) for 42 days.

Cold acclimation (CA) was performed by transferring the plants to a cold room at 2°C in a short day period (10h light/14h dark at 90 µmol quanta m-2 s-1). Plant leaf and crown tissues were harvested after; 0h (untreated), 1h, 2h, 3h, 8h, 24h, 48h, 7d, 14d and 42d of CA. The 0h untreated control plant was harvested at room temperature while the cold treated plants were harvested in a cold room. Triplicate samples (biological replicates) of both leaves and crown tissue from each genotype were harvested for each time point and stored at -80°C until time of processing.

## 2.2 Plant Material for Octoploid work: Jonsok, Elsanta, Frida and F1s. Protein and Transcript Analysis

The Jonsok, Elsanta, Frida and F1 generations, grown the same way as mentioned in (Koehler et al. 2012), and were provided by Dr. Muath Alsheikh, at Graminor, AS, Ridabu, Norway. Cold acclimation was performed in a cold room at 2 °C and 10 h light/14 h dark at 90 µmol quanta m-2s-1 for 0 hours (control) and 42 days (treatment). The F1 populations were grown in triplicates with three plants for each replicate giving a total of nine plants for a genotype in each treatment. Collection of 0 days control samples were performed at room temperature. Cold treated samples were harvested in a cold room. Two to three leaf samples were collected from each plant. Crown tissues were harvested by dividing longitudinally into four to six crown segments. After

harvesting of leaf and crown tissue, samples were immediately frozen in liquid nitrogen, and the tissues were stored at − 80°C for RNA and protein extraction.

## 2.3 Protein Extractions

Strawberry tissue samples were pulverized in liquid $N_2$ with a pestle and mortar until ground to a fine powder. One hundred mg of powder was combined with 500 uL extraction buffer (0.1 M Tris HCL, pH 8.5), 2% w/v Sodium dodecyl sulfate (SDS), 2 uL protease inhibitor mixture, and 2% (10 uL) 2-Mercaptoethanol (BME). The protease inhibitor mixture consists of: 0.2 uL 1 M Benzamidine, 0.2 uL 1 mg/uL aprotinin, 0.2 uL 1 mM pepstatin, 0.2 uL 1 mg/mL leupeptin, 0.25 uL 50X Roche Diagnostics Complete Protease Inhibitor Cocktail (contains 4-(2-Aminoethyl)-benzolsulfonylfluorid Hydrochlorid/4-(2-Aminoethyl)benzenesulfonyl Fluoride Hydrochloride), and 5 uL 0.5 M, pH 8.0, ethylenediaminetetraacetic acid (EDTA) for a final concentration of: 0.4 mM Benzamidine, 0.4 ug/uL aprotinin, 0.4 uM pepstatin, 0.4 ug/mL leupeptin, 0.025x RPIs, and 5 mM EDTA. Samples were homogenized with motorized pestle setting 1-2 for 90 seconds. Phenylmethylsulfonyl fluoride (PMSF) (0.5 uL of 1 M stock) in dimethyl sulfoxide (DMSO) was added per 500 uL, immediately after homogenization. Samples were spun in centrifuge at 4 °C for 10 min at 10,000 rpm. Supernatant was combined with 4x SDS-Page Sample Buffer (SSB) (0.25 mM Tris pH 6.8, 50% glycerol, 10% (w/v) SDS, small amount of bromophenol blue (Laemmli 1970)) containing 200 mM dithiothreitol (DTT); for every 60 uL of supernatant, 20 uL of 4x SSB was added. The mixture was heated for 4 minutes at 95 °C and then samples were either used immediately or stored at -80 °C.

## 2.4 Protein Determination - REVERT™

This method follows the LI-COR REVERT™ Total Protein Stain Instructions booklet. Membranes were rinsed in water and then gently shaken in 5 mL of REVERT™ Total Protein Stain for 5 minutes. Stain was decanted and membrane was washed twice with Wash solution (6.7% (v/v) Glacial Acetic Acid, 30% (v/v) Methanol, in water). Membrane was then imaged in the 700 nm channel using an Odyssey CLx system (LI-COR Biosicences, Lincoln, NE). Images were acquired under Automatic Mode (medium quality, 169 um resolution) to ensure a linear

range. No saturated pixels were detected. Image was quantitated using Image Studio Lite Ver. 5.2. Software.

## 2.5 Amido Black Protein Determination: Adaptation in the Dot-Blot

Sample aliquots of 20 uL were prepared at a concentration of 0.04x-0.05x SSB. Nitrocellulose was wetted in PBS for 10 minutes, then placed in the Bio-Dot Apparatus. Three washes with 100 uL PBS and a light vacuum was performed. Sample was then applied into the wells directly onto the nitrocellulose and allowed to gravity filter for 1-2 hours. After samples were filtered, 200 uL PBS washes with light vacuum were performed three times. Nitrocellulose was then taken out of the apparatus and stained and destained based on Kaplan and Pedersen (1985). Nitrocellulose was stained for 3 minutes in 200 mL Amido Black stain that consists of napthol blue black 0.1% (w/v) dissolved in methanol/glacial acetic acid/deionized water (45/10/45, v/v). Destain consisting of methanol/glacial acetic acid/water (90/2/8, v/v) was used to wash the nitrocellulose three times for one minute. Nitrocellulose was then rinsed with DI $H_2O$. The membrane was dried on filter paper, after ~15 minutes, sample circles were cut out and placed in test tubes. One mL of 25 mM NaOH/ 0.05 mM EDTA/50% ethanol was added and tubes were incubated for 20 minutes with occasional vortexing. Two hundred microliters of each sample was pipetted into a 96-well plate. Absorbance was read at 630 nm using Molecular Devices SpectraMax M2$^e$ plate reader and SoftMax Pro 6.5 software. A standard curve was established each time this process was done using a dilution series of BSA standards.

## 2.6 Western Blotting – Immunofluorescence

Following protein assay, samples were diluted to 1 ug protein/uL with 1x SSB. A 12% acrylamide gel was loaded with 10 uL (10 ug) of sample in each lane. Gel electrophoresis was run at 80 volts for 10-15 minutes, and then at 150 volts until the dye front was almost run off of the gel (~90 minutes). The gel was then placed in western transfer buffer for 45 minutes. A ‘transfer sandwich’ with filter paper, gel, and 0.45 micron nitrocellulose paper (NitroBind, Maine Manufacturing, LLC) was assembled, put into a wet transfer apparatus at 4 °C, and run

overnight (Amp 0.2, constant current). Transfer was then removed, nitrocellulose was cut to size of the gel, put into 5% milk/Phosphate Buffered Saline (PBS) and blocked for 2 – 24 hours. Primary antibody was applied to nitrocellulose (1:4000, unless noted otherwise), and placed in 4 °C on a rocker overnight. Primary antibodies used in experiments were: Rabbi anti - ADH (Product No. AS10 685, www.agrisera.com), Rabbit anti – β-1,3-glucanase (Product No. AS07 208, www.agrisera.com), anti – HSC70 (Lot No. 02011356, Enzo Life Sciences), anti – thaumatin (e. coli expressed in strawberry, Randall *et* al., unpublished), and anti – COR47 and anti – XERO2 (Alsheikh et al. 2005)). Blot was then washed three times in 5% milk/PBS for 15 minutes each in shaker at room temperature. Secondary antibody, either Donkey anti-rabbit igG or Donkey anti-mouse igG (1:8000, Alexa Fluor) in PBS/5% milk was added to the blot and put on rocker for 35-45 minutes at room temperature. All subsequent steps containing Alexa Fluor were protected from light exposure. The blot was then washed three times in 5% milk/PBS for 15 minutes each. Blot was washed three times in PBS for 15 minutes each. Then blot was placed on filter paper to dry (~30 min). Image was taken using Li-Cor Odyssey CLx Imager (169 um resolution) and quantitated using Image Studio Lite Ver 5.2. For specific protein bands, rectangles of the same size that encompassed the band were used to quantitate the fluorescence intensity signal. For the entire lane on a gel, rectangles of the size of the lane were used to quantitate entire antibody signal.

## 2.7 Dot-Blot 'Western'

The BIO-RAD BIO-DOT™ APPARATUS was used to load small volumes. Nitrocellulose was cut to desired size and wet in PBS for 10 minutes (PVDF membranes were soaked in methanol). The membrane was placed in the apparatus and any unused wells were covered with Parafilm. The apparatus was assembled, tightened, and a full vacuum was applied, and the apparatus was tightened again. One hundred microliters PBS was added to each well and a light vacuum was applied until the wells drained; washing was repeated two more times. Samples were diluted so that they contained a maximum concentration of 0.05x SSB. The sample (50 uL) was applied and filtered (without vacuum) for 1-2 hours. A light vacuum was sometimes applied if samples had not filtered by two hours. The wells were washed 3 times with 200 uL PBS with light vacuum. The membrane was immediately removed and treated as described for western blots or for amido black protein assay. When quantitation of images was done using Image

Studio Lite Ver 5.2, circles of the same size that encompassed the dot were used to quantitate fluorescence intensity signal.

## 2.8 DNA Purification

This method follows the Plant DNAZOL DNA Extraction Modified Method, modified from Invitrogen Plant DNAZOL Protocol. Frozen tissue was pulverized in liquid $N_2$ and weighed 0.05 g in a 1.5 mL Eppendorf tube without being allowed to thaw. Then 150 uL of DNAZOL was added, samples were thawed and were then homogenized with a motorized pestle for ~1 minute at speed 1.5. Following mixing on a rotator for 5 mintues, 150 uL of chloroform was added, vortexed for 3-5 seconds, and the sample was mixed on the rotator for 5 more minutes. Samples were centrifuged at 17 k x g for 10 minutes. The top 150 uL of upper phase, avoiding interface was carefully removed and placed in a new sterile 1.5 mL tube. Then 108 uL 100% ethanol was added, vortexed for 3-5 seconds, and let stand for 5 minutes. Samples were centrifuged again at 17 k x g for 10 minutes, afterwards the supernatant was removed and discarded. Then 300 uL of 75% ethanol was added, vortexed 5-8 seconds, and centrifuged at 5 k x g for 4 minutes. Ethanol wash was removed by pipet, avoiding the pellet. Tubes were left open on their side for 10-15 minutes for evaporation. The DNA pellet was then dissolved in 50 uL autoclaved DI water and centrifuged at 12 k x g for 4 minutes. The supernatant was removed and placed in a fresh sterile 1.5 mL tube, which was used immediately or stored at -20 °C. A further precipitation step was done by adding equal volume of phenol/chloroform/isoamyl alcohol 25:24:1 (250 uL), and vortexing for 20 seconds followed by centrifugation at 12 k x g for 5 min. The supernatant was transferred to a clean tube (220 uL) and $1/10^{th}$ the volume of 3 M Sodium (or potassium) Acetate (NaOAc) (22 uL), and 2.5 to 3x volumes of 100% ethanol (~600 uL) were added to the supernatant, placed in freezer for 30 minutes to overnight before being centrifuged at 12 k x g for 5 minutes. EtoH solution was removed, and pellet was washed 2 volumes 70% EtoH (1 mL). Centrifugation and wash step was repeated with 2 volumes 76% EtOH (1 mL), EtOH was removed, and then air-dried pellet for 10-15 minutes. DNA was resuspended in 100 uL $H_2O$ and centrifuged at 12 k x g for 4 minutes. DNA was quantified using Nanodrop 2000 software. DI water was used to blank instrument. DNA was measured using 1 uL of sample on spec and a record of A260, A280, A260/A280, and concentration values were

taken. This was repeated for each sample. A range 1.6-1.8 for A260/A280 was utilized in further experiments.

## 2.9 RNA Purification

Sigma Spectrum Plant Total RNA Kit was used according to the manufacturer's protocol. Since crown is starchy material, lysed samples (lysis solution supplemented with 1% v/v 2-mercaptoethanol) were incubated at room temperature for 3-5 minutes. RNA was bound to the column using Protocol A, which used twice the volume of Binding Solution compared to protocol B. Purified RNA was quantitated using Nanodrop 2000 software. Samples were used immediately or stored at -80 °C.

## 2.10 cDNA Synthesis

This method is adapted from Invitrogen SuperScript III First-Strand cDNA Synthesis following the manufacturer's protocol with the following changes. Total RNA (500 ng) was added to 1 uL 50 uM oligo (dT), 1 uL 10 mM dNTP mix, in a total volume of 10 uL. The mixture was incubated at 65 °C for 5 minutes to denature the RNA, then placed on ice for one minute. The following cDNA Synthesis Mix was prepared, adding each component in the indicated order. One reaction contains 2 uL 10X RT buffer, 4 uL 25 mM $MgCl_2$, 2 uL 0.1 M DTT, 1 uL RNase OUT (40 U/uL), and 1 uL SuperScript III RT (200 U/uL). Ten uL of cDNA Synthesis Mix was added to each RNA/primer mixture, mixed gently, and collected by brief centrifugation. The RT mix was incubated at 50 °C for 50 minutes, followed by termination of the reactions at 85 °C for 5 minutes, then it was chilled on ice. Following a brief centrifugation, 1 uL of RNase H was added to each sample and incubated for 20 min at 37 °C. The cDNA synthesis reaction was stored at -20 or -80 °C or was used for PCR immediately.

## 2.11 RT-qPCR

Primers (Invitrogen) were hydrated to a concentration of 100 uM so that the final concentration in primer mixtures was 5 uM. The cDNA from RT synthesis was diluted at a 1:4 ratio to be equivalent to 6.25 ng RNA. Generally the RT-qPCR reactions were prepared by addition of 5 uL autoclaved $H_2O$, 1 uL cDNA (1:4), 2 uL of 5 uM Forward Primer, 2 uL of 5 uM Reverse Primer,

and 10 uL Thermo Scientific Maxima SYBR Green/ROX qPCR Master Mix (2X) for a total of 20 uL. The 20 uL reaction solutions had three technical replicates for each biological replicate and were added to PCR plate wells, sealed, and spun for 3 minutes at 12,000 rpm in a Beckman GS-6R centrifuge. Applied Biosystems 7300 Real PCR System was used in conjunction with Applied Biosystems Sequence Detection Software Version 1.2.3 for each run. The first stage of each run was at 50 °C for 2 min, the second stage was at 95 °C for 10 minutes, and the third stage was at 95 °C for 15 sec and 60 °C for 1 min for 40 cycles. The final dissociation stage was at 95 °C for 15 sec, 60 °C for 30 sec, and 95 °C for 15 seconds to generate a melting curve. At times, a 15 uL reaction was performed where the total amount of RNA loaded was 2.343 ng. These reactions were prepared by addition of 1.5 uL $H_2O$, 3 uL cDNA (0.78125 ng/uL), 1.5 uL Forward Primer, 1.5 uL Reverse Primer, and 7.5 uL Thermo Scientific Maxima SYBR Green/ROX qPCR Master Mix (2X). PP2A was used to normalize samples (Rob Wilson, personal communication).

## 2.12 Semi-Quantitative PCR & Gel Electrophoresis

Master Mix consisted of 5 uL 5X Green GoTaq Reaction Buffer, 2 uL 25 mM MgCl, 0.5 uL 10 mM dNTP, 1 uL 5 uM Forward Primer, 1 uL 5 uM Reverse Primer, 0.125 uL GoTaq DNA polymerase, and 100 ng genomic DNA, bringing the total volume to 25 uL with DI $H_2O$. Samples were inserted into Perkin Elmer GeneAmp PCR System 2400 and programmed to melt at 95 °C for 2 minutes, then run 35 cycles melting, annealing, and extending at 95 °C, 60 °C, and 72 °C for 30 seconds at each temperature. The PCR terminated with holds at 72 °C for a total of 2 minutes. PCR samples were run on a 1.5% agarose gel using TAE (40 mM Tris, 20 mM Glacial acetic acid, and 1 mM EDTA (pH 8.0). Gel was loaded with PCR samples (25 uL) and standards (5 uL, NEB 100 bp ladder, 50 ng/uL). Gel was run at 50 Volts for 90 minutes. Gel was stained in 0.5 ug/mL ethidium bromide for 45 minutes, then destained in $H_2O$ for 45 minutes. Image was taken using the Bio-Rad Imager (UV/white, gel right side-up, Trans UV) and saved as a .tif file. For 12% polyacrylamide gels for western blotting lanes were loaded with 10 uL of sample and run at 80 volts for 10-15 minutes, then 150 volts until the dye front was almost run off of the gel (~90 minutes). The gel was then further processed following protocol for western blotting.

## 2.13 Primer Design

Primers were designed using NCBI (https://www.ncbi.nlm.nih.gov/) and Phytozome (https://phytozome.jgi.doe.gov/pz/portal.html) tools as well as JustBio Aligner tool (http://www.justbio.com/index.php?page=aligner) and NCBI's Primer Blast (https://www.ncbi.nlm.nih.gov/tools/primer-blast/index.cgi?LINK_LOC=BlastHome). Generated primers were checked with multiple parameters (Tm, GC content, and primer length) once the location in the gene was suitable and that there were no unintended targets (Table 1).

Table 1. List of Primers

| Primer Name | Gene ID | Sequence | Primer Length (bp) | Tm (°C) | GC% | Product Length (bp) |
|---|---|---|---|---|---|---|
| COR47_A | 101300217 | F: GCTCGTCTAGCAGTGACGAA | 20 | 59.83 | 55 | 81 |
| | | R: TGCTGGCGATCTTCTCCTTG | 20 | 60.11 | 55 | 81 |
| COR47_B | 101303769 | F: GCAAACCTGTTGAGCATGGC | 20 | 60.67 | 55 | 132 |
| | | R: CGTCACTTGACGAGCTGGAG | 20 | 60.73 | 60 | 132 |
| Nelson_COR47_B | 101303769 | F: GAGTACAACAAAGGCCACGAG | 21 | 59.2 | 52.38 | 148 |
| | | R: TCTCGAACTCGCTGACCATC | 20 | 59.55 | 55 | 148 |
| FvPP2A | 101300814 | F: CATCAAAGGACAGAGTACCCAACA | 24 | 60.5 | 45.83 | 94 |
| | | R: GTCTTCTCCACAACCGACTGA | 21 | 59.66 | 52.38 | 94 |
| COR47_B_Intron | 101303769 | F: TGGCTATCATCACGAGGAACC | 21 | 59.59 | 52.38 | 397 or 239 |
| | | R: CCTGCTCGTAGCCGTGT | 17 | 50.03 | 64.71 | 397 or 239 |
| COR47_B_Full | 101303769 | F: AACGCAGAGGTCGGTCATAG | 20 | 59.54 | 55 | 748 |
| | | R: GTGGAACTTCTCCACCGGG | 19 | 60 | 63.16 | 748 |

## 2.14 Gel Extraction and Purification

The extraction method followed QIAquick Gel Extraction Kit Protocol using a microcentrifuge from the QIAquick Spin Handbook (November 2006, www.QIAGEN.com). The DNA fragment was excised from the agarose gel with clean, sharp scalpel and was weighed.

## 2.15 DNA Isolation from *Fragaria* for Sequencing

Finely ground strawberry crown or leaf tissue was weighed (0.05 g) into a 1.5 mL tube and 5 mg insoluble Polyvinylpolypyrrolidone (PVPP) was added. Tissue was washed with 0.35 M sorbitol, 0.1 M TrisHCl pH 8.0, 5 mM EDTA, and 2% 2-Mercaptoethanol (BME) three times (with 1 mL), each time vortexing and incubating for two minutes, then centrifuging at 5200xg for 4 minutes. Next, the tissue was extracted with 600 uL of extraction buffer (0.1 M Tris HCL

pH 8.0, 20 mM EDTA pH 8.0, 2% CTAB, and 3 M NaCl) to each sample, along with: 65 uL 30% sarkosyl, 5 uL 10 mg/mL proteinase K, and 12 uL BME (Worden, 2009. Adapted from Winnepenninckx B. *et al*., 1993, TIG: 9 (12), 407 (Technical Tips). The extraction buffer was pre-warmed to 60 °C, added to the sample, vortexed, and incubated at 60 °C for 60 minutes. The samples were mixed by inversion every 5 minutes and incubation was terminated by putting samples on ice for 5 minutes. The mixture was then extracted with 600 uL of 24:1 (chloroform: isoamyl alcohol) followed by centrifugation at 13000xg for 5 minutes. To the aqueous phase, 1 uL RNase (DNase-free) was added and incubated for 30 minutes at 37 °C. The chloroform and isoamyl alcohol extraction step was repeated once more. Isopropanol was added at 0.67x the amount of recovered supernatant and held on ice for one hour, then centrifuged at max speed for 15 minutes in a microcentrifuge. The pellet was washed twice with 700 uL 70% ethanol, centrifuging for 5 minutes after each wash. The pellet was air dried for 30 minutes to let the ethanol evaporate completely, then resuspended in 50 uL $H_2O$. The concentration and purity were checked on Nanodrop 2000 software.

# CHAPTER 3. RESULTS

## 3.1 Evaluation of Biomarkers in Octoploids

Two octoploid varieties were chosen to be crossed based on their difference in cold tolerance. Jonsok is a very cold tolerant line while Elsanta has low cold tolerance. These octoploid parent varieties were crossed to obtain F1s of varying cold tolerance, which resulted with some F1s having a much higher, and others with a much lower degree of cold tolerance than that of the parents (Figure 1). The cross and filial generation survivability assays were done by collaborators in Norway (Alsheikh *et al*., unpublished). Evaluating the cold tolerance of the F1s and their parents with multiple potential protein biomarkers will give insight into which biomarkers might be the best predictors of survivability in the cold. The presence of a strong correlation can be further confirmed and ultimately used in breeding programs to select for more cold tolerant lines. Based on previous proteomic data (Koehler et al. 2012) several potential protein biomarkers were identified. We (note that some of this work was performed together with Shanti Pohkrel) selected five of these potential biomarkers to see if they might be good indicators of cold tolerance in a collection of F1s that has individuals with a wide range of ability to survive in cold temperatures. This could provide additional information to input into ongoing whole genome association studies and show that correlations with these potential biomarkers and the ability to tolerate cold temperatures can direct future screening and breeding selection for more cold tolerant lines.

Crown and leaf samples taken from the octoploid parents (Jonsok & Elsanta) and 30 F1s that varied in cold tolerance (Figure 1) were examined. Two time points, 0 hours in cold and 42 days in the cold, with three replicate plants per line were examined. Protein was quantified, and extracts were adjusted to 1ug protein/uL of SSB. Western blots were performed, testing 5 antibodies that targeted XERO2, β-1,3-glucanase, ADH, HSC70, or Thaumatin (Figure 2). For efficiency purposes antibodies to ADH/HSC70 and β-1,3-glucanase/Thaumatin were applied to the same blots. The use of both of the antibodies together was shown in a small sample set to visualize distinct bands of both proteins and it was clear that the specific protein bands could be quantitated for each antibody (Figure 3).

The F1s were evaluated with relation to percent survival and fluorescence signal intensity. In addition, the biomarkers were compared to total accumulation averages at 0 day and 42 day timepoints. The most apparent trend is with XERO2, where there is a strong increase in 42 day signal as percent survival increases in both the crown and leaf sets (Figures 4 & 8). ADH shows the same relationship in the crown and leaf, but to a lesser extent where clusters of 42 day expression accumulate higher than the corresponding 0 day samples (Figures 5 & 8). Overall, XERO2 and HSC70 total average signal is significantly higher in 42 days of cold compared to the 0 hour in the crown (Figure 9). It has been previously shown that ADH accumulates to a great extent in cold treated strawberry octoploid varieties (Koehler et al. 2012) and the results from this ADH set support what the literature suggests for the leaf (Figure 10). For ADH in the crown, the overall trend suggests higher accumulation in the 42 day samples (Figure 5), but the comparison of total average signal for 0 day and 42 day does not reflect that, possibly due to high variation in fluorescence intensity of 42 day samples (Figure 9). In the crowns, thaumatin and β-1,3-glucanase showed similar trends with 0 hour and 42 day expression (Figure 9), while showing little correlation to survival (Figure 7). Examination of leaves showed total dehydrin content, ADH, and thaumatin had significantly more expression at 42 days of cold than 0 day expression (Figure 10). For β-1,3-glucanase in leaves, the 0 day expression was significantly higher than expression at 42 days in the cold (Figure 10). In HSC70, a significant trend was observed in the crown samples for 42 day expression compared to 0 day expression (Figure 9). Interestingly, in the leaves it was the opposite where 0 day average HSC70 expression was significantly higher than expression at 42 days (Figure 10). The trend of 0 day HSC70 expression in the leaf increased as survival percentages increased (Figure 6).

Samples were also analyzed for their fluorescence intensity average to get average total protein present in a freezing tolerant group (> 10% survival at -8 °C) and a freezing intolerant group (< 10% survival at -8 °C). This type of analysis was done with all of the antibodies from 0 and 42 day crown and leaf data and unpaired two tailed t-tests were done to see if any of the results were significant (Figure 11 & 12). The 42 day crown analysis shows only XERO2 being statistically significant for having a much higher average protein quantitation in the above 10% survival compared to the less than 10% survival (Figure 11). Forty-two day crown and leaf in XERO2, 0 day leaf in HSC70, and 0 day crown and 42 day leaf in ADH showed statistically significant results (Figures 11 & 12). Overall, the trend noticed from this data analysis is that

potential biomarker expression on average is higher in the greater than 10% survival category for all sample types and timepoints for every biomarker except β-1,3-glucanase.

To summarize, the individual contribution of these potential biomarkers do not show convincing trends. There are no significant correlations with protein expression and increased survivability, but there are some significant correlations in comparing average 0 day and 42 day expression in the crowns and leaves. The best candidate is XERO2 with total dehydrin content showing the greatest correlation with survival at -8 °C in the F1s suggesting that the accumulation profiles of the dehydrin proteins would be useful in identifying more cold tolerant strawberry lines. In addition, the HSC70 trend seen in the leaf could be a particular advantage for the breeder because the plant does not need to be sacrificed to perform analysis.

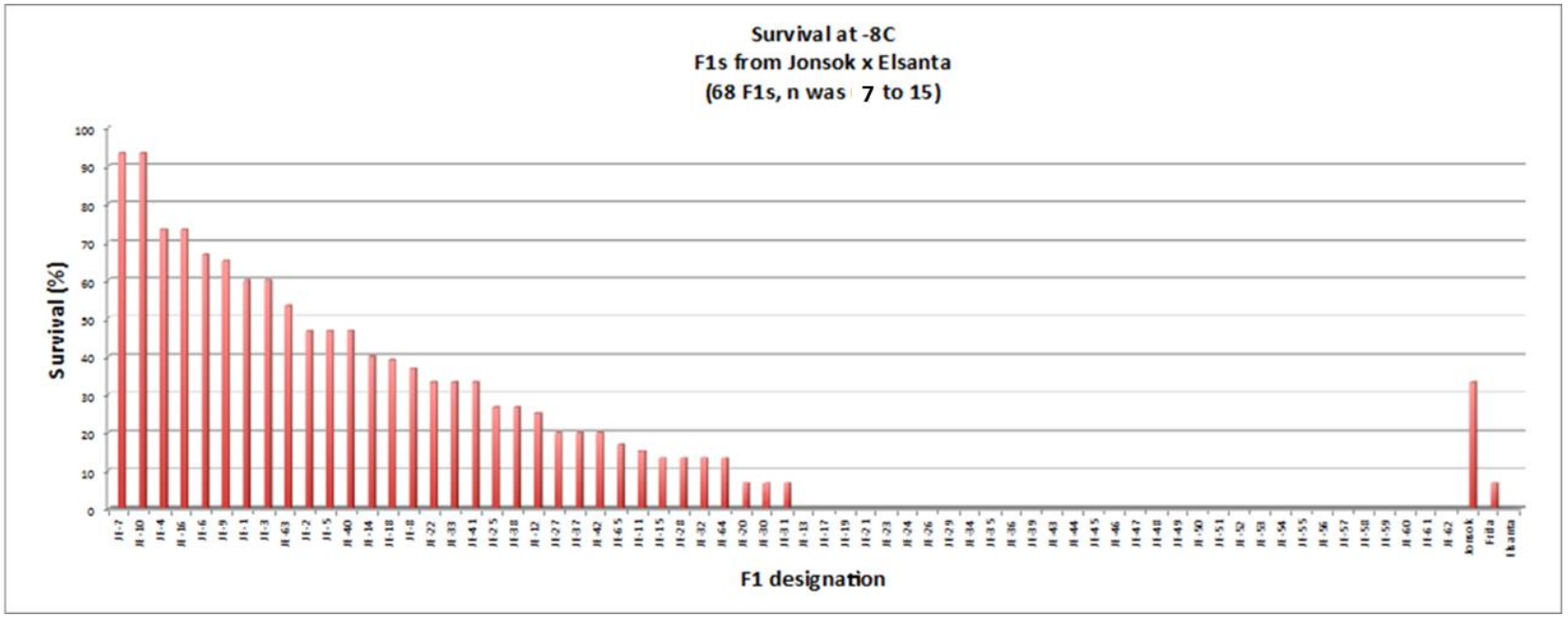


Figure 1. F1s resulting from a cross between Jonsok and Elsanta and their survival at -8 °C.

**Figure 1 Legend.** F1s resulting from a cross between Jonsok and Elsanta and their survival at -8 °C (Alsheikh et al, unpublished).

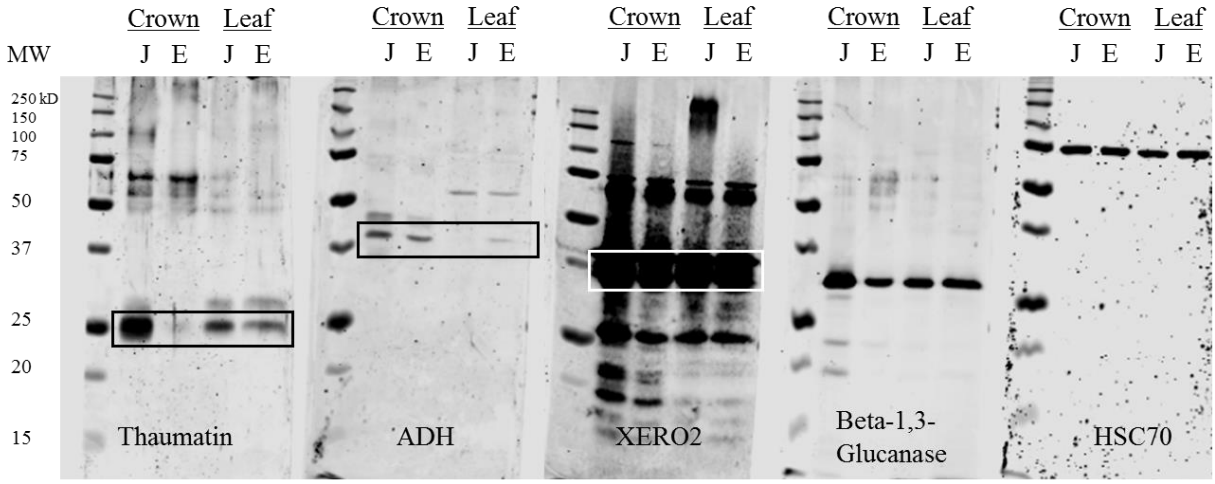


Figure 2. Probing Jonsok & Elsanta with potential biomarker antibodies.

**Figure 2 Legend.** Western blots showing the antibody applications of thaumatin, ADH, XERO2, β-1,3-glucanase, and HSC70. The five panels are loaded similarly with all tissue from plants exposed to cold for 42 days, with Jonsok and Elsanta crown in the first two lanes, and Jonsok and Elsanta leaf in the second two lanes. Lanes were loaded with 10 ug of protein. Antibodies were applied at a 1:2000 dilution except for HSC70, which was a 1:1000 dilution. Secondary antibody was applied at 1:4000 dilution.

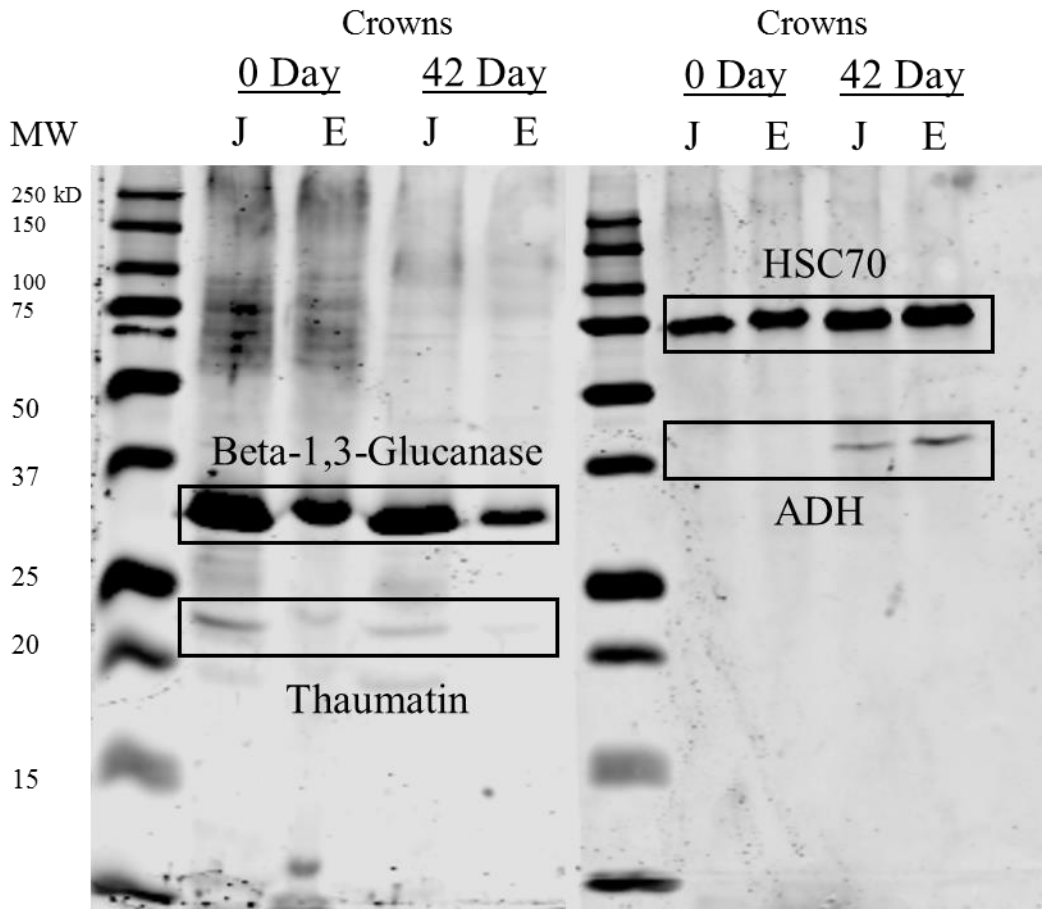


Figure 3. Simultaneous application of two antibodies on the same western blot

**Figure 3 Legend.** Proof of concept western blot showing one blot with both antibodies for thaumatin and β-1,3-glucanase applied, and the other with antibodies ADH and HSC70. The lanes were loaded with 10 ug of protein from crowns of either Jonsok or Elsanta at 0 and 42 days. Primary antibody dilutions were 1:2000 while secondary antibodies were 1:4000.

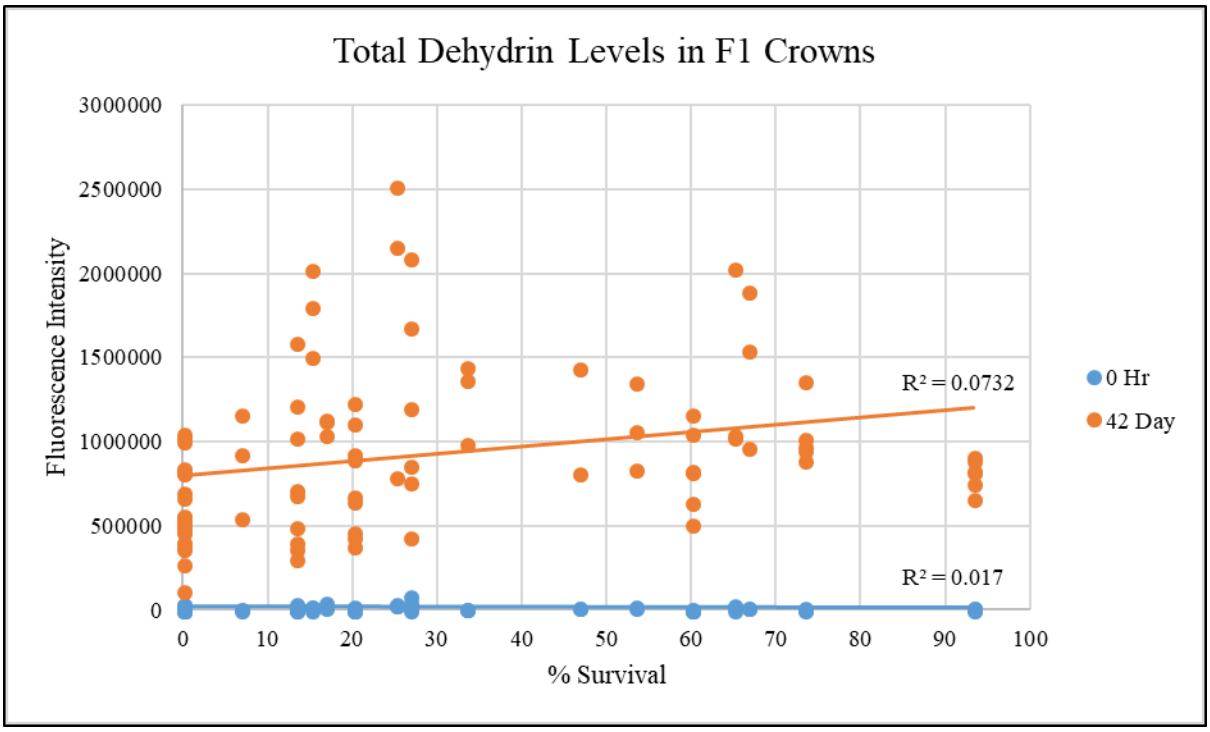


Figure 4. Crown: XERO2 entire lane quantitation

**Figure 4 Legend.** The XERO2 antibody is raised against the Arabidopsis XERO2, but reacts with most dehydrins, this antibody is suitable for examining all dehydrins on a gel. The XERO2 antibody was applied at a 1:2000 dilution with secondary antibody at 1:4000. The entire lane for each crown sample at zero hours and 42 days was quantitated to encompass the total antibody signal.

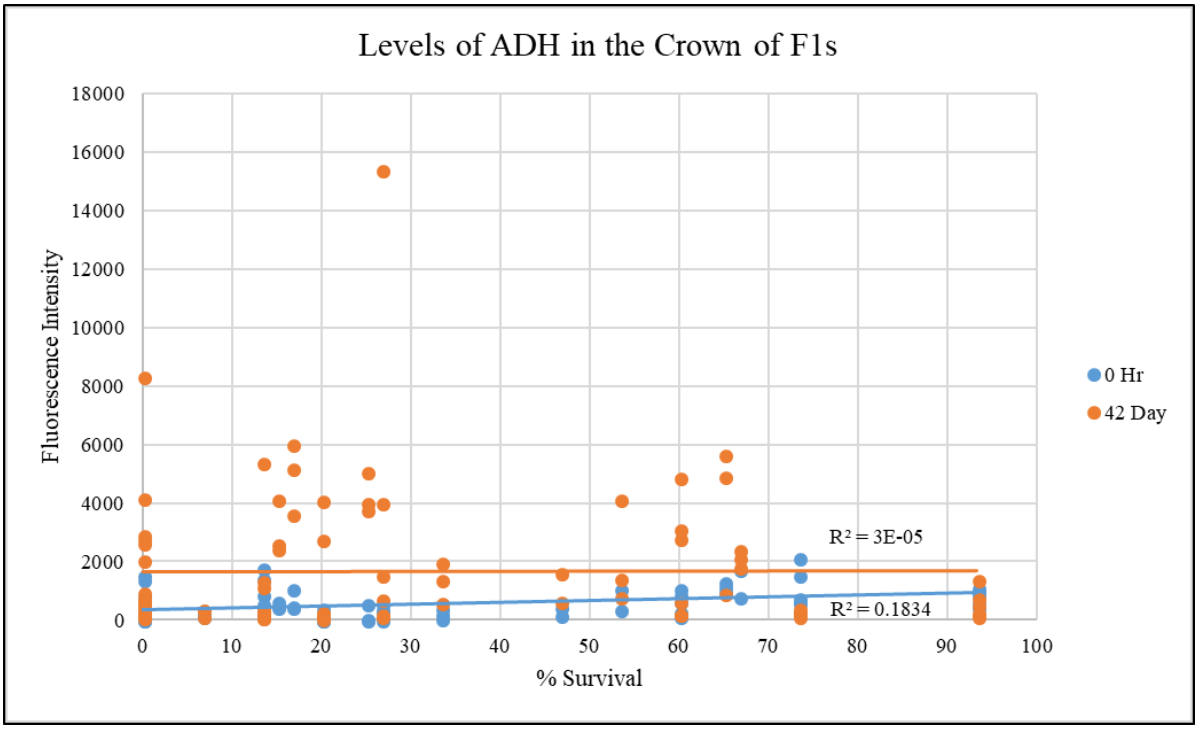


Figure 5. Crown: ADH band quantitation

**Figure 5 Legend.** ADH antibody was applied at a 1:2000 dilution with secondary antibody at 1:4000. The specific band quantitation was done for crown samples from F1s cold treated for 0 hours and 42 days. The clusters of 42 day samples had much higher signal than the 0 hour samples resulting in overall more induction at 42 days at all survival percentages.

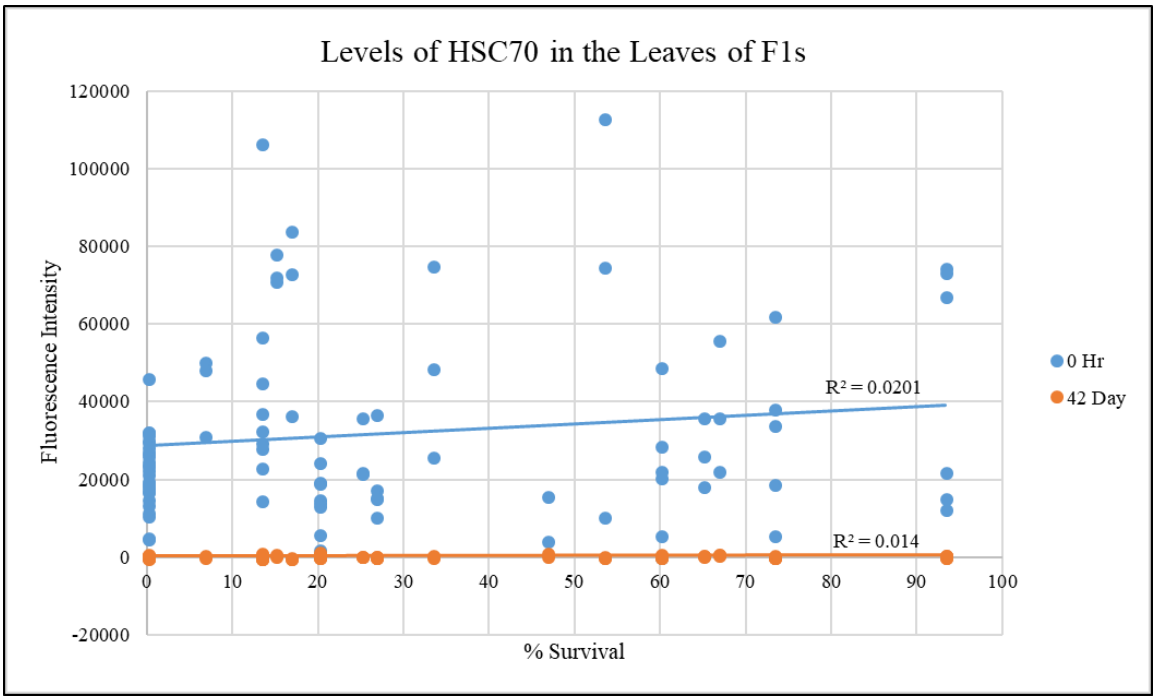


Figure 6. Leaf: HSC70 band quantitation

**Figure 6 Legend.** HSC70 antibody was applied at a 1:2000 dilution with secondary antibody at 1:4000. The specific band quantitation was done for leaf samples from F1s cold treated for 0 hours and 42 days. The expression of 0 hour samples was much higher than 42 day samples resulting in overall more induction at 0 hours at all survival percentages.

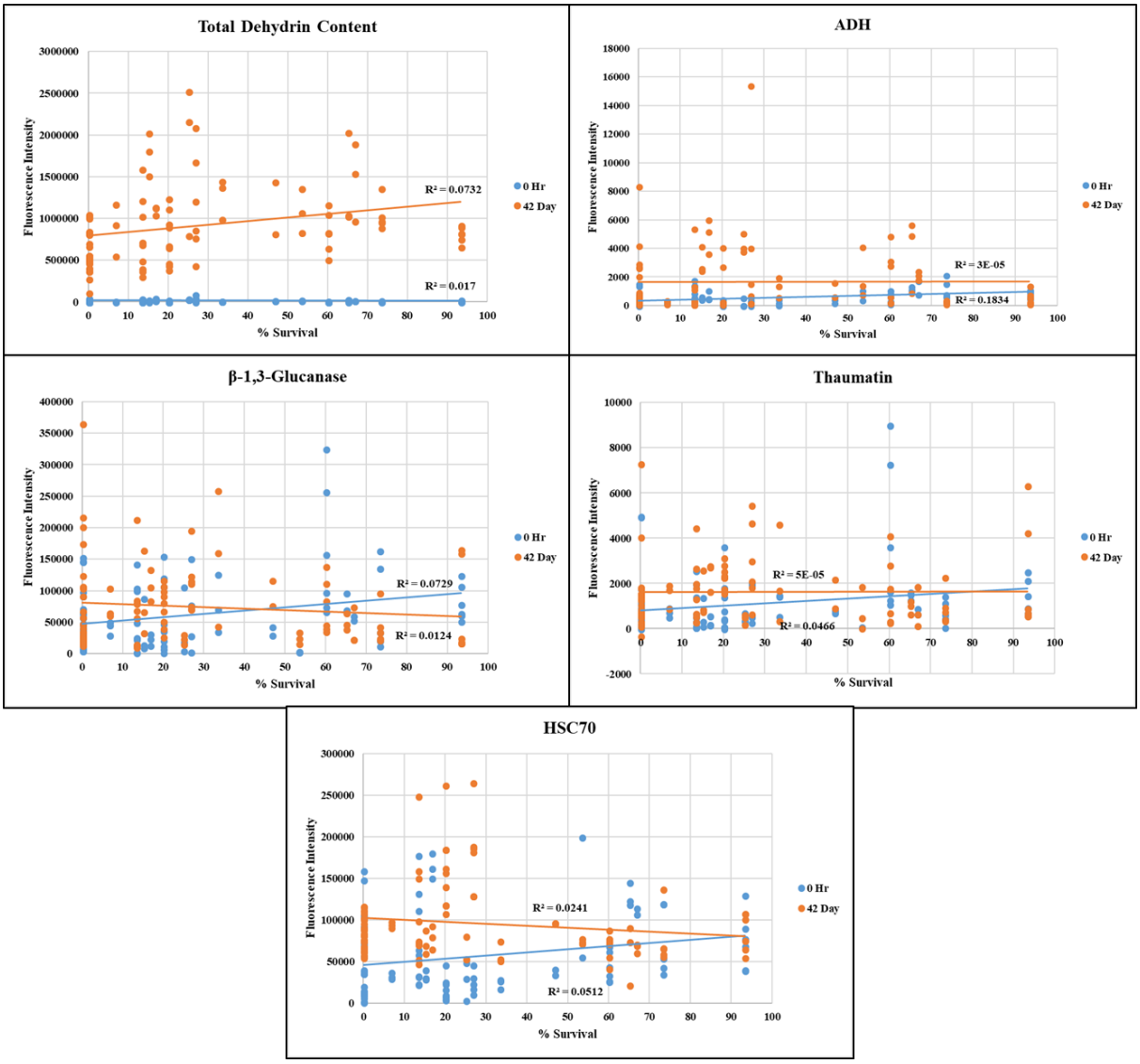


Figure 7. Crown Analysis of Octoploid F1s

**Figure 7 Legend.** Crown analysis of octoploid F1s and parents. Zero hour and 42 day samples were examined with 5 antibodies: XERO2, ADH, Thaumatin, β-1,3-glucanase, and HSC70.

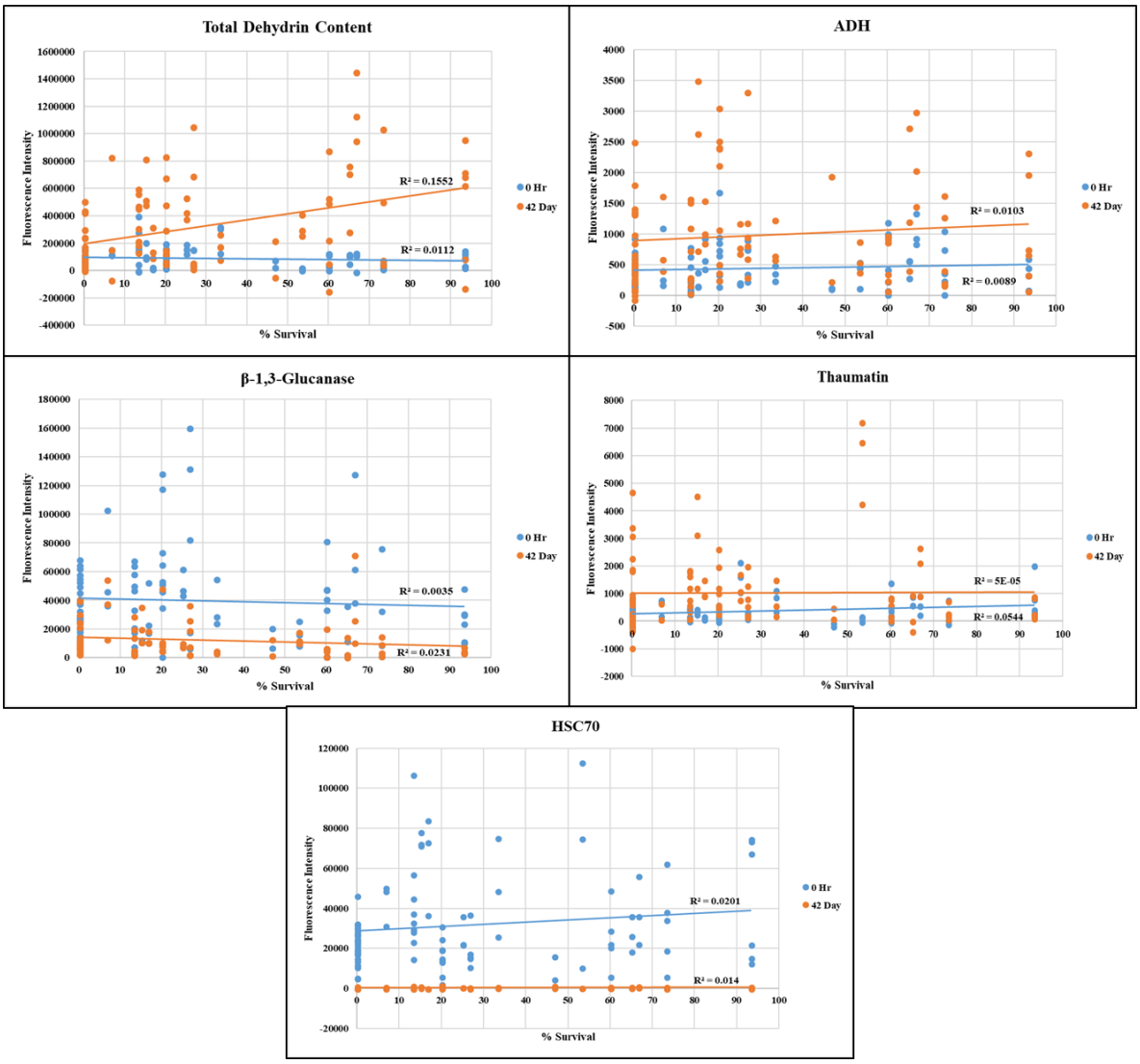


Figure 8. Leaf Analysis of Octoploid F1s

**Figure 8 Legend.** Leaf analysis of octoploid F1s and parents. Zero hour and 42 day samples were examined with 5 antibodies: XERO2, ADH, Thaumatin, β-1,3-glucanase, and HSC70.

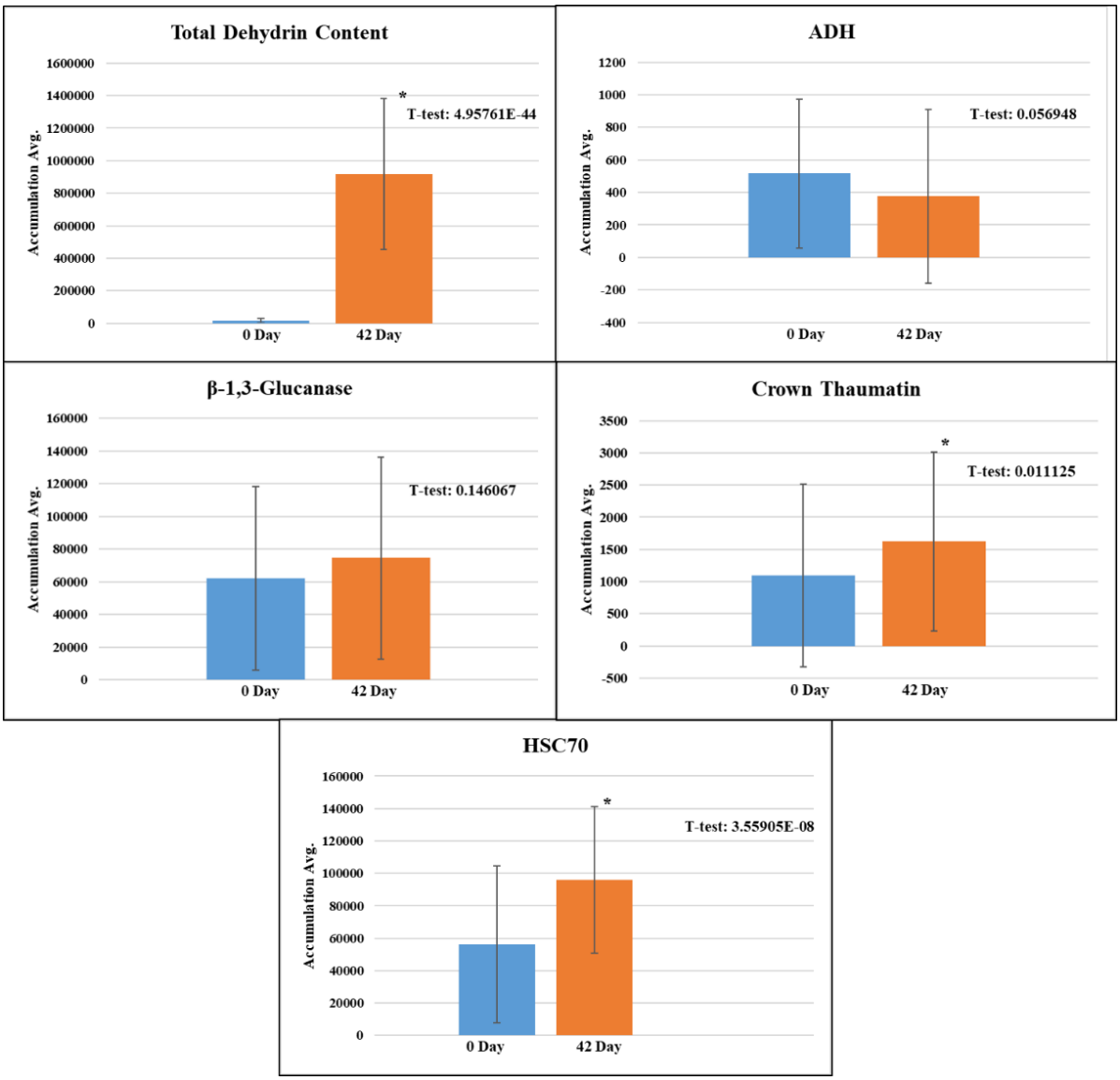


Figure 9. Crown Analysis of 0 Day vs. 42 Day Accumulation Averages

**Figure 9 Legend.** Analysis of the crowns of octoploid F1s and parents at 0 days and 42 days for total fluorescence intensity accumulation average. Samples were treated with five different antibodies: XERO2, ADH, β-1,3-glucanase, Thaumatin, and HSC70. Error bars represent standard deviation. Asterisks denote statistically significant t-tests where $P \leq 0.05$.

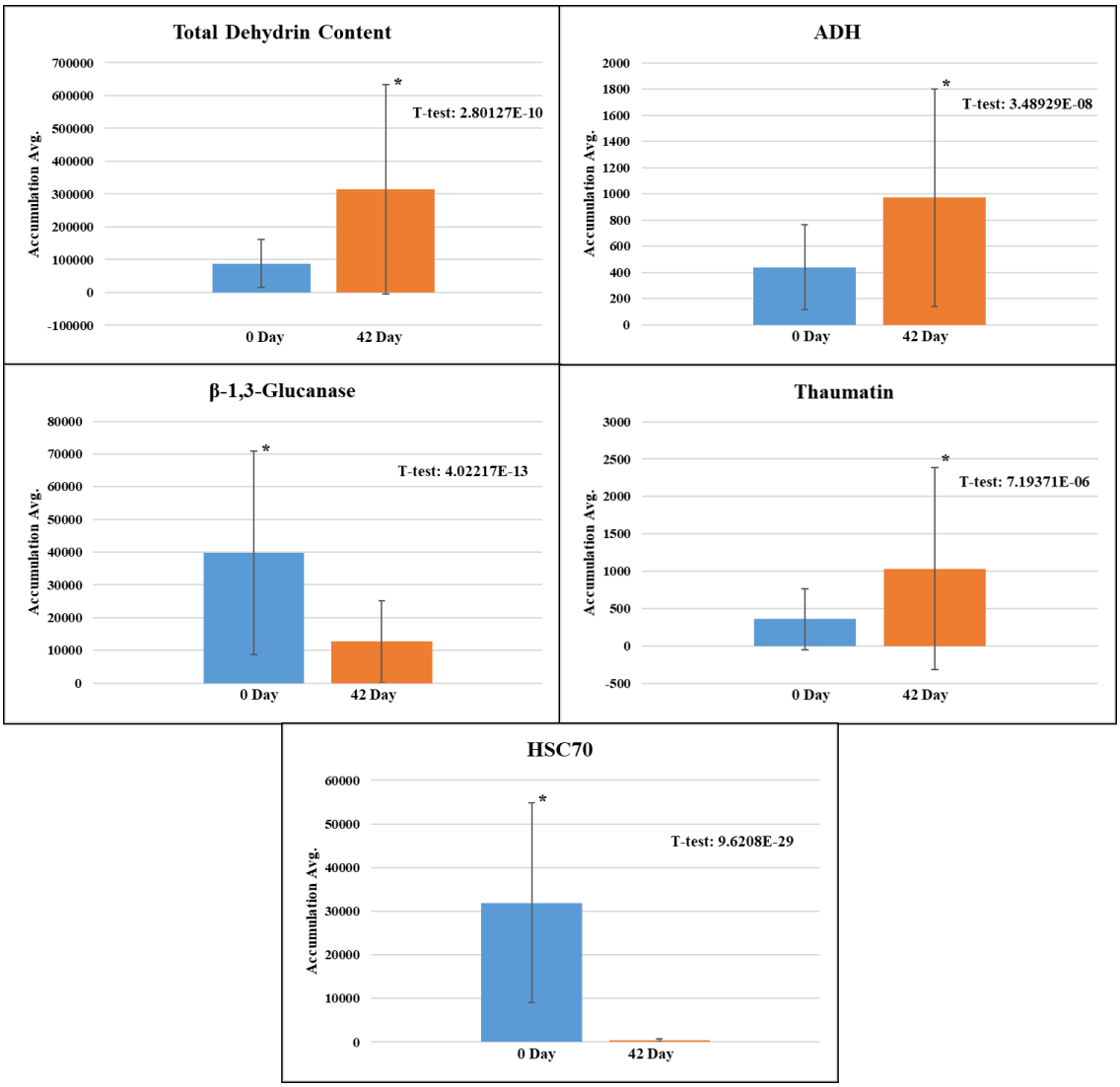


Figure 10. Leaf Analysis of 0 Day vs. 42 Day Accumulation Averages

**Figure 10 Legend.** Analysis of leaves of octoploid F1s and parents at 0 days and 42 days for total fluorescence intensity accumulation average. Samples were treated with five different antibodies: XERO2, ADH, β-1,3-glucanase, Thaumatin, and HSC70. Error bars represent standard deviation. Asterisks denote statistically significant t-tests where $P \leq 0.05$.

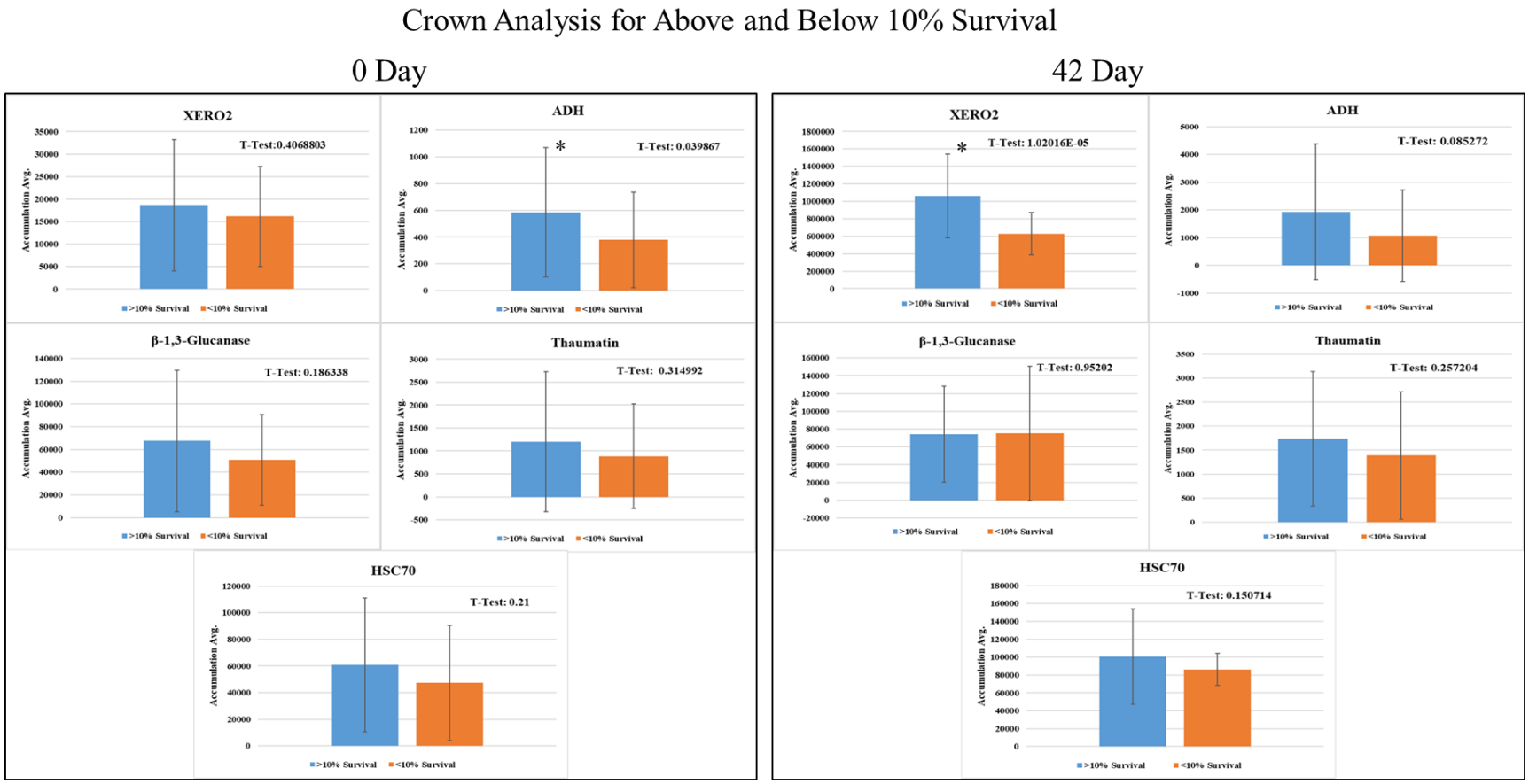


Figure 11. Levels of potential biomarkers in freezing intolerant and freezing tolerant offspring of Jonsok & Elsanta: Crowns

**Figure 11 Legend.** Samples were analyzed for their fluorescence intensity average in a freezing tolerant group (> 10% survival at -8 °C) and a freezing intolerant group (< 10% survival at -8 °C) in 0 day and 42 day cold treated crowns with five different antibodies applied: XERO2, ADH, β-1,3-glucanase, Thaumatin, and HSC70. There were 64 samples in the freezing tolerant group while 31 samples were in the freezing intolerant group. Error bars represent standard deviation. Asterisks denote statistically significant t-tests where $P \leq 0.05$.

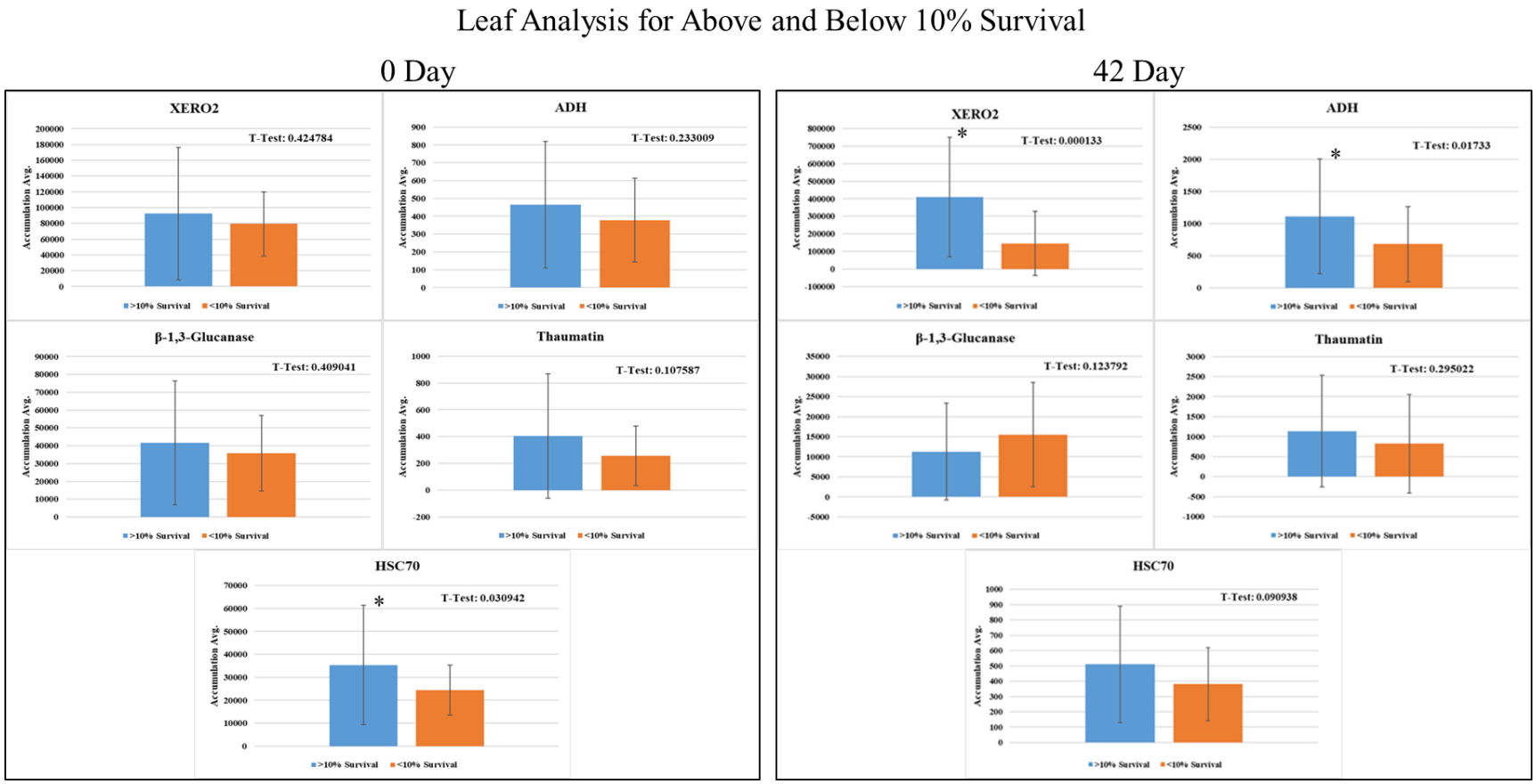


Figure 12. Levels of potential biomarkers in freezing intolerant and freezing tolerant offspring of Jonsok & Elsanta: Leaves

**Figure 12 Legend.** Samples were analyzed for their fluorescence intensity average in a freezing tolerant group (> 10% survival at -8 °C) and a freezing intolerant group (< 10% survival at -8 °C) in 0 day and 42 day cold treated crowns with five different antibodies applied: XERO2, ADH, β-1,3-glucanase, Thaumatin, and HSC70. There were 64 samples in the freezing tolerant group while 31 samples were in the freezing intolerant group. Error bars represent standard deviation. Asterisks denote statistically significant t-tests where $P \leq 0.05$.

## 3.2 Analysis of diploid strawberry mRNA and protein levels for two dehydrins, XERO2 and COR47

Three diploid strains were selected for their differences in cold tolerance to be evaluated at different timepoints in the cold for two specific dehydrins' transcript and protein accumulation. Alta is a very cold tolerant line, while NCGR1363 and FDP817 are much less cold tolerant. Transcript and protein work with the dehydrins XERO2 and COR47 in crown and leaf tissue in these diploid varieties were evaluated at nine different timepoints from 0 hours to 42 days in the cold (plant material was prepared by our collaborators, Jahn Davik and Anne Langerud in Norway). Initially, lane smearing was apparent in the blots of many Alta samples where the area above the major band had high signal (Figure 13). The possibility that the dehydrin (COR47) was forming aggregates resulting in streaking was tested by introducing 8 M Urea into the samples. All of the Alta crowns electrophoresed in the presence of 8M urea show much clearer bands from COR47 and little smearing in the upper part of the lane (Figure 13). Quantitation of the bands led to higher confidence in the identity of the protein being quantified. The overall trends in the data were not drastically changed which suggests that the signal above the band was due to aggregation of COR47.

Diploids were tested by RT-qPCR and western blots to estimate transcript and protein levels. XERO2 expression (obtained by Nelson Osuagwu) in all genotypes, both crowns and leaves, shows a clear peak of accumulated RNA transcripts at 48 hours, is typical for early transcript accumulation based on Arabidopsis RNA time courses following cold (Kreps et al. 2002). In all diploids an increase in RNA leads to an increase, after a lag, in protein. The expression of XERO2 transcript is increasing at later timepoints in the cold with accumulation at 48 hours and 7 days and greatest accumulation at 42 days (Figure 14). The changes in Alta protein are much greater than NCGR1363 and FDP817 protein, which have less XERO2 induction.

The expression profile of COR47 was more complex. For the transcripts, there is a distinct 48 hour peak similar to what we see with XERO2. The accumulation of COR47 protein in Alta genotype seems to increase immediately at early timepoints between one and eight hours in the cold, before sharply increasing again after seven days in the cold (Figure 15). In NCGR1363 crowns, Alta leaves, and FDP817 leaves there is a weak response of protein accumulation, even in the timepoints after the 48 hour transcript spike of RNA. In FDP817 crowns, there is an

increase in protein from 48 hours to seven days, following the increase of transcripts at 24 and 48 hours.

Interestingly, and particularly with the Alta genotype, an increase in protein is seen without a previous increase in transcripts. This is most notable at early timepoints of one to eight hours in Alta crown and NCGR1363 leaves and at later timepoints in the Alta crowns between seven and 14 days. Since this observed discrepancy is mostly seen in the crown of the most cold tolerant line, it raises the question of whether this regulation resulting in rapid increase in protein levels could contribute to this variety being better able to withstand cold stress. Therefore, identification of the basis for this phenomenon would be of value in understanding the regulation of this dehydrin's expression.

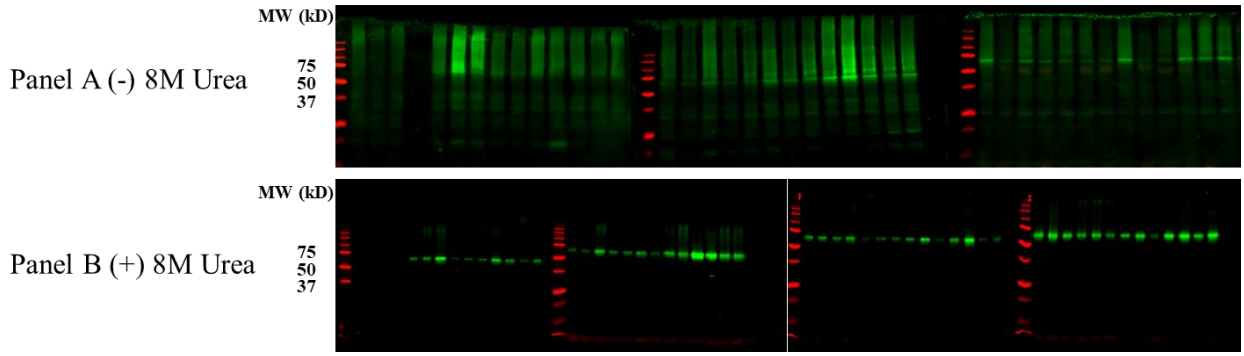


Figure 13. Optimization of COR47 resolution on SDS-PAGE

**Figure 13 Legend.** Panel A. Western blot image showing lane smearing in the upper part of the lane. COR47 was used as the primary antibody. Panel B: Western blot image showing protein samples treated with 8 M urea and COR47 primary antibody applied. The 8M urea alleviated the issue of smearing in the upper part of the bands.

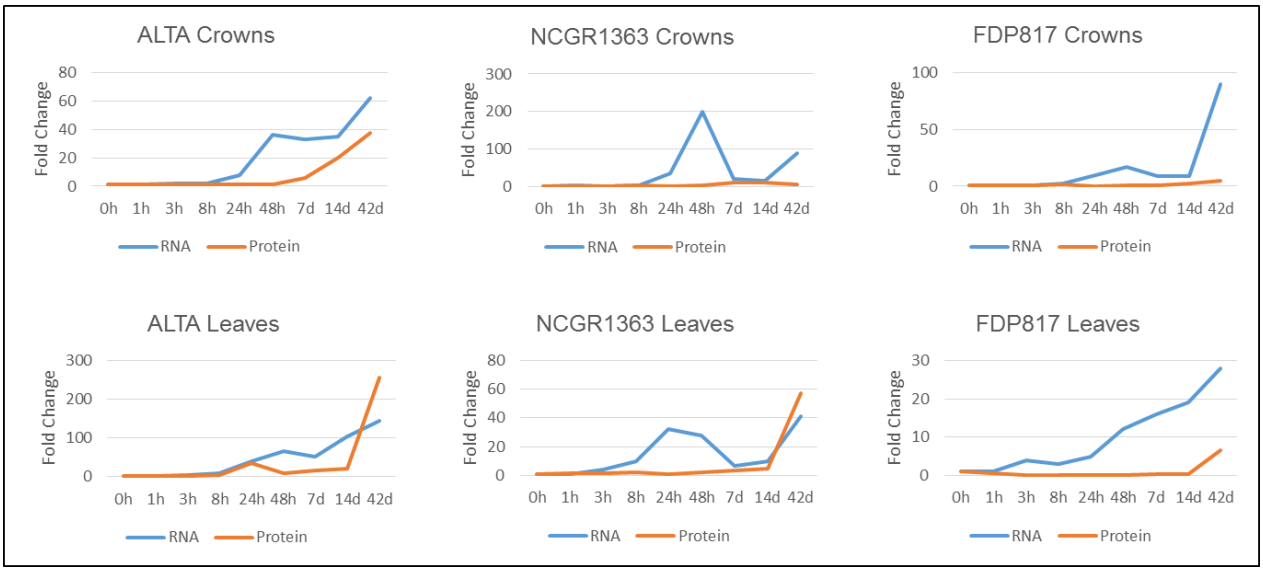


Figure 14. XERO2 transcript and protein levels in response to cold in diploids

**Figure 14 Legend.** RNA and protein fold change of XERO2 from Alta, NCGR1363, and FDP817 varieties. Plants were grown and triplicate samples (n = 3) were taken at eight timepoints throughout a 42 day exposure to the cold and evaluated in single technical replicates. Ten micrograms of protein from leaves and crowns were probed with XERO2 primary antibody and visualized with Alexa Fluor 790 donkey anti-rabbit secondary antibody using the Odyssey Imager. XERO2 transcript and protein data was obtained by a collaborator (Osuagwu 2014).

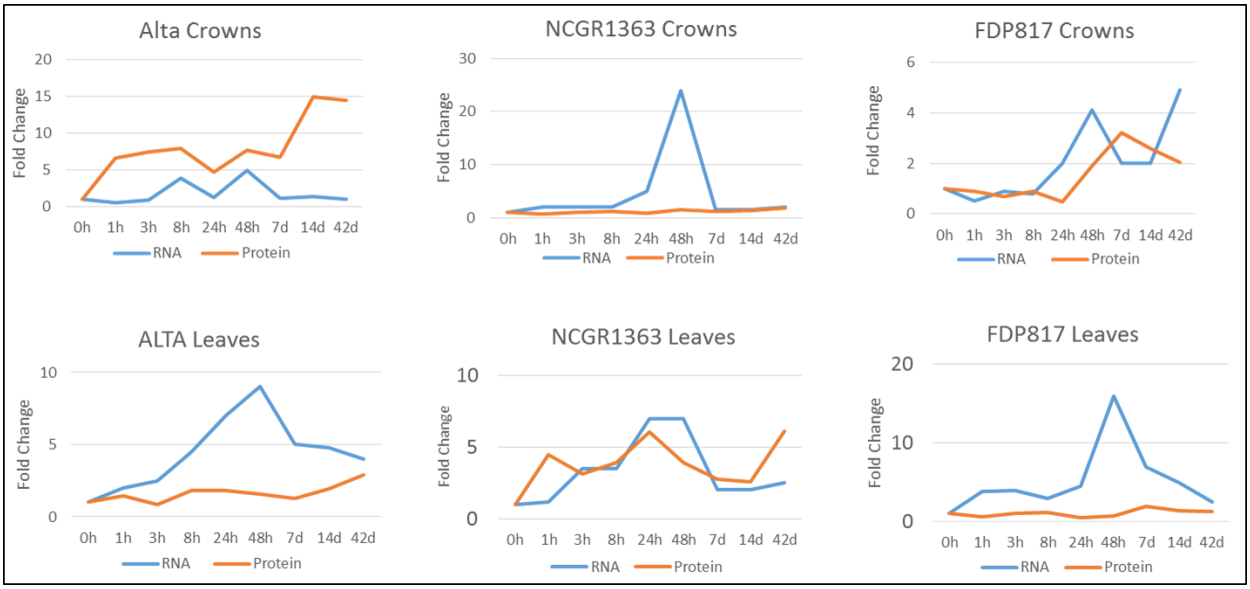


Figure 15. COR47 transcript and protein levels in response to cold in diploids

**Figure 15 Legend.** RNA and protein fold change of COR47 from Alta, NCGR1363, and FDP817 varieties. Plants were grown and triplicate samples (n = 3) were taken at eight timepoints throughout a 42 day exposure to the cold and evaluated in single technical replicates. Ten micrograms of protein from leaves and crowns were probed with COR47 primary antibody and visualized with Alexa Fluor 790 donkey anti-rabbit secondary antibody using the Odyssey Imager. COR47 transcript data was obtained by a collaborator (Osuagwu 2014).

## 3.3 Preliminary Investigation of the Level of Regulation of the COR47 gene in the diploid genotype, Alta

### 3.3.1 Sequence analysis of the two COR47-related genes

RNA-sequencing, nucleotide alignments and database searches (Phytozome & NCBI) led to the conclusion that COR47 in diploid strawberry is coded by two distinct isoforms, which we have described as COR47-like_A and COR47-like_B. COR47_A is predicted to be 179 amino acids with a mass of 19.98 kD, which is about 100 amino acids smaller than COR47_B. COR47_B is predicted to be 276 aa with a mass of 32.18 kD (Figure 16). A ClustalW alignment with wild type Arabidopsis COR47 against the diploid COR47-like_A and COR47-like_B fragment sequence translations is shown (Figures 17 & 18). Each of them shows a moderate amount of similarity yet when COR47-like_A and COR47-like_B are aligned against one another it is observed that they are sufficiently different from one another to be considered different forms of the same gene (Figure 19). Although dehydrins run anonymously high, it is likely that the COR47-like_A protein would run at a lower apparent molecular mass than the COR47_B protein, and that band would not have been included in the previous COR47 accumulation estimations (Figure 20). Since COR47-like_B version was identified by mass spectrometry (Isam Fattash et al, unpublished) from the band at 60-70 kD and found to be the only dehydrin present in that band, it was the major gene whose transcript and corresponding protein that were quantitated in previous experiments (Osuagwu 2014). Since COR47 runs aberrantly on a gel, it is a formal (but unlikely) possibility that COR47_A could be co-migrating with COR47_B and contributing to total protein accumulation of COR47. This might explain why the mRNA and protein data do not always agree because previously we were only examining one of multiple contributions to the COR47 protein. The transcripts between the two COR47s are sufficiently different from one another so that a primer designed specifically for COR47_B would not amplify COR47_A transcripts, and therefore would not be included in total COR47 transcript quantitation. The primers used in the previous experiments for RT-qPCR to quantitate transcripts of COR47 are only found in the COR47-like_B gene.

RNA-SEQ analysis of octoploid strawberry revealed six unique sequences for COR47 (Randall, Alsheikh, Wilson, Fattash, *et al*, unpublished). After translating their sequences, the six fragments were analyzed for relationship to one another and then compared to the diploid COR47-like_A and COR47-like_B. All sequences were identified as being most related to either

COR47_A or COR47_B. The phylogenetic tree shows a grouping of the six fragments into three pairs (Figure 21). The g1 pair are quite similar to COR47-like_A (Figure 22) while the g2 and g3 pairs are much more similar to COR47-like_B (Figures 23 & 24). The g3 pair are more similar to the N-terminus of the COR47-like_B sequence (Figure 23) while the g2 pair are more similar to the C-terminus of the COR47-like_B sequence (Figure 24). Transcript abundance over a time course in the cold with these octoploid transcripts shows that the sequences closely related to COR47_A do not change up to 48 hours but drop dramatically at 240 hours (Figure 25). The COR47_B transcripts show increased fold change at 48 hours of cold (Figure 25).

### 3.3.2 Sequencing Analysis of COR47_B in Alta, NCGR1363, FDP817

While examining the possibility that multiple transcripts of the same gene or alternative splicing were contributing factors to the discrepancy between transcripts and protein in Alta crown for COR47, it was noticed that the sequences for COR47 were slightly different between NCBI and phytozome databases. In NCBI there were two nucleotides missing in the COR47_B sequence that were present in the phytozome sequence (Figure 26). Translation of these two sequences gave two distinctly different proteins. The NCBI protein was 276 aas while the phytozome protein was 129 aa (Figure 27). The presence of the two nucleotides caused a premature stop codon leading to a truncated protein that did not contain a K-segment. Without the two nucleotides, the predicted protein follows the expected size and motifs known for COR47_B. However, the predicted mRNA sequence in NCBI is from the distinct diploid genotype (Hawaii IV), and therefore may have a slightly different sequence than in the varieties used in this study.

A new primer called COR47_B_Full, was designed to encompass a large portion of the COR47_B gene (748 bp) over the region containing the two nucleotide discrepancy, as well as covering the putative splice site. The COR47_B_Full primer generated a single band at the proper size from Alta, NCGR1363, and FDP817 DNA (Figure 28). The band was cut out, gel purified, and sent for sequencing. Sequencing was done for three reasons. The first was to check the similarity of the sequence to the predicted reference sequence in NCBI. The second was to check the predicted conserved splice site for the intron, to ensure that there was only one splice site and no other areas for alternative splicing. The third reason was to determine the true sequence for our varieties and see if the two nucleotide difference was present or absent in our

purified samples. Results from this would clarify the sequence of our genotypes' COR47_B gene.

A forward and reverse sequence were returned for each diploid variety. The sequences were aligned against one another and the corresponding chromatograms were used to clarify nucleotides not identified and potential sequencing errors. Sequences were then aligned against the NCBI database gDNA and mRNA sequences. In all 6 sequences, the two nucleotide sequence was present, thus giving us confidence that these two nucleotides were actually present. This however did not entirely resolve the issue because the translated database sequence with the two nucleotides included produces the truncated 129 aa protein. Upon further investigation it was found that a run of 8 As near the two nucleotide sequence was present in the sequenced Alta, NCGR1363, and FDP817 transcripts. In the database sequences (NCBI, Phytozome) there were only 7 As (Figure 29). When we translated our sequences with these three nucleotides in the correct spot, the resulting protein was nearly identical to the translated NCBI protein, except for two different amino acids, one being where the two nucleotides were present changing an arginine into a glutamic acid. The other amino acid was simply an additional lysine where the extra A was located. From these findings I concluded that the NCBI predicted mRNA sequence for COR47_B is incorrect and is missing three nucleotides. Two of them were present in the genomic DNA in NCBI and phytozome, but presumably due to curation, were not included in the predicted mRNA in NCBI. The third nucleotide was undetected by all of the reference sequences, which would have been a crucial factor in producing the correct protein with the other two nucleotides present or not. When the NCBI predicted mRNA sequence with the three nucleotides included is translated, a 277 amino acid protein results and its alignment is completely identical with sequenced data from Alta and NCGR COR47_B (Figure 30).

### 3.3.3 RT-qPCR quantitation and analysis

To determine if alternative splicing or accumulation of an additional transcript (i.e. COR47_A) could be contributing to the difference in mRNA and resulting protein in Alta responses to cold treatment, RT-qPCR was performed. While it seems unlikely that this would explain the discordance as the COR47_A and COR47_B predicted proteins are much different in mass and sequence, multiple primers were utilized to rule out this option.

Three biological replicates per timepoint were utilized, resulting in 27 samples total. The RT-qPCR used four different primers COR47_B, COR47_B_Intron, COR47_A, and PP2A. PP2A was used to normalize samples (Rob Wilson, personal communication). The primer design for COR47_B had the reverse primer split between the second exon and the first, so a 132 bp product would not be made if the intron was retained. The COR47_B_Intron primer was designed to be on the outside of the intron, so two distinct sized products would result depending on if the intron was being retained or not having 397 or 239 bp products, respectively (Figure 31). The COR47_A primer was designed the same way as B to have an 81 bp product, but from preliminary RT-qPCR data, the COR47_A transcript is hardly detectable near 38 cycles and at times undetectable under standard conditions (Figure 32). The COR47_B transcript is detected below 25 cycles at all timepoints, thus total levels of COR47_B would likely be several orders of magnitude greater than COR47_A, making the contribution of COR47_A to the whole gene accumulation insignificant (Figure 32). RT-PCR was utilized to confirm primers qualitatively before doing qRT-PCR for a quantitative analysis on these samples and it was found that all the primers were producing one band of predicted size (Figures 33 & 34).

The newly generated diploid Alta transcript data was compared to the previous results (Osuagwu 2014) and with the protein data (Deitch, unpublished). The intention was to either confirm that the RNA and protein are indeed not in agreement, or the new data will fall in line with the protein work, showing that another replicate of data was necessary to confirm results. The new results from the Alta transcript work show that COR47_B transcripts are increasing at 48 hours and again at 14 day and 42 days in the cold. This is similar to previous results generated except a strong increase in transcript at 8 hours was not seen. There is little change at early timepoints, with slight transcript decrease at 1 – 3 hours compared to 0 hour until the transcripts rise dramatically to under 4 fold change at 48 hours. The transcripts drop after this until 7 days but then rise after that at 14 and 42 days (Figure 35). Note that these samples are from the endpoint of RT-qPCR where accumulations are saturated, therefore they cannot quantitatively be compared. These results still do not explain the large increase in protein accumulation at the early timepoints in the cold, but the trends of the transcript more closely match what is going on at the later timepoints.

The COR47-like_B qPCR products were run out on an 8% polyacrylamide gel to check for alternative splicing products at various timepoints in the cold. One sample from each timepoint

was loaded into the wells. The results from running this gel showed that bands at 148 bp (spliced product) were found for every timepoint and only one band was found for each sample (Figure 36). This suggests that alternative splicing is not occurring during the cold exposure treatment. But if there was alternative splicing happening where the intron was not being spliced out, there would be no observed product because the reverse primer is split across the intron. Therefore, we cannot be completely certain that there are no alternative spliced products because these products would not be made (or be detectable) based on the primer design.

To resolve this possibility, the COR47_B_Intron primer was utilized because it would make two different sized products based on intron retention or splicing. If the intron was being retained the expected size of the band was 397 bp while if the intron was being spliced out, a band is expected at 239 bp. An initial RT-PCR product was run on a gel and shows a band near 240 bp (Figure 34). There is a possibility that alternative splicing could occur at different timepoints so RT-qPCR products of COR47_B_Intron were separated on a 1% agarose gel with one sample from each timepoint to get an additional qualitative result (Figure 37). The gel shows one strong band around 240 bp is consistent with the intron being properly spliced out and alternative splicing via intron retention is not occurring in the COR47_B gene.

When the COR47_B protein is translated with the intron present, the protein hits multiple stop codons less than 50 nucleotides into the intron. This would imply that if intron retention were occurring it would create a truncated protein of a much smaller size than expected. But to further characterize the conclusion that mechanisms of alternative splicing are not occurring, RT-qPCR products of COR47_B_Intron primer were purified at 4 critical timepoints, 0 hr, 3 hr, 48 hr, and 7 day and sent for sequencing. These samples are crucial time points where either the transcript or protein are differing greatly from one another and confirmation of conserved splice sites occurring at different time points in the cold was necessary. Our hypothesis was that sequencing the splicing region of the intron would confirm a lack of alternative splicing happening during the transcription of the mRNA. From the sequencing results, it was found that alternative splicing of the intron was not observed and no alternative 3’ or 5’ splice sites were identified. The splice sites in all of the samples were in the same location and 100% conserved (data not shown). These results further confirm that the COR47_B protein is not being alternatively spliced and that posttranscriptional and post-RNA splicing mechanisms are likely to be regulating expression of the gene.

For COR47_A, the levels were too low to get quantitation of samples and it was concluded that there was likely no significant contribution of this isoform to total transcript counts.

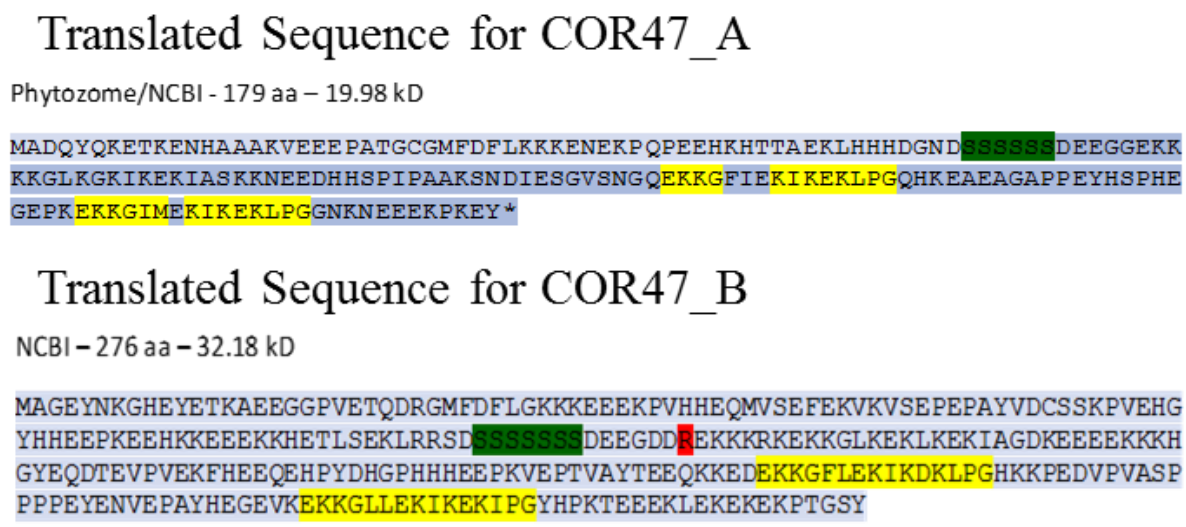


Figure 16. Translated Sequences for COR47_A and COR47_B

**Figure 16 Legend.** Translated sequences for the two isoforms of the COR47 gene. The top sequence is COR47_A which is 179 amino acids and has a predicted mass of 19.98 kD. The bottom sequence is COR47_B which is 276 amino acids and has a predicted mass of 32.18 kD. The highlighted green regions are S-segments, the highlighted yellow regions are K-segments, and the highlighted red amino acid is a sequencing discrepancy that was investigated.

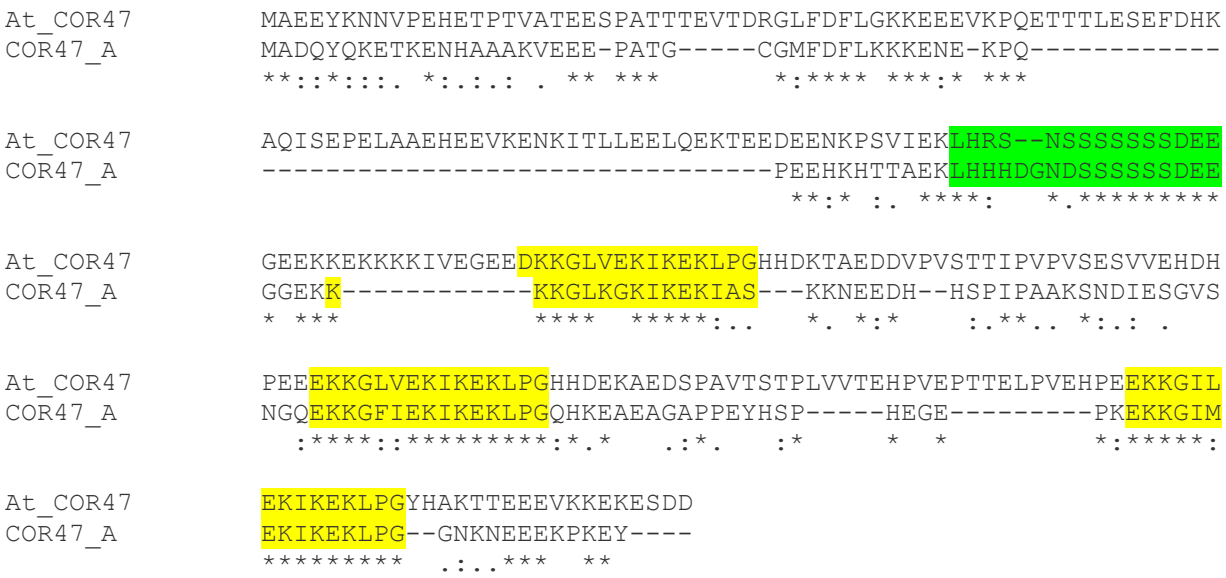


Figure 17. Sequence Alignment with Arabidopsis COR47 and *Fragaria vesca* COR47_A

**Figure 17 Legend.** Amino acid sequence alignment of Arabidopsis COR47 and diploid *Fragaria vesca* COR47-like_A translation (Performed with Clustal version 2.0.12). Green highlighted areas show S-segments, while yellow highlighted areas show K-segments. The most conserved areas in the alignments fall within these regions.

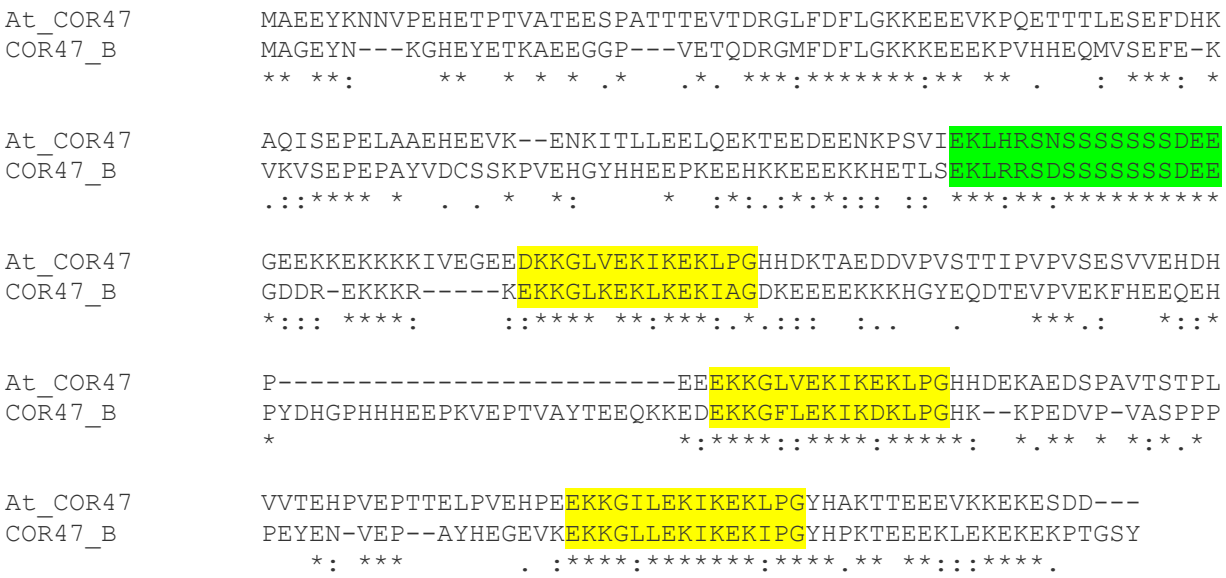


Figure 18. Sequence Alignment with Arabidopsis COR47 and *Fragaria vesca* COR47_B

**Figure 18 Legend.** Amino acid sequence alignment of Arabidopsis COR47 and diploid *Fragaria vesca* COR47-like_B translation (Performed with Clustal version 2.0.12). Green highlighted areas show S-segments, while yellow highlighted areas show K-segments. The most conserved areas in the alignments fall within these regions.

```
COR47-like_A_Translation    MADQYQKETKENHAAAKVEEEPATGCGMFDFL-KKKENEKPQPEEHKHTT
COR47-like_B_Translation    MAGEYNKGHEYETKAEEGGPVETQDRGMFDFLGKKKEEEKPVHHEQMVSE
                            **.:*:*  : :  * :     : . ****** ****:***  .*:  :

COR47-like_A_Translation    AEKL--------------------HHHD----------------------
COR47-like_B_Translation    FEKVKVSEPEPAYVDCSSKPVEHGYHHEEPKEEHKKEEEKKHETLSEKLR
                             **:                    :**:

COR47-like_A_Translation    -GNDSSSSSSDEEGGE------KKKKGLKGKIKEKIASKKNEED------
COR47-like_B_Translation    RSDSSSSSSSDEEGDDREKKKRKEKKGLKEKLKEKIAGDKEEEEKKKHGY
                             .:.**********.:      *:***** *:*****..*:**:

COR47-like_A_Translation    -HHSPIPAAKSND-----------------IESGVSNGQE------KKGF
COR47-like_B_Translation    EQDTEVPVEKFHEEQEHPYDHGPHHHEEPKVEPTVAYTEEQKKEDEKKGF
                             :.: :*. * ::                 :*. *:  :*      ****

COR47-like_A_Translation    IEKIKEKLPGQHK----EAEAGAPPEYH----SPHEGEPKEKKGIMEKIK
COR47-like_B_Translation    LEKIKDKLPGHKKPEDVPVASPPPPEYENVEPAYHEGEVKEKKGLLEKIK
                            :****:****::*     . : .****.    : **** *****::****

COR47-like_A_Translation    EKLPGGN-KNEEE---KPKE-----Y
COR47-like_B_Translation    EKIPGYHPKTEEEKLEKEKEKPTGSY
                            **:** : *.***   * **     *
```

Figure 19. Sequence Alignment with *Fragaria vesca* COR47_A and COR47_B

**Figure 19 Legend.** Amino acid sequence alignment of diploid *Fragaria vesca* COR47-like_A and COR47-like_B translations (Performed with Clustal version 2.0.12). Green highlighted areas show S-segments, while yellow highlighted areas show K-segments. The most conserved areas in the alignments fall within these regions. The two sequences are different enough to be considered different forms of the same gene.

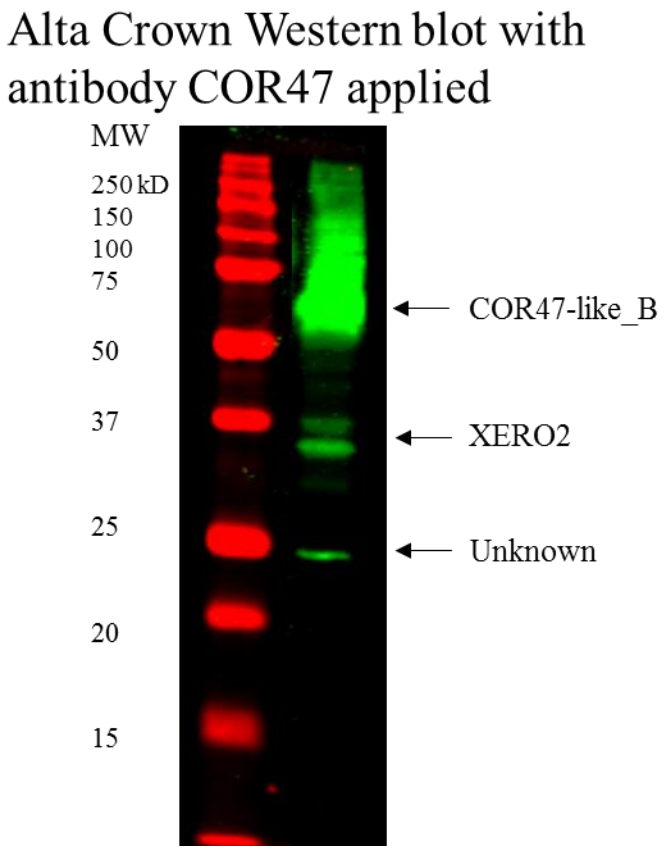


Figure 20. Multiple bands produced from COR47 antibody

**Figure 20 Legend.** Western blot probed with anti-COR47 (with gain turned up) shows additional minor bands present in Alta crown extracts. Gel run in the absence of 8M Urea so clear smearing in the upper part of the lane is present. The presence of unidentified protein band (possibly COR47_A-like) is indicated.

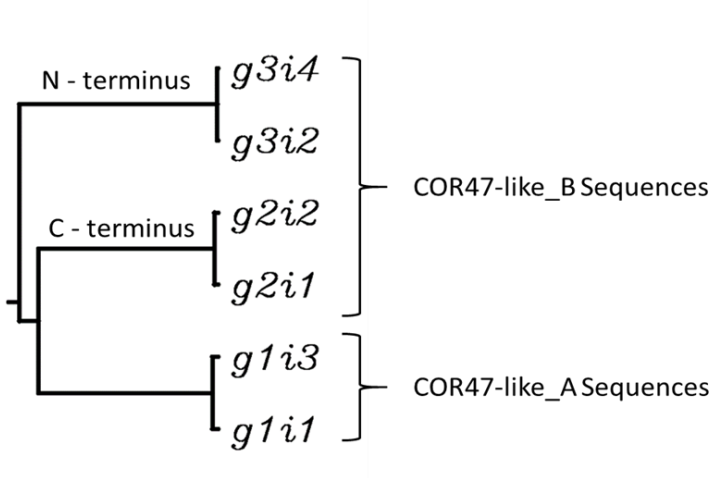


Figure 21. Phylogenetic tree of octoploid COR47 transcripts

**Figure 21 Legend.** Phylogenetic tree of relatedness between the octoploid COR47 transcript (all) sequences translated into amino acid sequences. Sequences were obtained from a RNA-SEQ experiment examining all COR47 sequences obtained from a 0 – 10 day cold treatment. The g1s are quite similar to COR47-like_A (Figure 28), while the g2s and g3s are much more similar to COR47-like_B. The g3s are more similar to the N-terminus of the COR47-like_B sequence (Figure 29) while the g2s are more similar to the C-terminus of the COR47_like_B sequence (Figure 30).

```
g1i3                        TITQSIIKSLISNHILLFKAFFLCSLSTSTMADQYQKETKENHAAAKVEE
COR47-like_A_Translation    ------------------------------MADQYQKETKENHAAAKVEE
                                                          ********************

g1i3                        EPATGCGMFDFLKKKENEKPQPEEQKHTLAEKLHHHDGNDSSSSSSDEEG
COR47-like_A_Translation    EPATGCGMFDFLKKKENEKPQPEEHKHTTAEKLHHHDGNDSSSSSSDEEG
                            ************************:*** ********************

g1i3                        GEKKKKGLKGKIKEKIASKKNEEDHHAPIP--KSNDIQSGVSNGEEKKGF
COR47-like_A_Translation    GEKKKKGLKGKIKEKIASKKNEEDHHSPIPAAKSNDIESGVSNGQEKKGF
                            ***************************:***  *****:******:*****

g1i3                        IEKIKDKLPGQHKEAEAGAPPQNHAPHEGEPKEKKGIMEKIKEKLPGGNK
COR47-like_A_Translation    IEKIKEKLPGQHKEAEAGAPPEYHSPHEGEPKEKKGIMEKIKEKLPGGNK
                            *****:***************: *:*************************

g1i3                        NEEKKPKEY
COR47-like_A_Translation    NEEEKPKEY
                            ***:*****
```

Figure 22. Sequence Alignment with octoploid g1i3 COR47 translation and *Fragaria vesca* COR47-like_A

**Figure 22 Legend.** Amino acid sequence alignment of octoploid g1i3 COR47 translation and diploid *Fragaria vesca* COR47-like_A translation (Performed with Clustal version 2.0.12). The two sequences are almost identical to one another.

```
g3i2                          ------------RVRESQGSGEPQ-----------PPSPPPVHHEQEEVM
COR47-like_B_Translation      MAGEYNKGHEYETKAEEGGPVETQDRGMFDFLGKKKEEEKPVHHEQ---M
                                          *. *. *.*             .  ******   *

g3i2                          ASEFEKVKVSEPEPAYVDCSSKPAEHGYHHEEPKEEHK--EEKKHETLSE
COR47-like_B_Translation      VSEFEKVKVSEPEPAYVDCSSKPVEHGYHHEEPKEEHKKEEEKKHETLSE
                              .**********************.**************  **********

g3i2                          KLRRSDSSSSSSSDEEGDDEEKKKKRKEKKGLKEKIKEKISGDKEEEEKK
COR47-like_B_Translation      KLRRSDSSSSSSSDEEGDDREKKK-RKEKKGLKEKLKEKIAGDKEEEEKK
                              ******************.**** **********:****:*********

g3i2                          KHGYEQX-------------------------------------------
COR47-like_B_Translation      KHGYEQDTEVPVEKFHEEQEHPYDHGPHHHEEPKVEPTVAYTEEQKKEDE
                              ******

g3i2                          ------------------------------------------------
COR47-like_B_Translation      KKGFLEKIKDKLPGHKKPEDVPVASPPPPEYENVEPAYHEGEVKEKKGLL


g3i2                          -------------------------------
COR47-like_B_Translation      EKIKEKIPGYHPKTEEEKLEKEKEKPTGSY
```

Figure 23. Sequence Alignment with octoploid g3i2 COR47 translation and *Fragaria vesca* COR47-like_B

**Figure 23 Legend.** Amino acid sequence alignment of octoploid g3i2 COR47 translation and diploid *Fragaria vesca* COR47-like_B translation (Performed with Clustal version 2.0.12). The g3 sequences align closely with the amino-terminus of the COR47-like_B sequence.

```
g2i1                          --------------------------------------------------
COR47-like_B_Translation      MAGEYNKGHEYETKAEEGGPVETQDRGMFDFLGKKKEEEKPVHHEQMVSE

g2i1                          --------------------------------------------------
COR47-like_B_Translation      FEKVKVSEPEPAYVDCSSKPVEHGYHHEEPKEEHKKEEEKKHETLSEKLR

g2i1                          ---------SDEEGDDEEKKKKRKEKKGLKEKIKEKISGDKEEEEKKKHG
COR47-like_B_Translation      RSDSSSSSSSDEEGDDREKKK-RKEKKGLKEKLKEKIAGDKEEEEKKKHG
                                      *******.**** **********:****:************

g2i1                          YEQDTEVPVEKFHEEHERPYDHGPVVHHHEEPKVEPTVAYTEEEKKEEEK
COR47-like_B_Translation      YEQDTEVPVEKFHEEQEHPYDHGP--HHHEEPKVEPTVAYTEEQKKEDEK
                              ***************:*:******  *****************:***:**

g2i1                          KGFLEKIKDKLPGHKKPEDVPVASPSPPEYEKVEPAYHEGEVKEKKGLLE
COR47-like_B_Translation      KGFLEKIKDKLPGHKKPEDVPVASPPPPEYENVEPAYHEGEVKEKKGLLE
                              *************************.*****:******************

g2i1                          KIKEKIPGYHPKTEEEKLEKEKEKPTGSY
COR47-like_B_Translation      KIKEKIPGYHPKTEEEKLEKEKEKPTGSY
                              ****************************
```

Figure 24. Sequence Alignment with octoploid g2i1 COR47 translation and *Fragaria vesca* COR47-like_B

**Figure 24 Legend.** Amino acid sequence alignment of octoploid g2i1 translation and diploid *Fragaria vesca* COR47-like_B translation (Performed with Clustal version 2.0.12). The g2 sequences align closely with the carboxyl-terminus of the COR47-like_B sequence.

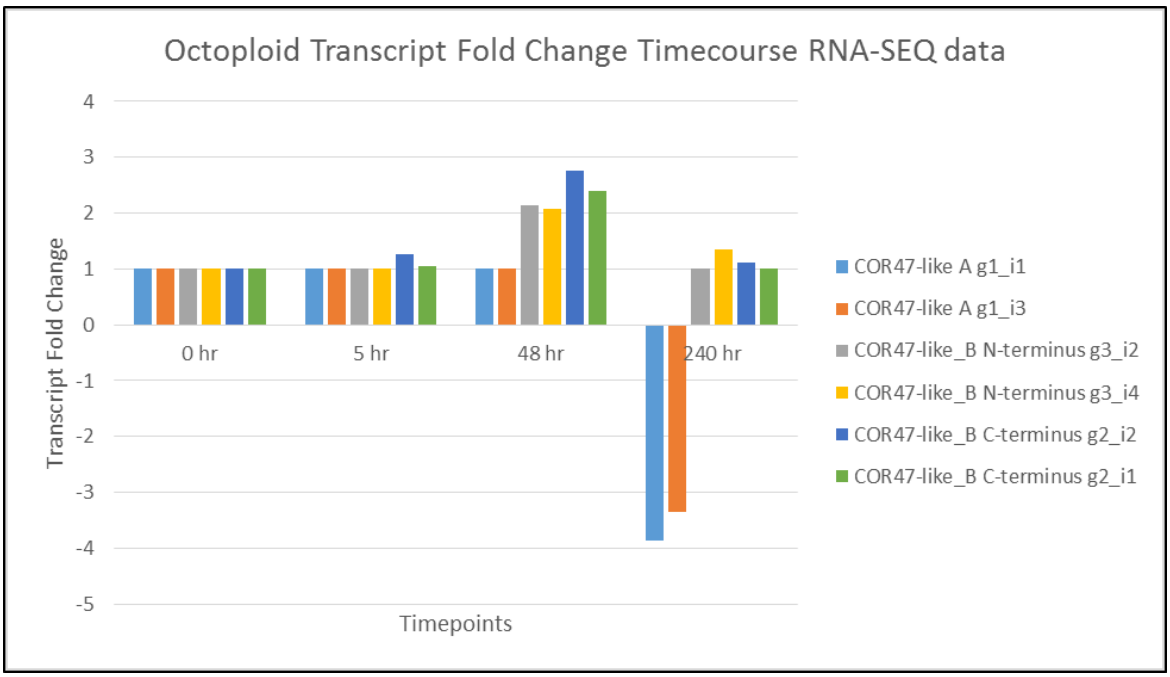


Figure 25. Octoploid COR47 transcript levels

**Figure 25 Legend.** Octoploid COR47 transcript levels over a 240 hour cold treatment analyzed from RNA-SEQ data (Ahmad *et al*. unpublished). All data is expressed as fold change compared to the 0 hour time point.

COR47_B coding sequence

ATGGCGGGTGAGTACAACAAAGGCCACGAGTACGAGACCAAGGCCGAGGAGGGCGGTCCAGTTGAGACCCAAGA
TCGTGGGATGTTTGATTTCTTGGGGAAGAAGAAGGAGGAGGAGAAGCCTGTTCATCATGAACAGATGGTCAGCG
AGTTCGAGAAAGTCAAGGTGTCTGAGCCTGAGCCAGCTTATGTAGACTGCAGCAGCAAACCTGTTGAGCATGGC
TATCATCACGAGGAACCTAAGGAGGAACATAAGAAGGAGGAGGAGAAGAAGCATGAAACTCTCTCCGAGAAGCT
TCGCCGATCCGACAGCAGCTCCAGCTCGGTAAGTCGATCACCTCTTACTACAATGATACGTTTCAATTGAACTA
CTTAACCAACCAGTTCACTGCTACCTACTACTATAGTGATCTTTCTTAAACGCATTGTGTTTCATGATTAATAT
GTTTGACTAATAATATATTGGACGATGAATTTGCAGTCAAGTGACGAGGAAGGAGACGATGAAGAGAAAAAAAG
AAGAGGAAGGAGAAGAAGGGACTGA

Figure 26. Nucleotide Sequence Discrepancy between Databases

**Figure 26 Legend.** Part of the COR47_B coding sequence showing a two nucleotide difference between databases. Highlighted blue regions are the two exons, while the un-highlighted region is the intron, and the highlighted red region is the two nucleotide discrepancy. In phytozome and NCBI both genomic sequences contain the GA, but in the mRNA sequence, phytozome contains the GA while NCBI does not, leading to two quite different predicted proteins.

NCBI

MAGEYNKGHEYETKAEEGGPVETQDRGMFDFLGKKKEEEKPVHHEQMVSEFEKVKVSEPEPAYVDCSSKPVEHG
YHHEEPKEEHKKEEEKKHETLSEKLRRSDSSSSSSSDEEGDDREKKKRKEKKGLKEKLKEKIAGDKEEEEKKKH
GYEQDTEVPVEKFHEEQEHPYDHGPHHHEEPKVEPTVAYTEEQKKEDEKKGFLEKIKDKLPGHKKPEDVPVASP
PPPEYENVEPAYHEGEVKEKKGLLEKIKEKIPGYHPKTEEEKLEKEKEKPTGSY

Phytozome – No K-segment

MAGEYNKGHEYETKAEEGGPVETQDRGMFDFLGKKKEEEKPVHHEQMVSEFEKVKVSEPEPAYVDCSSKPVEHG
YHHEEPKEEHKKEEEKKHETLSEKLRRSDSSSSSSSDEEGDDEEKKRRGRRRRD*

Figure 27. Database sequences translate into different sized products

**Figure 27 Legend.** Translated sequences of COR47_B from two different databases, NCBI and Phytozome. Green highlighted regions represent S-segments. Yellow highlighted regions represent K-segments. Red highlighted regions show the amino acid where the two nucleotide difference is, causing the translated protein to be quite different.

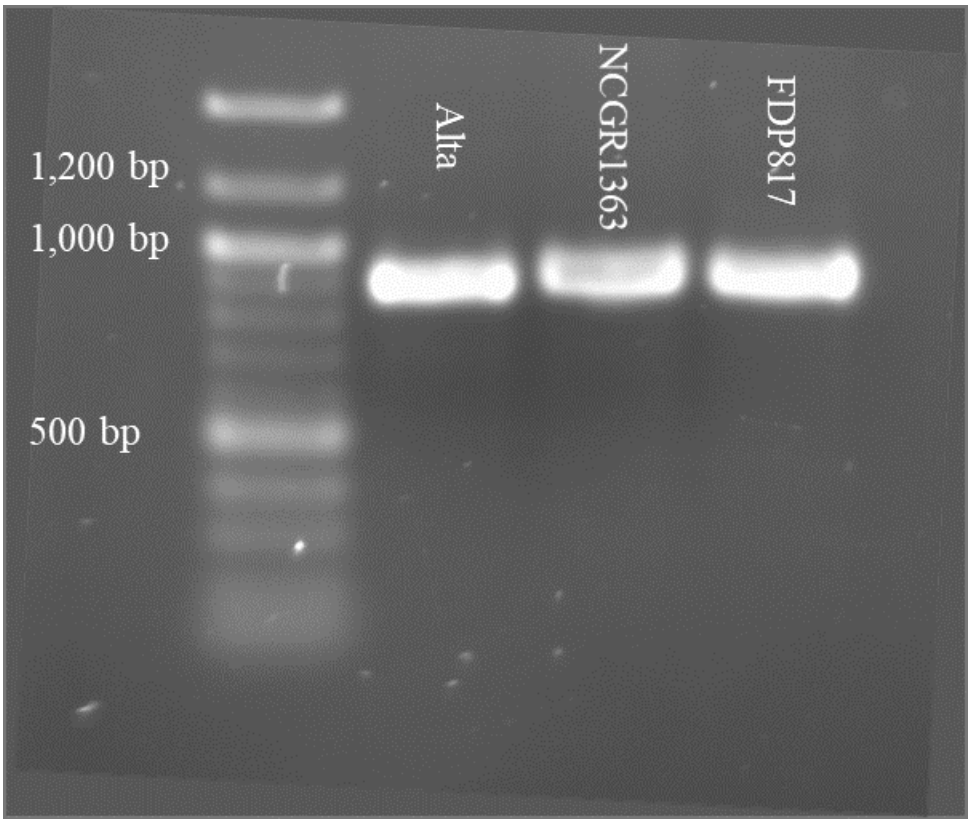


Figure 28. PCR of COR47 from Genomic DNA

**Figure 28 Legend.** DNA was purified from leaf samples of Alta, NCGR1363, and FDP817 and PCR was performed using the COR47_B_Full primer. Bands of expected size were cut-out from a 1% agarose gel and further purified before being run again on a 1% agarose gel to confirm the purity of the products. NEB 100 bp standards were used to determine the size of the bands.

Nucleotide alignment from second exon

```
Hawaii_gDNA       GGAGACGATGAAGAGAAAAAAA-GAAGAGGAAGGAGAAGAAGGGACTGAAGGAGAAGCTC
Hawaii_mRNA       GGAGACGAT--AGAGAAAAAAA-GAAGAGGAAGGAGAAGAAGGGACTGAAGGAGAAGCTC
Alta_Forward      GGAGACGATGAAGAGAAAAAAAAGAAGAGGAAGGAGAAGAAGGGACTGAAGGAGAAGCTC
                  *********  *********** ************************************
```

Figure 29. COR47 sequences of Alta genotype suggests curation errors in NCBI database

**Figure 29 Legend.** Nucleotides alignment with genomic DNA and mRNA sequences from NCBI diploid Hawaii 4 compared with returned sequencing data in Alta COR47_B. NCGR and FDP sequences were 100% identical to the shown Alta_Forward sequence.

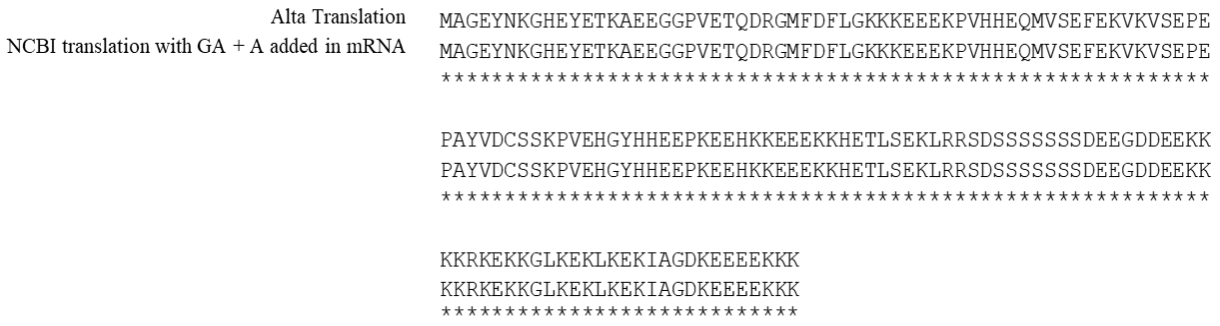


Figure 30. Translated Sequence Alignment with Alta and NCBI mRNA with added nucleotides for COR47_B Sequencing Results

**Figure 30 Legend.** Translated sequence alignment between Alta COR47_B and NCBI database COR47_B mRNA containing three nucleotides, GA and A, that are omitted from the published sequence. The alignment is identical with the returned Alta sequencing results and NCBI with three added nucleotides. With this sequence the predicted size of the COR47_B protein would be 277 amino acids.

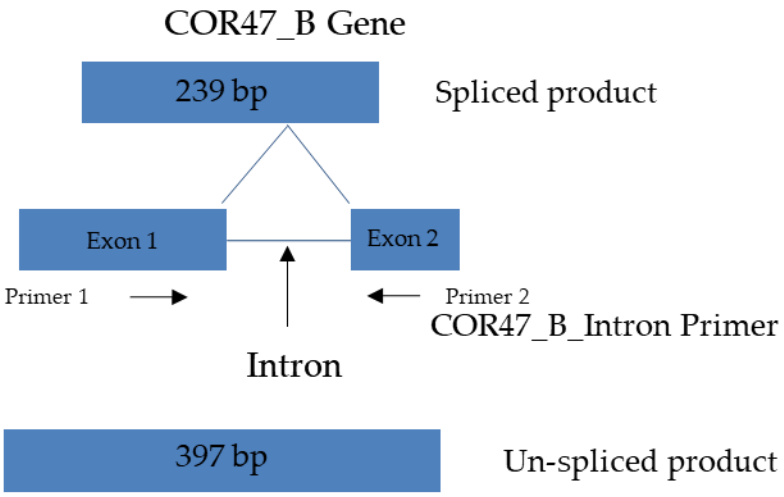


Figure 31. COR47_B gene diagram showing COR47_B_Intron Primer Location

**Figure 31 Legend.** The COR47-like_B gene contains two exons and one intron. A primer was designed to span the intron region, where two different sized products would be formed depending if intron retention was occurring (not drawn to scale).

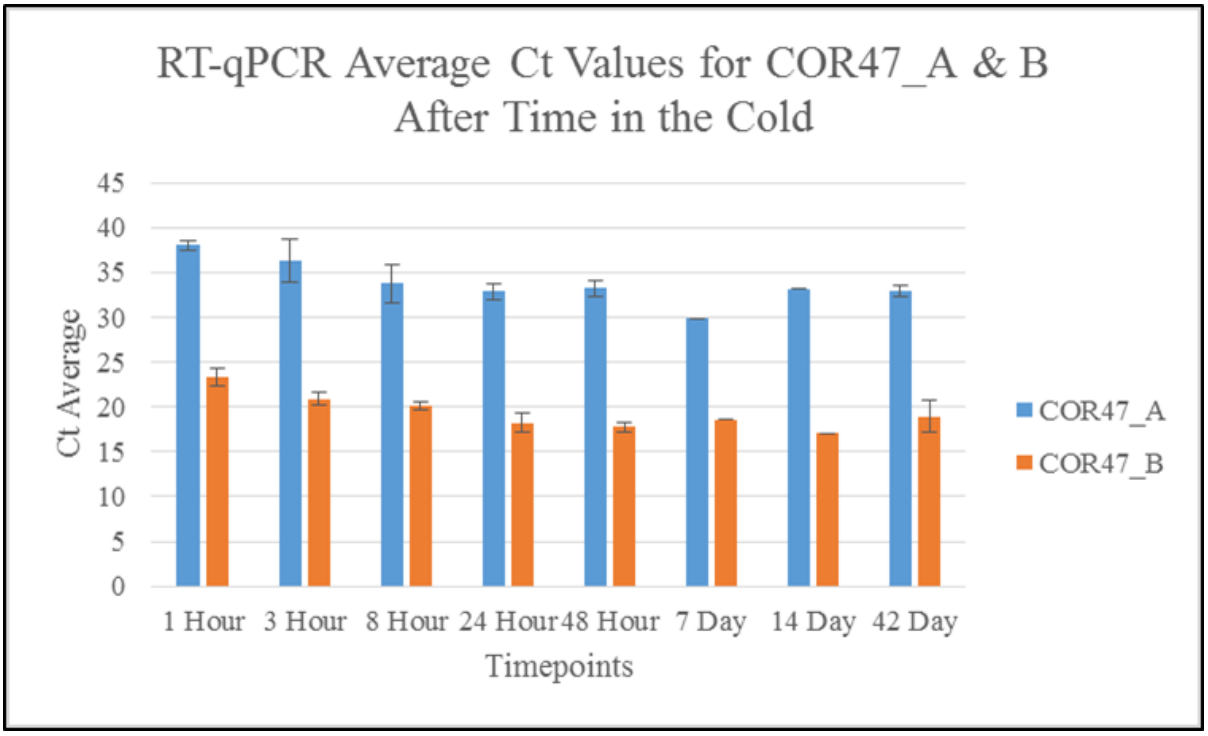


Figure 32. RT-qPCR COR47_A & COR47_B Ct Averages

**Figure 32 Legend.** RT-qPCR Ct averages of Alta crown samples at eight different timepoints for COR47_A and COR47_B primers. COR47_A is detected much later in the rounds of doubling compared to COR47_B suggesting that the amount of COR47_A is much less than COR47_B.

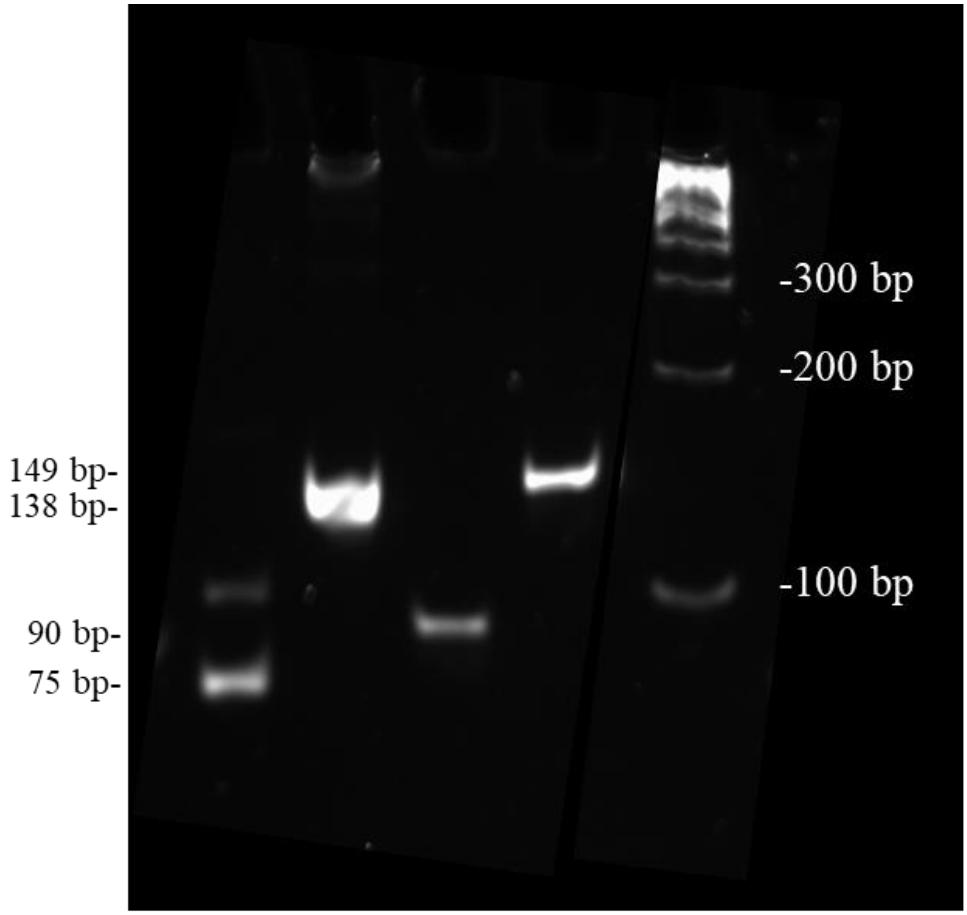


| COR47_A | COR47_B | PP2A | Nelson_COR47_B | Primer |
|---|---|---|---|---|
| 81 | 132 | 94 | 148 | Expected Size (bp) |
| 75 | 138 | 90 | 149 | Calculated Size (bp) |

Figure 33. RT-PCR confirmation of primers

**Figure 33 Legend.** RT-PCR test of CO47_A, COR47_B, PP2A, and Nelson_COR47_B primers. Samples were loaded into wells on an 8% acrylamide gel. Multiple bands from COR47_A are likely due to the conditions not being optimized.

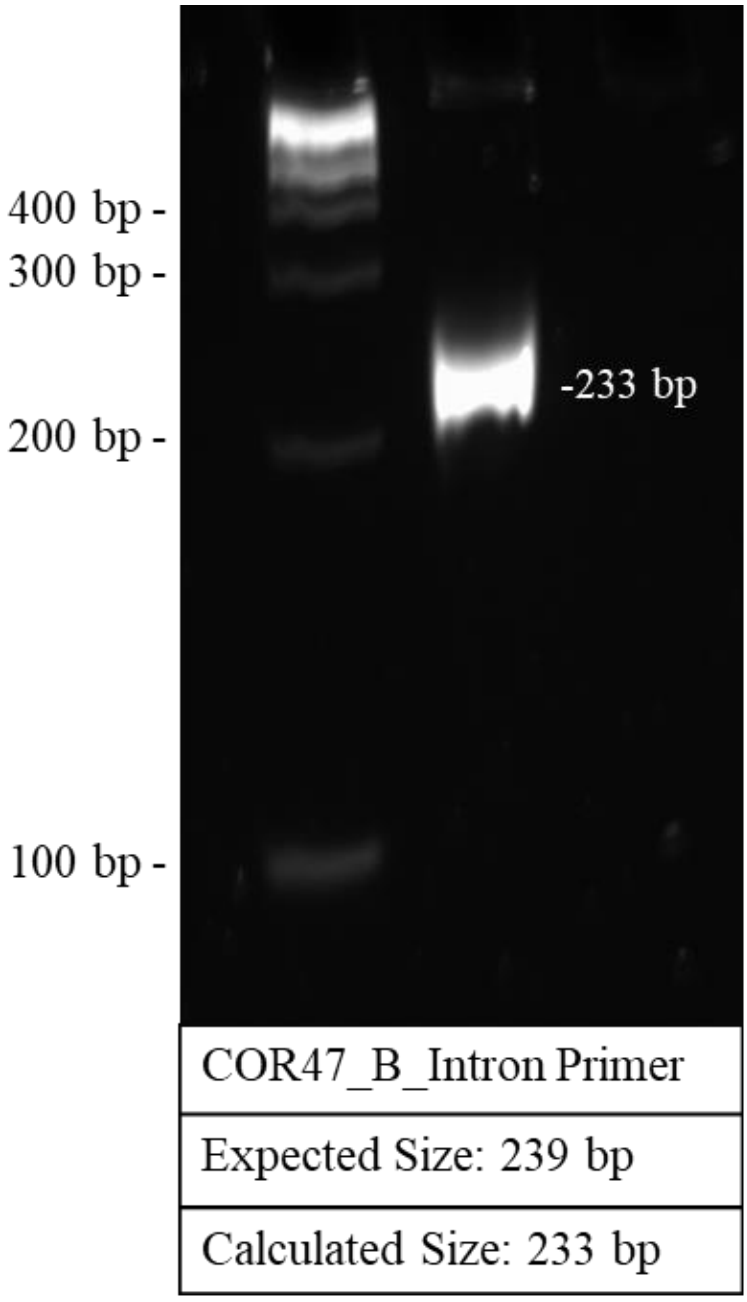


Figure 34. RT-PCR of COR47_B_Intron Primer confirms expected intron splicing

**Figure 34 Legend.** RT-PCR product for primer spanning the intron of COR47_B. If the intron was being spliced out properly, a 239 bp band was expected. If the intron was being retained, a 397 bp band was expected. The resulting calculated band is shown at 233 bp.

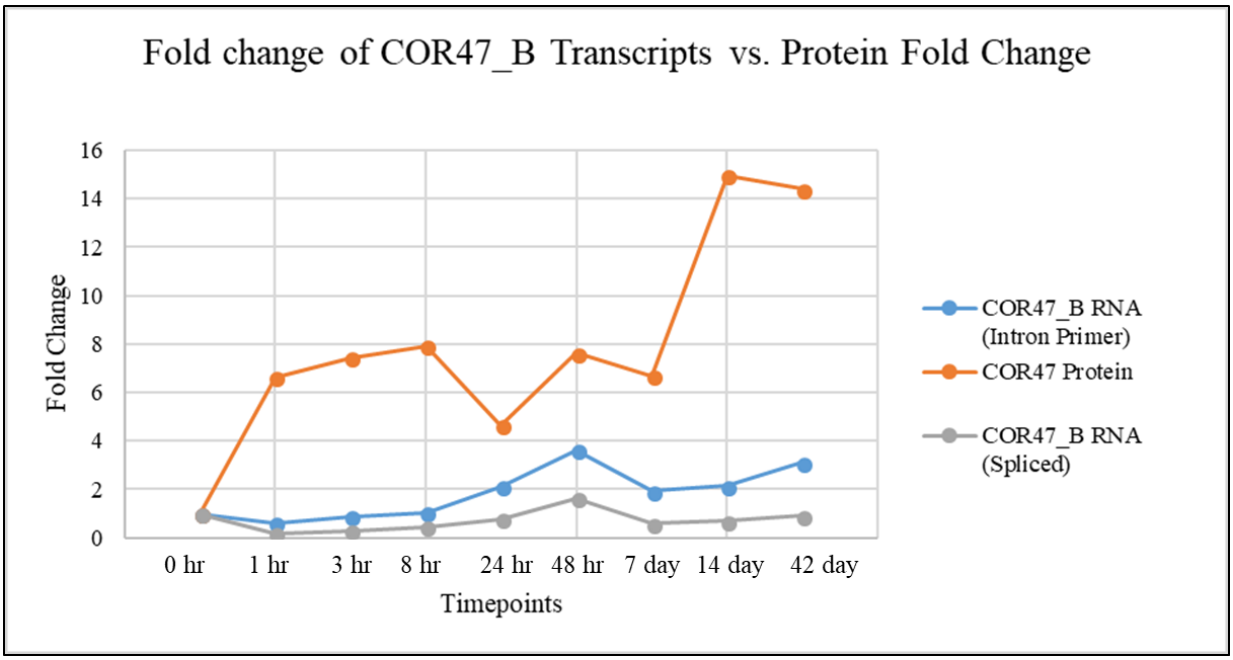


Figure 35. Transcript fold change with COR47_B_Intron primer vs. protein fold change

**Figure 35 Legend.** Graph showing transcript fold change of the COR47_B gene (average of three biological replicates for each timepoint, three technical replicates for each biological replicate) in comparison to protein fold change over 42 days in the cold. Transcript increases are seen at 48 hours and at 14 and 42 days. The observed trends may explain later protein accumulations but do not explain early timepoint protein accumulation while transcripts go down or do not change.

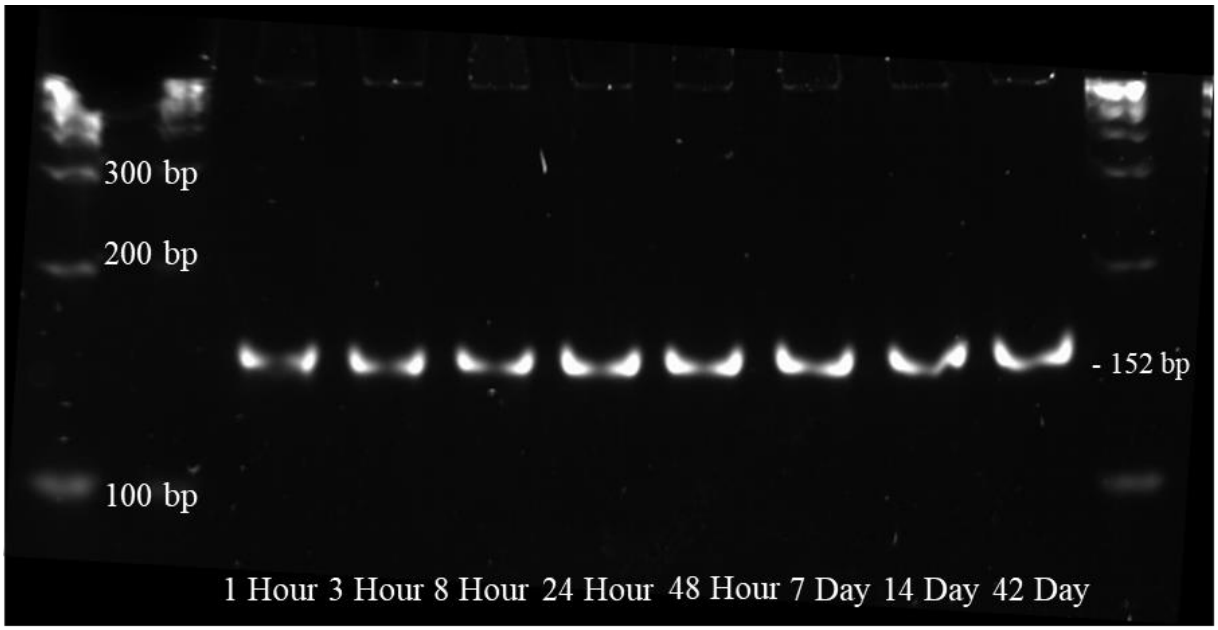


Figure 36. RT-qPCR products of COR47_B at different timepoints do not show a change in abundance or alternative spliced products

**Figure 36 Legend.** RT-qPCR products for COR47_B were run on an 8% polyacrylamide gel. Each lane was loaded with one replicate from each timepoint of cold treatment. Expected product size is 148 bp and corresponding calculated product size is 152 bp.

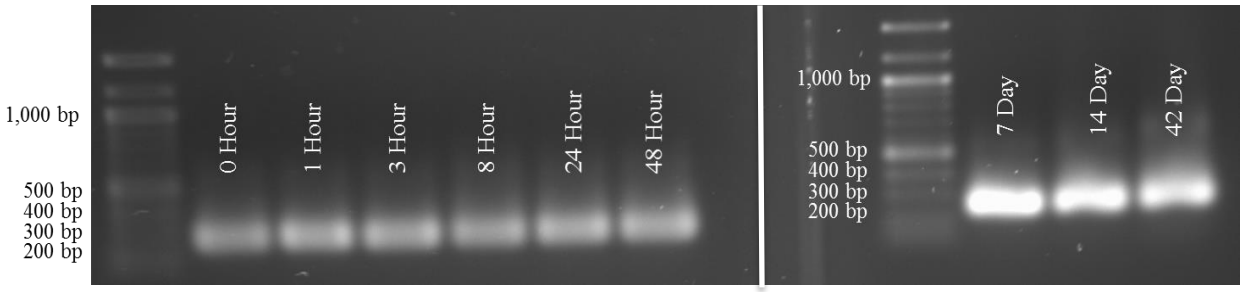


Figure 37. RT-qPCR products of COR47_B_Intron run on a 1% agarose gel

**Figure 37 Legend.** One sample from all nine timepoints was taken and run on a 1% agarose gel to qualitatively see if there is any alternative splicing occurring in the COR47_B gene. The expected size of the band with the intron being properly spliced out is 239 bp. All of the sample could not be run on the same gel, so the exposure between gels is slightly different but the results seen on the gel do not show the presence of any products at 397 bp where the intron would be retained.

# CHAPTER 4. DISCUSSION

## 4.1 Octoploid Analysis

Koehler et al. (2012), taking a proteomic approach, identified proteins with major changes in response to cold in octoploid varieties Jonsok and Elsanta. F1s produced from a cross between Jonsok and Elsanta, including the parental lines and with Frida (another cold intolerant variety) were analyzed for protein levels and cold-associated changes in XERO2, Thaumatin, β-1,3-glucanase, ADH, and HSC70. The lines chosen had varying degrees of cold tolerance (previously determined) and observing changes in expression from 0 hours to 42 days in the cold gave a snapshot perspective of beginning and end timepoints in cold expression. From this dataset, XERO2 (total dehydrin content) showed the strongest correlation with accumulation in relation to the cold. ADH, Thaumatin, β-1,3-glucanase, and HSC70 were not as convincing, showing variable accumulations across varying degrees of cold tolerance. It was observed for β-1,3-glucanase that higher levels of the protein were observed in the cold intolerant group compared to the cold tolerant group. Since β-1,3-glucanase has been implicated to defend against plant pathogens, it could be that lines from the cold intolerant group are more vulnerable to infection. Therefore, production of higher amounts of β-1,3-glucanase are occurring in low survival conditions to protect against pathogen attack. We gain from this dataset a confirmation that XERO2 and total dehydrin content can be utilized as biomarkers in breeding programs, and that breeders should look for lines with high levels of these proteins to select for more cold hardy lines.

HSC70 in the leaf had significantly higher abundance at the 0 hour timepoint compared to the 42 day timepoint across the range of survivability. But although the overall trend of HSC70 at the 0 hour timepoint was increasing slightly with cold survival, it was not statistically significant. However, this brings up the potential for a biomarker that could be detected at 0 hour timepoint in the leaves. Having a marker like this would be extremely valuable because the plant would not need to be sacrificed in order to test it, and the presence of high levels of the biomarker at 0 hours would save a huge amount of time by not having to grow the plants in the cold for long periods of time. The freezing tolerant group (> 10% survival at -8 °C) of HSC70 at 0 days was statistically significant in comparison to the freezing intolerant group (< 10% survival

at -8 °C). But the correlation of 0 hour protein level and survival percentage does not necessarily indicate that high amounts of HSC70 lead to higher survival in the cold, but it could definitely be a contributing factor.

The cold response in strawberry is quite complex, for example, more than 100 genes are controlled by the cold responsive transcription factor, CBF. A possible explanation that makes analyzing biomarkers of octoploid F1s so difficult is the involvement of many different coordinated changes and mechanisms involved in the octoploid cold response that could be coded by as many as eight different alleles on eight different chromosomes, which makes analysis of a contributing single allele quite difficult.

Another possible explanation for the low correlations of potential markers with cold tolerance could be that heterosis is masking the gene expression changes and therefore we see a lack of strong correlation in the data. Heterosis occurs when two widely different varieties are crossed and is broadly defined as the increased vigour of hybrids in comparison to their parents (Romagnoli et al. 1990). It has been suggested that differential gene expression and protein synthesis may be the basis of heterosis in plants (Rohde et al. 2004; Romagnoli et al. 1990). In Arabidopsis, a significant heterosis effect on leaf-freezing tolerance was observed in the F1s of a cross between two parental lines (Rohde et al. 2004). In our octoploid strawberry cross of parental lines, the F1s created were very diverse in their cold survivability compared to the parents as well (Figure 1). Thus in some cases, expression of specific genes can be higher in the F1 plants compared to the parents, indicating a direct role of the corresponding proteins in heterosis (Song and Messing 2003). Clear candidates for a functional role in the observed heterosis in freezing tolerance are COR proteins. In Arabidopsis, no indication was found from testing mRNA levels of different COR genes (including COR47) that the increased freezing tolerance was correlated with increased levels of COR gene transcripts (Rohde et al. 2004). This was very similar with the results of testing protein accumulations of specific potential biomarkers with relation to cold tolerance. This possibility could indicate that heterosis was based on a different molecular mechanism than the differences in freezing tolerance between accessions (Rohde et al. 2004). Further work is also being done by examining mRNA transcripts for each of the 5 genes examined at the protein level. Statistical analysis done by collaborators (Pokhrel, *et al*.) will allow a more complete perspective of this dataset.

In the processing of the western blots to generate these results, it was very difficult to normalize between membranes, and with many samples per dataset, this likely contributed to error in the outcomes. In order to alleviate this issue in the future, finding a way to compare all of the samples of one set on the same gel or blot would be extremely useful. Since this is often not possible with many samples per set, a control sample of known amount could be utilized to normalize each gel. In addition, creating a mixed lysate of the biological replicates would create more normalized samples with less variability. To normalize for protein load (in addition to amido black), using REVERT$^{TM}$ on membranes to stain all blot for total protein and normalizing before applying antibody would allow for quantitation and comparison of equal loading on the western blots.

## 4.2 Diploid Analysis

Isam *et al.* (unpublished) began to analyze the transcript and protein correlations in XERO2 and COR47 in diploid varieties Alta, NCGR1363, and FDP817. XERO2 is known to accumulate at later timepoints in the cold (Koehler et al. 2012) and we saw just that, mimicking the transcript accumulation. From these data, XERO2 is a very strong biomarker for indication of cold tolerant lines. Overall, larger increases of XERO2 and COR47 protein levels were detected in Alta compared to the other two lines, supporting the evidence that Alta has a much stronger cold induction of dehydrins than the less cold tolerant lines. COR47 protein accumulated early on in the time course, decreased, and then increased again later on. This pattern did not correlate with transcript levels, especially in Alta crown, which is the most cold hardy variety. Investigation into what mechanism or level of regulation causing this discrepancy was undertaken. Alternative splicing is not a likely factor because the spliced region was purified and sent for sequencing and was found to be the only splice site used at all timepoints. The possibility of intron retention was also resolved by translating the sequence and the presence of multiple stop codons within the first 50 nucleotides of the intron showed that a truncated protein product would be a result. In addition, primers were designed to create products of different sizes if intron retention was occurring or not, and no evidence for the intron being retained was observed. Contribution of more than one isoform is not likely a factor because the COR47_A isoform is not only much smaller in size than the COR47_B isoform and is likely not a

component of accumulation measurement because it accumulates to amounts much smaller in magnitude than the COR47_B transcripts, making its potential contribution insignificant.

Another potential contributor to the discrepancy of COR47 transcript and protein in Alta is the possibility of post-translational modifications. Phosphorylation seems to be the major post-translational modification of dehydrins because the S-segment is easily phosphorylated (Rorat 2006). But is it possible that COR47 is being ubiquitinated? We performed a western blot using ubiquitin antibody and noticed that many of the proteins are ubiquitinated, although we did not have the tools or the time to perform a co-IP, which could have answered this question (data not shown).

Transcript levels for Arabidopsis COR47 increased dramatically between 1 and 4 hours of cold exposure (Guo et al. 1992). Those levels remained high for the duration of the cold before returning to basal levels within 4 hours after returning to normal temperatures, which was also noted in wheat COR39 (Guo et al. 1992). The nuclear run-on results from (Hajela et al. 1990) indicate that both transcriptional and post-transcriptional mechanisms are involved in the temperature-regulated accumulation of Arabidopsis COR gene transcripts. Specifically for COR47, steady state transcript levels changed dramatically in the cold, while transcription rate in the cold barely changed at all, suggesting primarily posttranscriptional control mechanisms (Hajela et al. 1990).

## 4.3 Sequence Analysis of COR47_B

Many factors could be involved in preventing the COR47 protein from being translated with full efficiency and often times more than one mechanism can be at play. It was hypothesized that the discrepancy between protein and transcript responses to cold seen in Alta crown could be explained by post-transcriptional regulation and a large focus was dedicated to investigating this observed trend.

Conclusions from the sequencing results are that the COR47_B sequence of the diploids used in this study are identical to the NCBI and Phytozome databases, except for three missing nucleotides in the mRNA sequence of NCBI database resulting in a protein one amino acid larger than predicted. Lastly, the truncated protein predicted from Phytozome can be attributed to a missing nucleotide in the NCBI and Phytozome database sequence. An extra A in a run of As

is present that was not shown in NCBI or Phytozome database sequences, and the presence of this extra A fixes this discrepancy.

In addition, sequenced genomic DNA regions were aligned and translated, with only one predicted intron being found. cDNA sequences derived from transcripts isolated from 0 hr, 3 hr, 48 hr, and 7 days, all show an appropriately spliced junction at the single predicted intron border. This data suggests that alternative splicing does not have a role in post-transcriptional regulation of COR47 protein expression and that the COR47_B isoform is the dominant contributor to the COR47 gene expression.

To further characterize if COR47_B transcripts and protein can be used as a reliable biomarker, experiments testing translational and post-translational mechanisms would be useful in narrowing down the regulation of the COR47_B protein. A possible translational control experiment would be to see the efficiency of translation through polysomal fractionation. Polysomes generally represent actively translated transcripts, and thus the number of mRNA molecules engaged in polysomes should be a robust indicator of the synthesis rate of the corresponding protein. Hybridization of northern blots (or RT-qPCR) could then reveal the distribution profile of specific mRNAs between ribosome-free and polysome-bound fractions. The comparison between the total and polysome-bound mRNAs enables transcriptional and translational regulation to be distinguished (Pradet-Balade et al. 2001). A possible post-translational control experiment would be to perform a Co-IP experiment using anti-ubiquitin and anti-COR47. This would show if the COR47 protein was being marked for degradation. These experiments would be useful follow-up experiments to the post-transcriptional work presented here.

# APPENDIX

## A1.1 Investigation of the use of a Bio-Dot (Dot-Blot) Apparatus for high throughput protein assays and western blots.

The feasibility of replacing western blots and protein assays with a high throughput method in the Bio-Rad, Bio-Dot™ Apparatus was examined. This method is designed to assay protein amount and subsequent signal from an applied antibody on the same blot. This would allow for internal normalization and a direct correlation with many samples in less time than traditional methods. It would be particularly useful in analysis of biomarkers for cold-tolerance by speeding up the processing of a high number of samples and would allow for a direct comparison of 96 samples on one nitrocellulose membrane. This would eliminate any potential disjunction between comparing and analyzing multiple membranes from western blots (15 lanes/blot). Classical amido black protein quantitation is known to be very reliable, but with many samples it is tedious, time consuming, and the samples quantitated cannot then be used for antibody application, making it impractical for our purposes. The ability to apply an antibody to a nitrocellulose membrane, and get a signal that can be directly compared to the amount of protein on the same membrane is the ultimate goal. This would be a very efficient process that would not only save time but would also generate more reliable data amongst replicates.

### A1.1.1 Protein Assays in Dot-Blot

In this investigation three methods for protein quantitation were explored consisting of REVERT™ Total Protein Stain (Li-Cor), Ponceau S stain (Sigma-Aldrich), and amido black (Kaplan & Pedersen, 1985). Using the Bio-Rad Bio-Dot™ Apparatus, 96 samples were processed at the same time by applying prepared sample directly onto the nitrocellulose membrane and letting them gravity filter, where they become irreversibly bound. Membranes were then washed, further processed, and quantitated.

#### A.1.1.1.1 REVERT™

The first method tested was REVERT™ Total Protein Stain (Li-Cor) to assess protein quantitation accuracy with strawberry extracts. This method has a linear range of 1-60 ug but more importantly, once the protein quantitation is complete the stain can be washed off and an

antibody can be directly applied, allowing for direct comparison of a sample between total protein amount and antibody signal. Protein extractions are generally in 1xSSB. So the first question was to ask if any components in this buffer might interfere with REVERT™. Testing the contribution of glycerol, SDS, bromophenol blue, and Tris revealed that SDS was a major contributor to SSB interfering with the reliability of the assay (Appendix 1). Through more testing, we found that while SDS inhibits the signal of the REVERT™ /protein interaction, SDS at 0.1% or less minimally interfered, while still having enough protein for quantitation.

A comparison of REVERT™ with Bovine Serum Albumin (BSA) versus Alta crown samples with and without SDS showed an interference with the accuracy of the REVERT™ process, possibly small yet variable amounts of chlorophyll (Appendix 2). Washing the blots with methanol and extra PBS washes did not alleviate this issue. This suggested high signal from chlorophyll effectively made accurate quantitation of protein samples unreliable (Appendix 3). These results showed that the REVERT™ stain would produce different results based on the type of sample being used (and amount of chlorophyll present). Other methods to extract chlorophyll were not attempted as my goal was to develop a low manipulation, high throughput system.

#### A1.1.1.2 Amido Black

A comparison between Amido black and REVERT™ was conducted. Protein was loaded on the dot-blot apparatus as before. Amido black was linear between 1-50ug with an ideal range between 5-20ug (Appendix 4, compare to Appendix 1 for REVERT™). Using this method, SDS and chlorophyll do not interfere and the results are quite reliable, although it is not possible to apply an antibody after amido black. A comparison of REVERT™ and amido black on a full set of Alta crowns showed REVERT™ samples having extremely high pixel counts compared to the BSA standards, potentially due to the presence of chlorophyll in the samples (Data not shown). The amido black samples were within the expected range of the standards and it was concluded that using the amido black method would be most quantitative and reliable.

#### A1.1.1.3 Ponceau S Stain

The utility of Ponceau S stain, a fast and reversible but non-fluorescent method for locating protein bands on western blots was investigated. The stain is easily reversed with water washes,

and does not interfere with antibody reactivity or with fluorescence signal. It was concluded that the sensitivity of the Ponceau S Stain was not high enough to detect differences in the low amounts of protein being added to the wells in the Bio-Dot Apparatus (Appendix 5).

Overall, the presence of chlorophyll, SDS, and other unknown interfering components precluded the direct use of REVERT$^{TM}$ Total Protein Stain, so it was not further considered. Ponceau S stain was found to be not sensitive enough of an assay. Amido black, even though it is not a direct comparison method, was concluded to be the optimal method for protein quantitation in the Bio-Dot Apparatus. Even though the western blots and protein assays cannot be performed on the same blot, the amido black technique in the Bio-Dot Apparatus still saves a large amount time compared to the traditional method from Kaplan and Pedersen (1985).

### A1.1.2 Antibody Application in Dot-Blot

In addition to high throughput protein quantitation we were also interested in seeing if the Bio-Dot Apparatus could be utilized to do antibody quantitation. Even if REVERT$^{TM}$ could not be used, the use of the bio-dot apparatus would still allow for more samples to be analyzed than traditional western blotting methods. When increasing amounts of protein are applied on a traditional western blot, the quantitation of these results is linear for the specific protein band, and the entire lane (Appendix 6). Preliminary testing in the dot-blot was done to test binding of an antibody to protein to see if the resulting signal was entirely produced by the fluorescence of the primary antibody on protein. A dilution series using only SSB (no protein) and another with Alta protein was compared with two identical sets, one receiving COR47 antibody and the other with no primary antibody added. Both sets were incubated with secondary antibody. The results from this confirmed that secondary antibody does not generate a false positive signal through nonspecific binding to Alta extracts (Appendix 7) and that the primary antibody was responsible for the signal being produced and was quantitative. The detection limit appeared to be approximately 30 – 50 ng total Alta crown protein (Appendix 7). Unfortunately 0.04x SSB did interfere, creating a workable, but high background.

It was demonstrated that primary antibody can be analyzed quantitatively in the dot-blot, but there is potential for varying amounts of unknown contaminants in the crowns and leaves to have a significant impact on signal. One approach to continue refining this process for experimental application was to investigate potential chlorophyll interference with antibody

signal and to establish a standard protocol for sample processing to remove chlorophyll. It was determined that chlorophyll is not directly interfering with antibody signal at low levels (Appendix 8) but may be quenching the signal at higher concentrations (Appendix 8), at 1 or 3 ug leaf protein. As mentioned earlier, it was concluded that chlorophyll sufficiently interfered with protein assays (Appendix 3), producing an extremely high signal. Chlorophyll signal shows up in the 700 channel and can be easily seen in leaf samples where chlorophyll levels would be quite high, but not the 800 channel (antibody signal) with antibody application (Appendix 8). The conclusions from these results are that antibody and chlorophyll are not interacting, yet some unknown interfering component (background, small molecules) at low protein levels is, which can be seen by variable and high levels of the $H_2O$ samples (Appendix 8).

The dot-blot apparatus was compared with classic gel western blots with equivalent protein load and the identical samples followed by blotting with anti-COR47, to see if quantitation was comparable. In the dot-blot, the total pixel count was much greater for all samples compared to the total pixel count for the western (Appendix 9). When these total pixel amounts were analyzed for fold changes, the dot-blot values were under 2-fold change while the values from the Western blot (specifically the COR47 band) showed much greater changes, with fold changes up to 15-fold (Appendix 9B). When the entire lane of COR47 signal on the Western blot was quantitated, values were under 3-fold change. By comparing the two methods, there is much better distinction between sample variations using traditional Western blots where the specific COR47 band is quantitated. The dot-blot was likely quantitating the total signal that would be from multiple bands of an entire lane had it been run on a gel. Concentrating the entire sample to the small area in the dot-blot results in a general background fluorescence signal that obscures the ability to detect variation in the COR47 protein. Being able to isolate the band on a gel allows for much more direct testing of the changing amounts of COR47 protein, without minimal noise, background, other proteins, or contaminants.

PVDF (Polyvinylidene Fluoride) membranes were compared to nitrocellulose to determine if PVDF might not bind the interfering component(s) that we observed on the nitrocellulose membrane. A dilution series of BSA, Alta crown, and Alta leaf on PVDF and probed with COR47 antibody, showed much lower background (Appendix 10). The total pixel count was much lower on dot-blot PVDF compared to the Western which is the opposite of how the

nitrocellulose behaved (Appendix 11). But the values resulted in little detectable variation and similarly were under a 3-fold change like the dot-blot nitrocellulose fold changes.

Future experiments with high through-put techniques for westerns in the dot-blot apparatus still have the major hurdle of eliminating unknown interfering components at low protein levels and require a demonstration of a specific antibody signal. Chlorophyll also could have the potential to interact with different antibodies or sample types. A possible solution could be to include two antibodies that require fluorescent characteristics different from chlorophyll; an antibody that probes a "housekeeping" protein with one color and probe the blot with another color for a different direct comparison. Another option would be to do extractions that remove the chlorophyll, but this may be such a tedious step that it negates any time saved by using the dot-blot. An alternative analysis could be done with an enzyme-linked immunosorbant assay (ELISA). This method would use an antibody and color change to detect the presence of a substance. The ability to get reliable results without interference of chlorophyll would be of paramount importance for progress in high through-put techniques using plant samples in the dot-blot apparatus. The results of comparing PVDF and nitrocellulose in the dot-blot did not alleviate the effects of the interfering components while both methods were shown to not be able to detect much variability between different samples.

### A1.2 High-Throughput Methodology Discussion

For large scale breeding experiments, new techniques and methods that streamline a process are integral to saving field and lab time. In particular, being able to process a higher number of samples and generate larger and more comprehensive datasets allows for analysis of more replicates, reducing error. This increases certainty that observed trends reflect true experimental findings and are not skewed due to inherent variability and a low number of replicates. Investigation into developing a high throughput method for protein assay and western blotting using the Bio-Dot$^{TM}$ Apparatus was undertaken to save time, increase sample volume processing, and lower the potential error generated from small sample sizes. We conclude that using the protein assay for amido black in the dot-blot is an effective way to quantitate protein accurately, while saving time and removing tedious steps from the traditional method. Instead of filtering each sample one at a time, all samples can be loaded into the apparatus and filtered without a great deal of attention. Finding a method that allows for the washing of stain and

antibody quantitation is still not resolved. REVERT™ and Ponceau S stain were candidates that proved unusable for our purposes, due to chlorophyll interference, other unknown contaminants, and a lack of sensitivity for low protein loads.

The use of the bio-dot for antibody application also needs further investigation. It was shown that antibody quantitation on the dot-blot does not show fluorescence variability well with different protein loads. This is likely due to the entire signal being concentrated and expressed on the small surface area of the dot. When an antibody is applied to a traditional western, the proteins separate during gel electrophoresis and run with their molecular weight. The utility of the dot-blot also depends on antibody specificity, where many antibodies recognize multiple bands of different masses on a nitrocellulose membrane that will fluoresce. If the mass of the specific protein is known, then quantitation can be directly correlated with that band's signal. With the dot-blot, all proteins are expressed on the membrane in each well, so we cannot be certain that the signal we are getting is specific to our protein of interest. It is likely that the signal we are getting could be compared to quantitation of an entire lane on a western blot membrane. A possible solution to this issue would be to choose an antibody that has been shown to only recognize one band. For example, HSC70 would be a great candidate for use in the dot-blot because it only fluoresces one strong band at a known molecular weight. We could therefore predict that the signal from applying HSC70 antibody to a dot-blot would be exclusively signal from that specific protein.

One hypothesis that would explain the small quantitative variability in the dot-blot is increased non-specific background binding; perhaps due to lack of removal by electrophoresis. Without electrophoresis run, the entirety of a lane's signal is concentrated on just the dot, which could have minimal variation from sample to sample. The COR47 antibody signal on a western blot has three or more bands in addition to non-band specific signal in the higher molecular weight regions of the blot. The difference between specific band related signal from an antibody may not be possible in the dot-blot, unless the goal is to see total antibody signal, which theoretically could be comparable to the entire lane on a western gel. When trying to detect COR47 specifically, the amount of signal of the specific band compared to the entire lane would be only a fraction of the total signal. Choosing a particular antibody (that produces one band e.g. HSC70) would generally be necessary for successful quantitation of a specific protein in the dot-blot.

Overall, this method could be useful if the entire antibody signal was desired instead of a specific band. The comparison of an entire lane on a gel would theoretically be the same as the quantitation of the whole dot from the dot-blot. If done using an antibody like XERO2 that detects many bands, and the change in overall antibody signal from the bio-dot to the western blot full lane signal was very similar, then the bio-dot could be used for entire lane comparison of samples that do not need a specific band analyzed. For an antibody like anti-COR47, which also recognizes multiple bands it was seen that total lane quantitation had under a 3-fold change which was very similar to the results obtained from the dot-blot. Alternatively, an antibody like anti-HSC70 that has been shown on western blots to only detect one band could be a good potential candidate for use. It is likely that the signal produced on the blot would be more similar to the entire band signal since only a specific protein is being detected by the antibody.

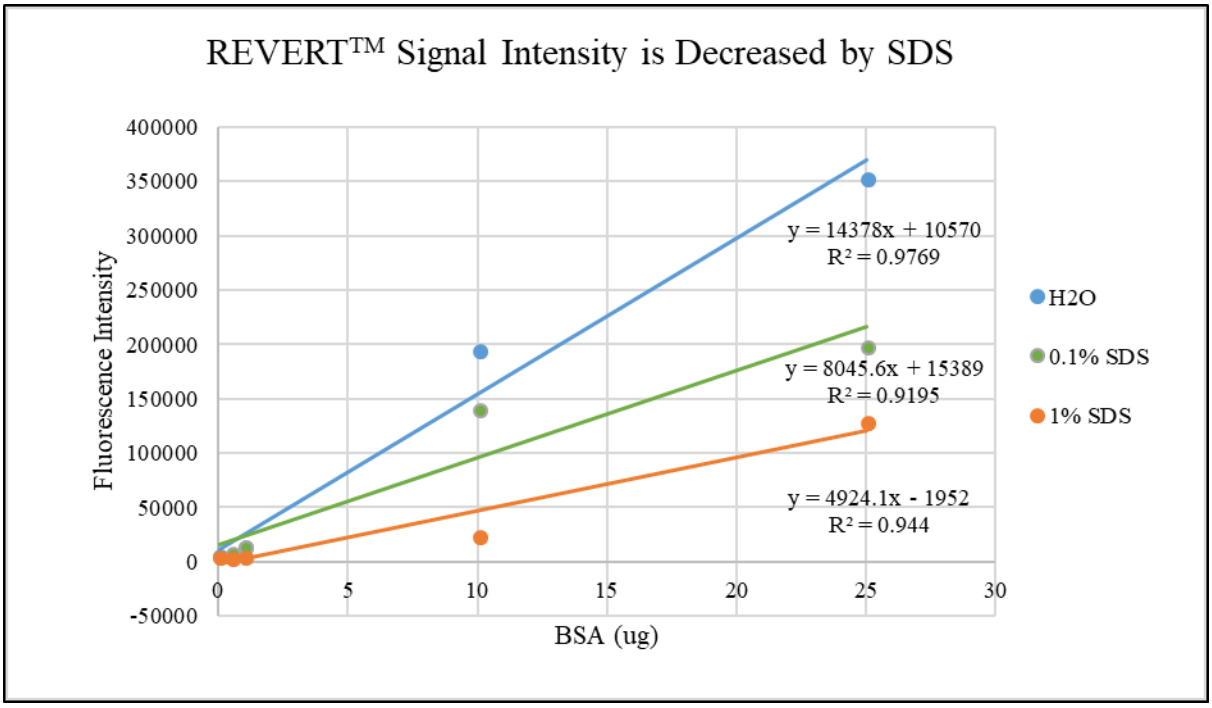


Figure 38. REVERT™ Signal Intensity is decreased by SDS

**Figure 38 Legend.** Interference of REVERT™ stain by differing amounts of SDS. BSA in water, 1% SDS, or 0.1% SDS were loaded onto nitrocellulose membrane in a dot-blot apparatus and then treated with REVERT™ total protein stain. The resulting spots were imaged using the Odyssey Imager CLx and pixel quantitation was done using Image Studio Lite Ver. 5.2.

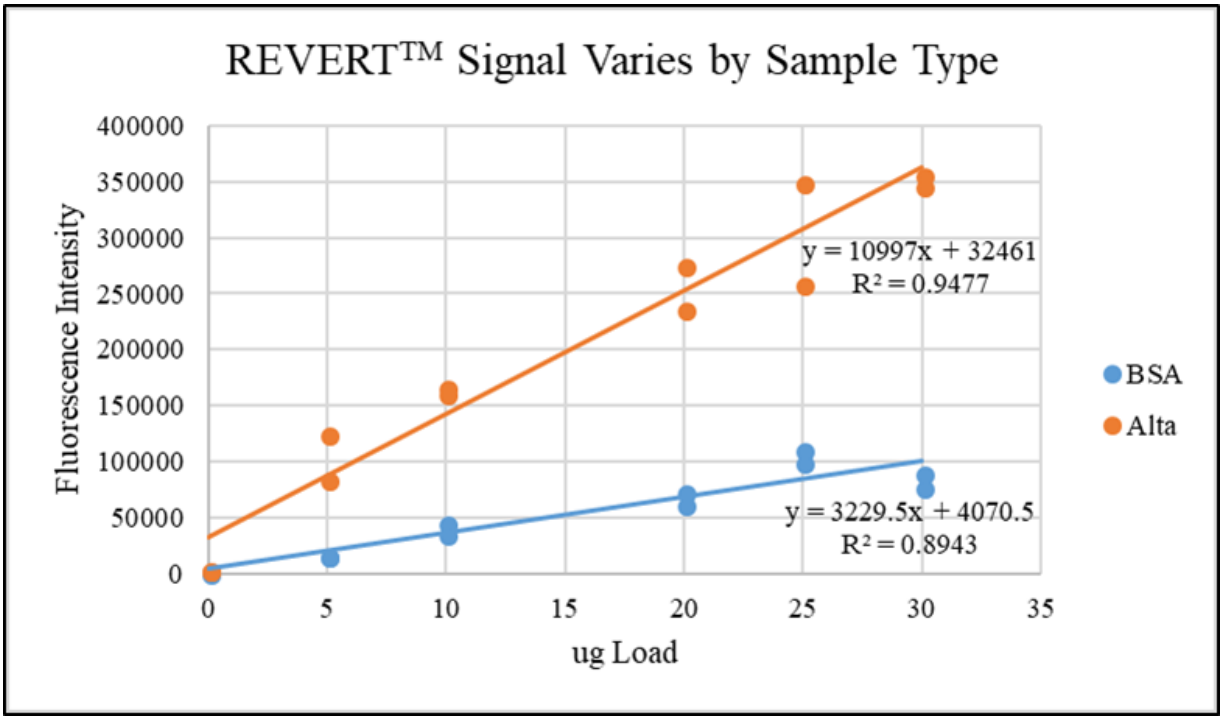


Figure 39. REVERT™ Signal Varies by Sample Type

**Figure 39 Legend.** REVERT™ stain comparing two different sample types, BSA and Alta crown. The extraction process for Alta protein uses a minimal amount of SDS that cannot be omitted. Therefore, samples were diluted with $H_2O$ without additional SDS. Two data sets each with 0-30 ug of BSA or Alta crown (protein previously determined by amido black assay using BSA as a standard) were loaded onto the dot-blot apparatus and processed with REVERT™. The results were imaged using the Odyssey Imager CLx and pixel quantitation was done using Image Studio Lite Ver. 5.2. A clear enhanced signal is observed in the Alta samples.

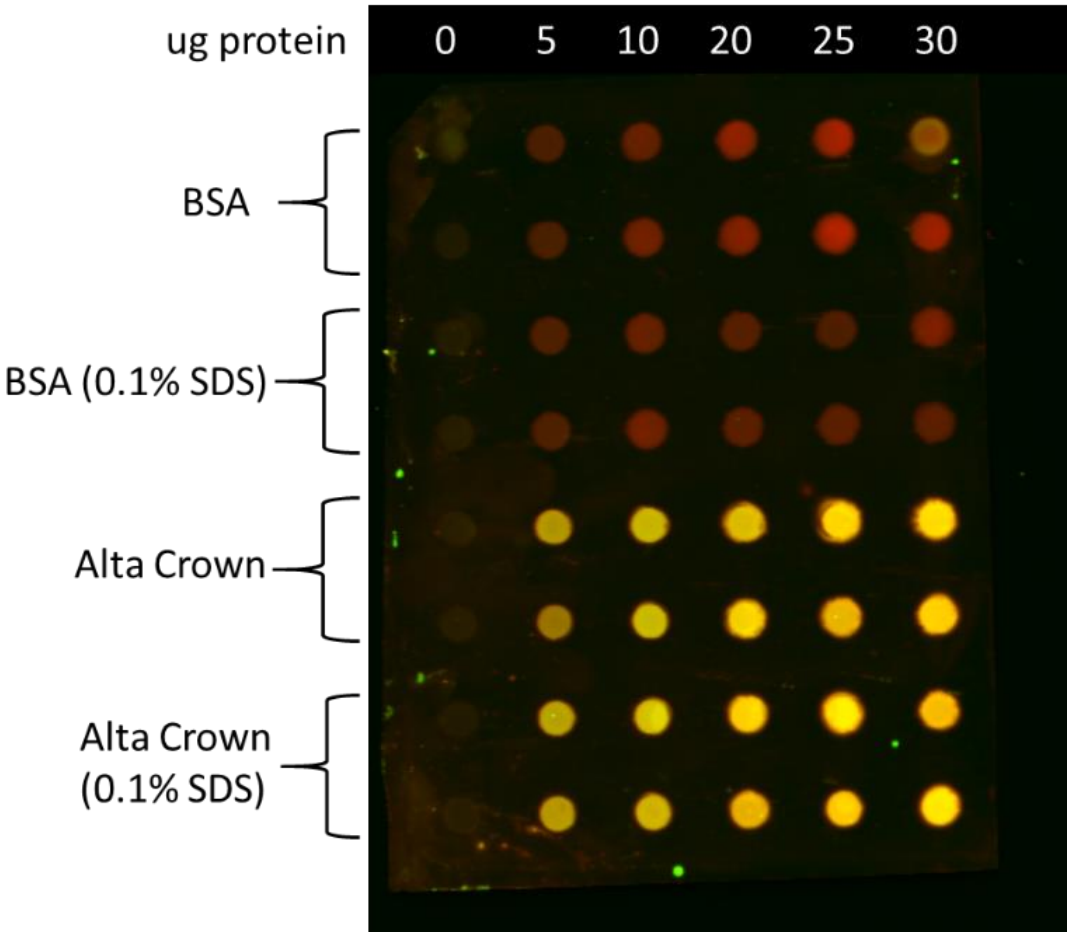


Figure 40. Interference of Chlorophyll in Plant Samples with REVERT™

**Figure 40 Legend.** Odyssey image of 700/800 nm channel of BSA and Alta samples with and without 0.1% SDS on dot-blot and treated with REVERT™ total protein stain. The top set of replicates only contained BSA protein while the bottom set of replicates only contained Alta crown protein. A yellowing in the Alta samples is apparent and due to the presence of chlorophyll fluorescence in both the 700 and 800 nm channels, leading to artificially high pixel counts for these samples.

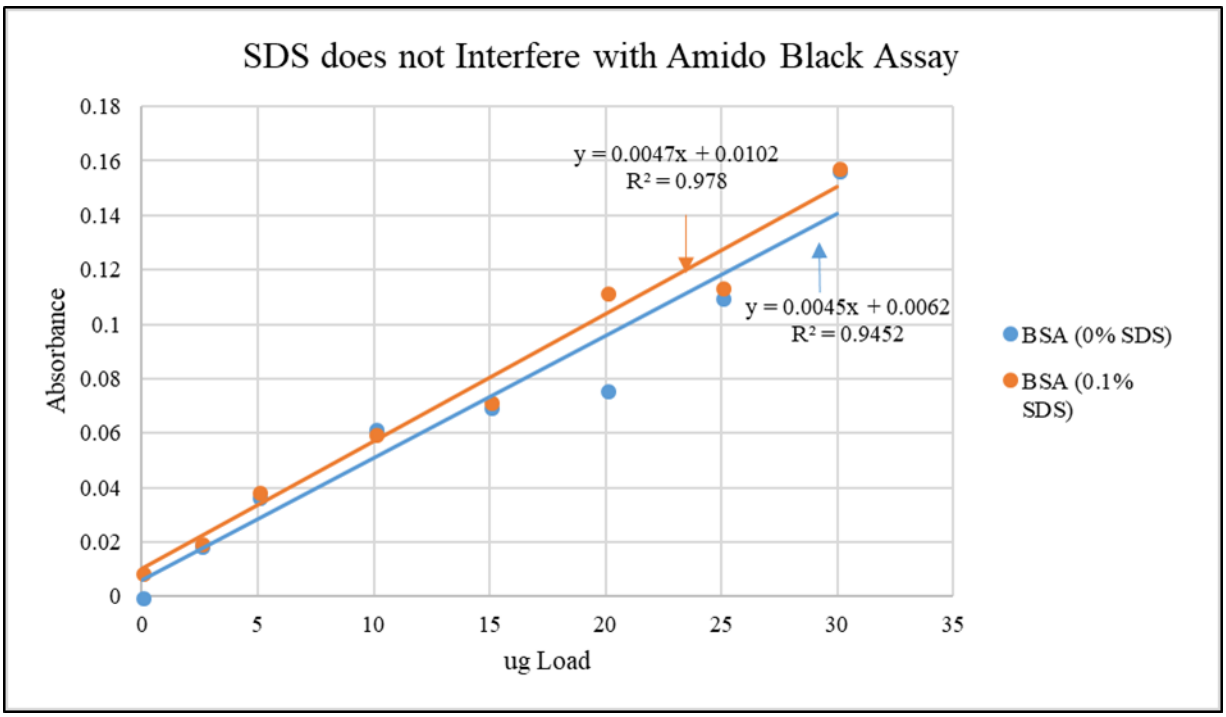


Figure 41. Protein assay using Amido Black is not effected by SDS

**Figure 41 Legend.** Amido black protein assay performed with differing amounts of BSA with and without the presence of SDS. This graph demonstrates the linear range of BSA and that there is no significant interference with SDS.

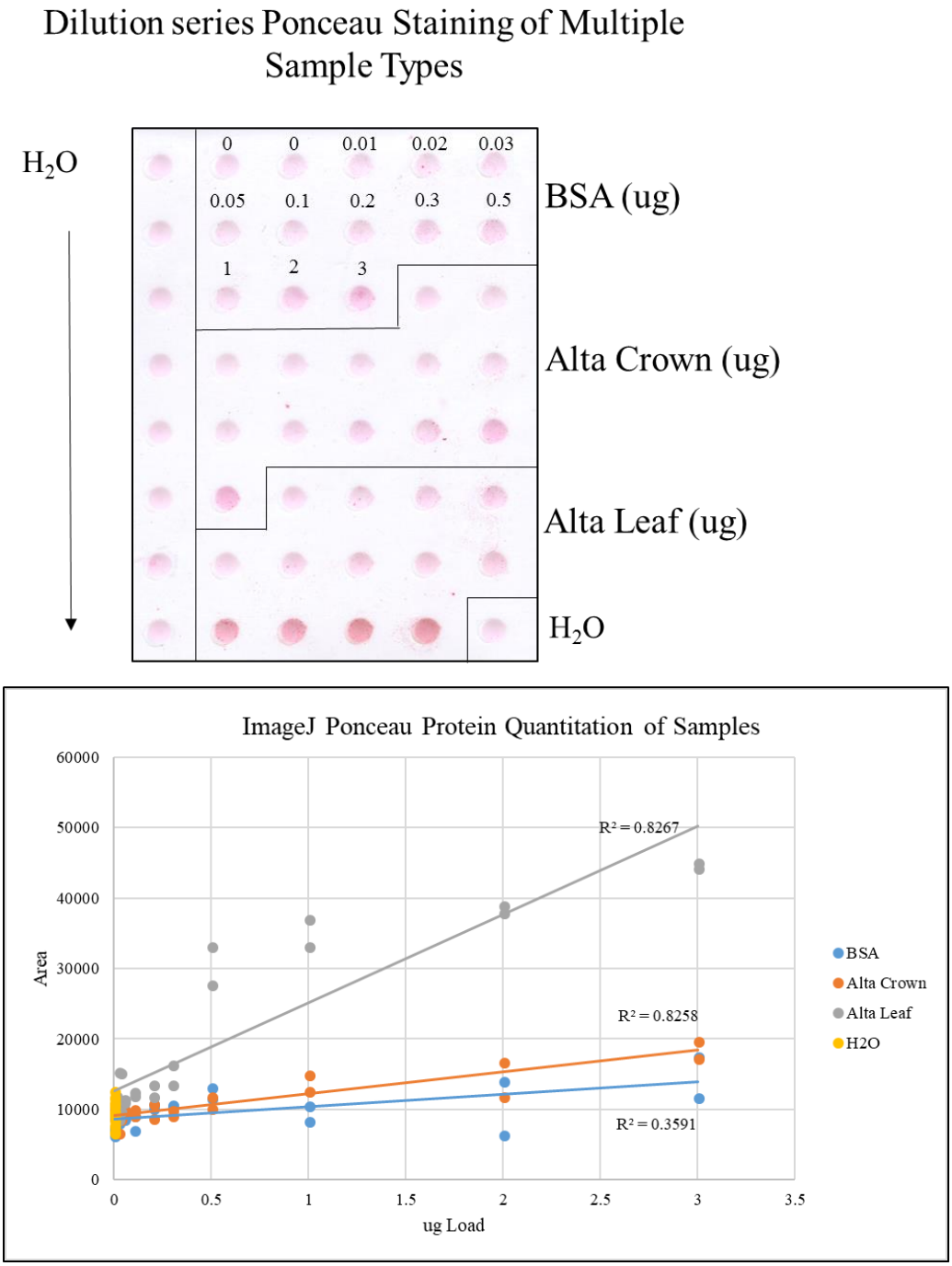


Figure 42. Ponceau S staining dilution series of multiple sample types.

**Figure 42 Legend.** Ponceau S Staining of BSA, Alta Crown, and Alta leaf protein in a dilution series on a nitrocellulose membrane. Quantitation of the dots showed that the stain was not sensitive enough with a low protein load and had variable detection based on sample type (For example Alta crown and leaf at 1 – 3 ug).

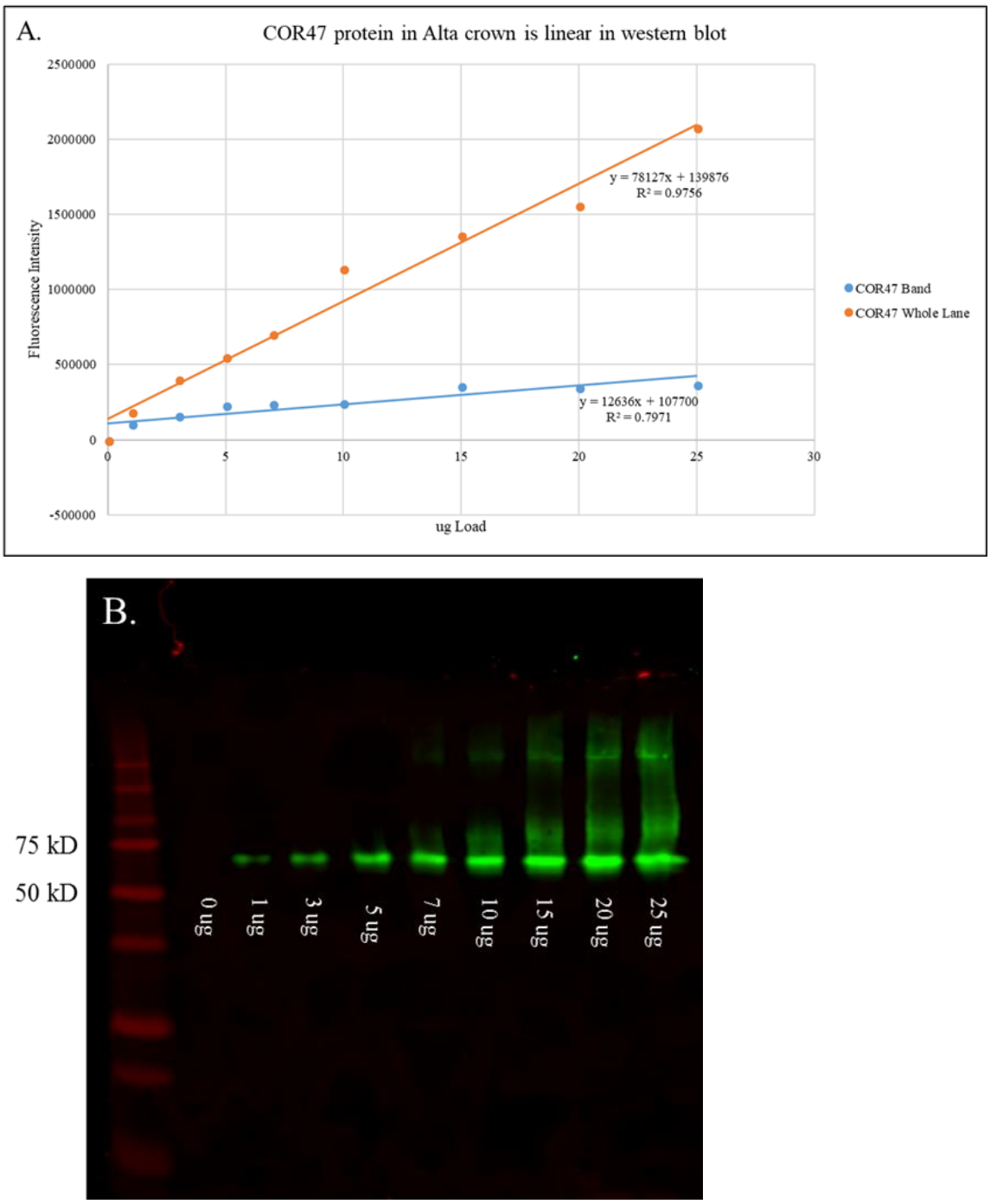


Figure 43. Dilution series of Alta crown protein on a western blot shows linearity with COR47 antibody application

**Figure 43 Legend.** A. Western blot quantitation of Alta crown protein dilution series with COR47 antibody applied (1:4000). The specific COR47 band and the entire lane were quantitated to see the signal from each. B. Odyssey image of the western blot with increasing amount of Alta protein applied (no 8 M urea) to the wells. As the amount of protein increased, so did the amount of background in the lane.

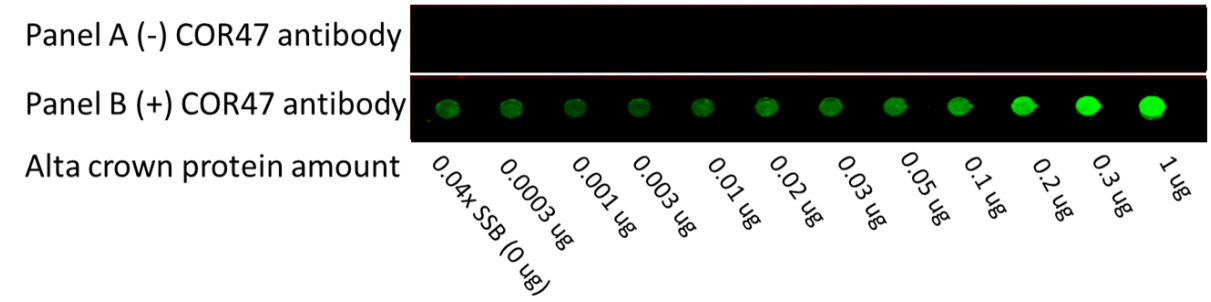


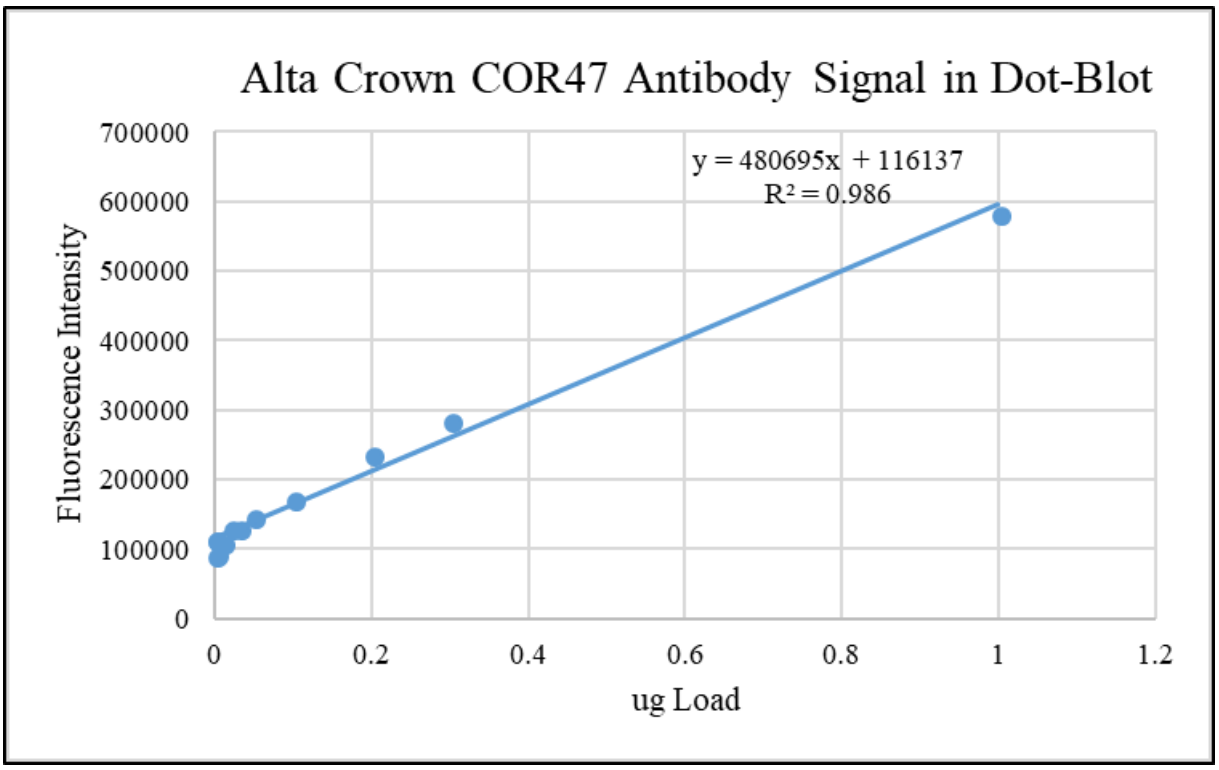


Figure 44. Primary Antibody is Responsible for Signal Produced in Alta Crown

**Figure 44 Legend.** Odyssey image in 800 nm channel comparing blots without (Panel A (top)) and with (Panel B (bottom)) COR47 primary antibody. On each panel is a dilution series of Alta protein (0.0003 – 1 ug) containing the same amounts of SSB. Secondary antibody donkey anti-rabbit was added to both blots prior to imaging. Signal from primary antibody is clearly detected for the increasing Alta protein in the presence of secondary antibody. A small amount of primary antibody signal is seen even in a sample without any protein loaded. Subsequent quantitation of the COR47 antibody signal shows linearity among the samples.

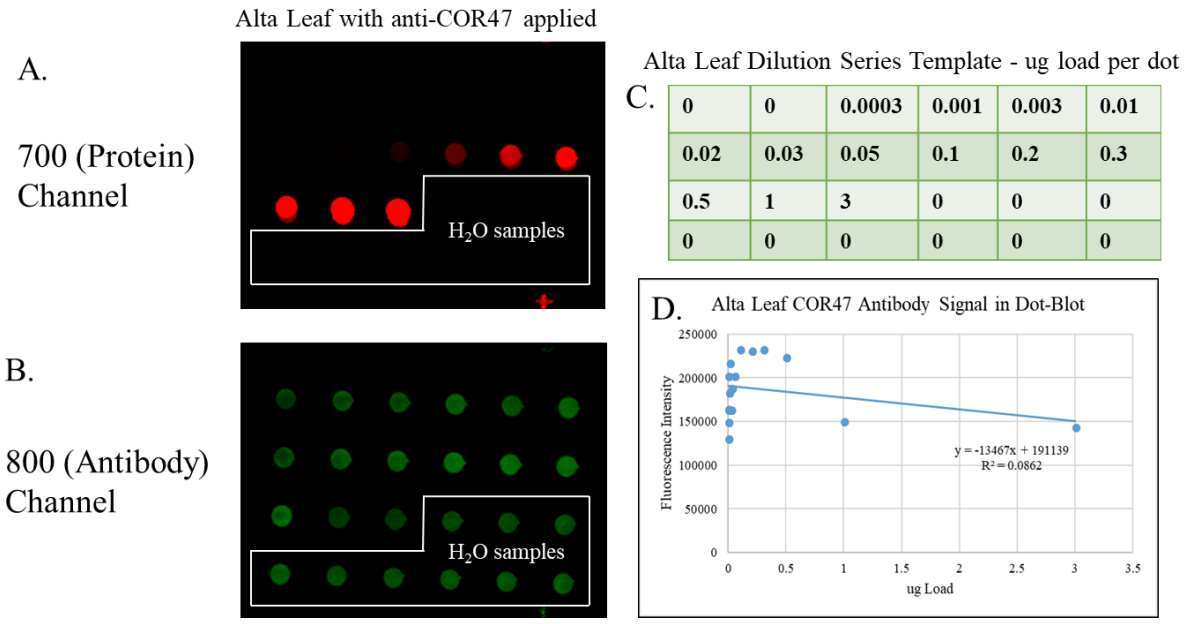


Figure 45. Chlorophyll at low levels does not appear to impact antibody signal in Alta leaf

**Figure 45 Legend.** A. Odyssey image in 700 nm channel showing a dilution series of Alta leaf protein. Extremely high signal likely from chlorophyll in the samples is seen. B. Odyssey image showing the same image as panel A, but in the 800 nm channel. The high signal previously seen in the 700 nm channel is not observed in the 800 nm channel. Comparable levels of water well signal to protein loaded wells suggests background signal from the antibody application, or an unknown interfering component is contributing to the signal, even without protein application C. Template of Alta leaf dilution series showing what ug load was put into each well. There were 11 water wells to test the variability of background signal. D. Graph quantitating the COR47 antibody signal for the Alta leaf dilution series in the 800 nm channel. Samples were found to not be linear in relation to the amount of protein loaded.

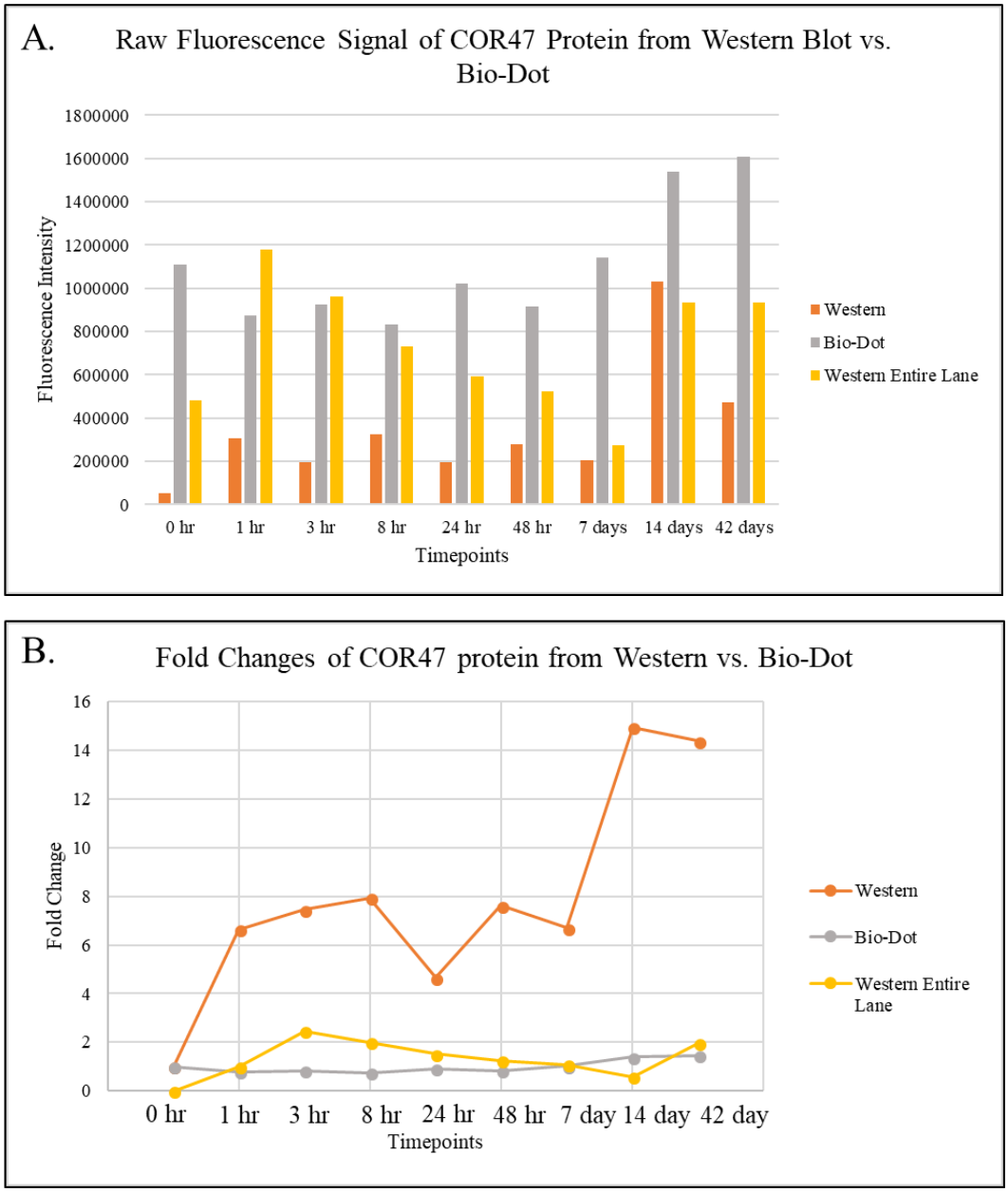


Figure 46. Quantitative Comparison of Dot-blot and Western blots

**Figure 46 Legend.** A. Comparison of raw total pixel count of COR47 signal for Alta crowns with normalized amount loaded for the same samples in the dot-blot apparatus (1 ug) and Western blot (10 ug) using nitrocellulose membranes. The pixel count was much higher in the dot-blot samples compared to the Western results. The entire lane of each sample in the Western results was also quantitated. B. Fold change comparison between dot-blot and Western blot results from samples taken at different timepoints during cold exposure. Since the 0 hour timepoint had a high pixel quantitation in the dot-blot, fold change was very low and data did not show trends similar to western fold changes. Entire lane quantitation was also evaluated for fold change and shows a trend more similar to the dot-blot results which is also likely due to a high 0 hour signal.

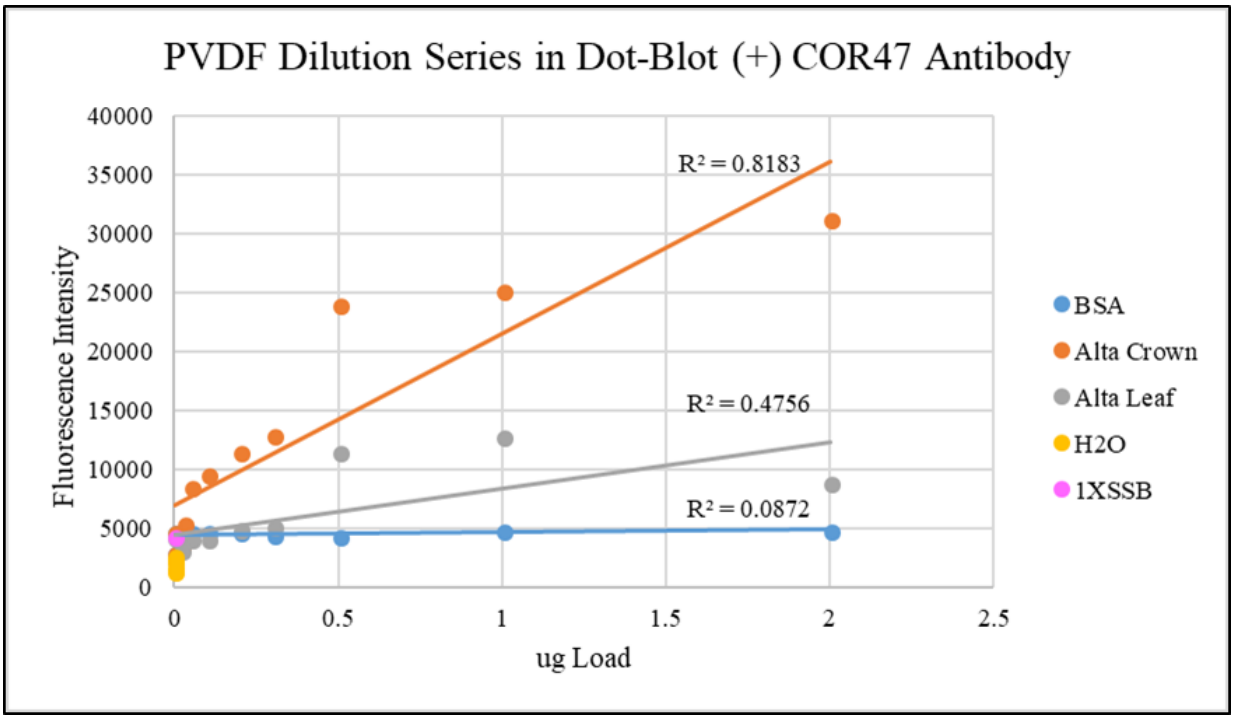


Figure 47. Detection of COR47 signal with PVDF and multiple sample types

**Figure 47 Legend.** Dot-blot dilution series using BSA, Alta crown, and Alta leaf on PVDF membrane. COR47 antibody was applied to samples that were loaded from 0 ug protein to 2 ug protein. Lower background levels were obtained using PVDF membrane, allowing quantitation of lower levels of protein and minimizing background interference.

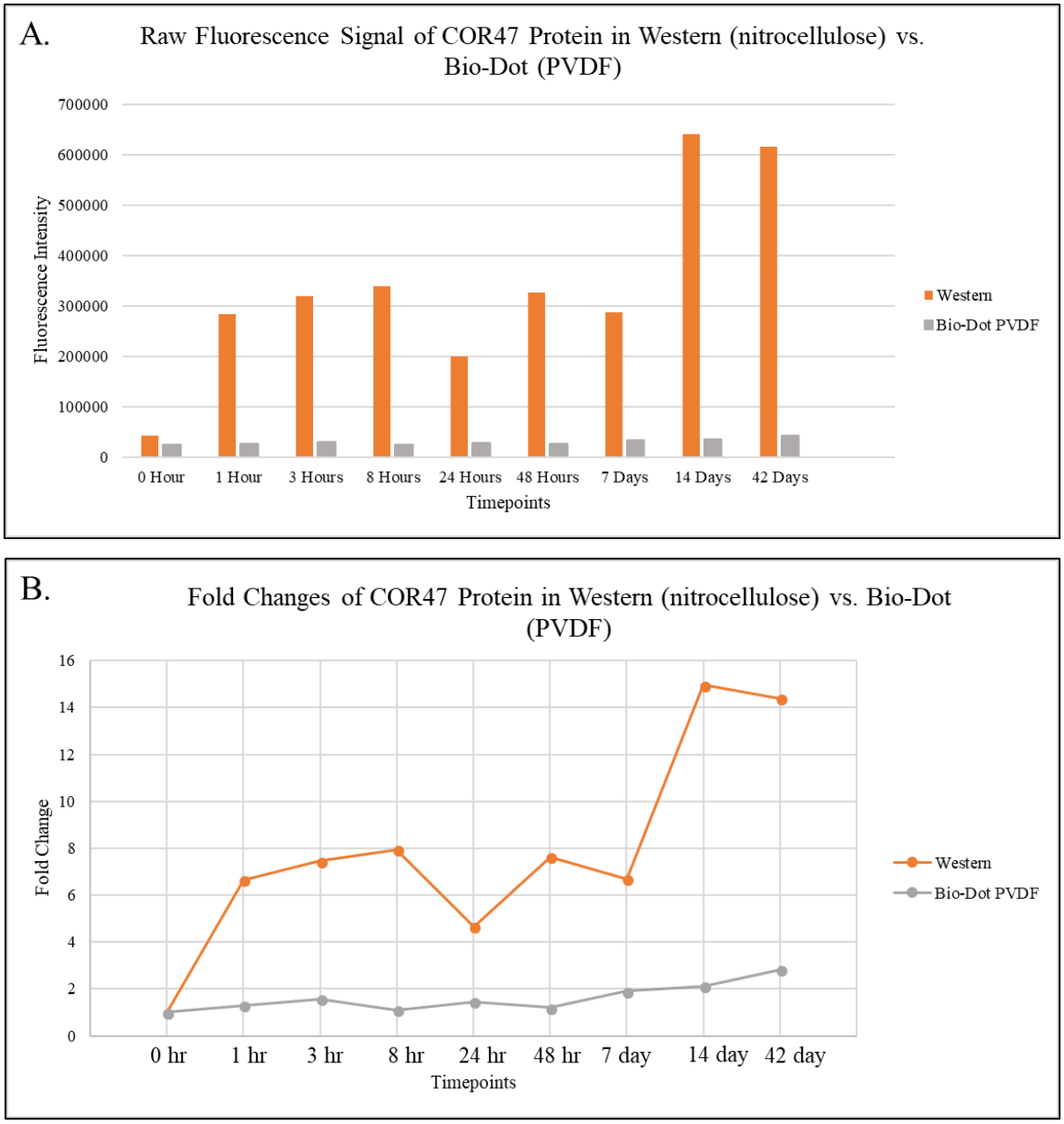


Figure 48. Comparison of Dot-blot and Western data with the same samples using PVDF membranes

**Figure 48 Legend.** A. Comparison of raw total pixel count of COR47 signal for Alta crowns with normalized amount loaded for the same samples in the dot-blot apparatus (1 ug) using a PVDF membrane, and Western blot (10 ug) using nitrocellulose membranes. The pixel count was much lower in the dot-blot samples compared to the Western results. B. Fold change comparison between dot-blot and Western blot results from samples taken at different timepoints during cold exposure. The 0 hour timepoint had a low pixel count, but the rest of the samples did not show much variation either, resulting in the fold changes being very minimal. This data did not correlate with the western protein fold changes observed.

## A1.3 Localization of dehydrins XERO2 and COR47 in Jonsok cold and not cold treated plants

Localization of tissue-specific expression of dehydrins in an octoploid (Jonsok) had not been previously done. Plants were treated for 42 days at 22 °C or 4 °C and extracts or tissue blots were prepared for leaves, crowns, roots, stems, and flowers. XERO2 and COR47 antibodies were applied to see accumulation of dehydrins in the different strawberry tissues using tissue blots (Data not shown). The results from this were not clear, so western blots were done using anti-COR47 and anti-XERO2 to get a more distinct result. The westerns showed a clear induction of dehydrins in the cold treated plants. The COR47 and XERO2 antibodies show a clear induction in cold treated tissues and were most strongly induced in young leaf and crown tissues (Appendix 12).

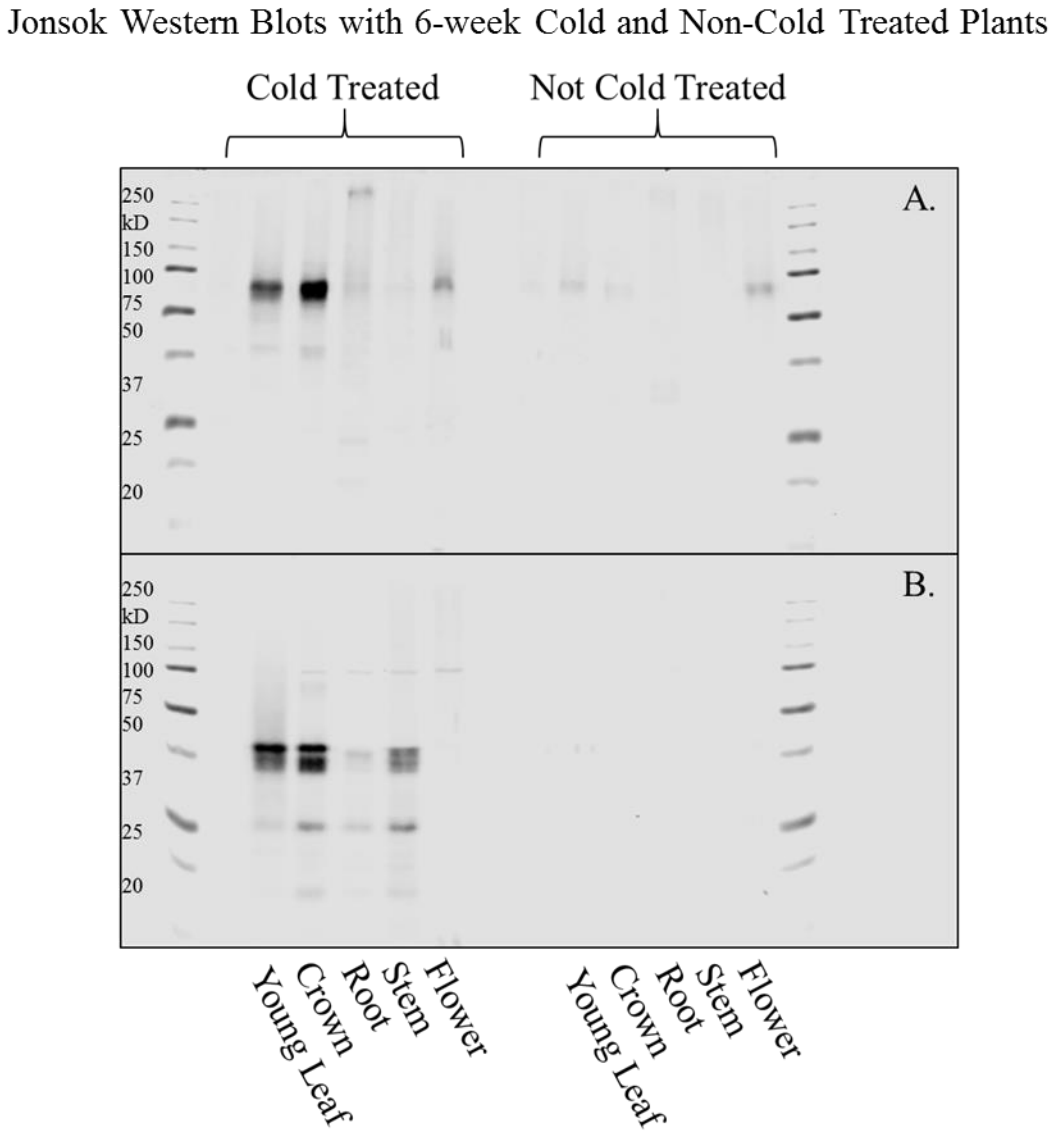


Figure 49. Western Blot of Cold and Non-Cold Treated Jonsok Tissues

**Figure 49 Legend.** Forty-two day cold treated and 42 day not cold treated Jonsok western blot with different tissue samples using the COR47 and XERO2 antibodies. Extracts (10 ug protein) were derived from young leaf, crown, root, stem, and flower. Panel A shows a western blot treated with COR47 antibody. Panel B shows a western blot treated with XERO2 antibody.

# REFERENCES

Abu-Abied M, Golomb L, Belausov E, Huang S, Geiger B, Kam Z, Staiger CJ, Sadot E (2006) Identification of plant cytoskeleton-interacting proteins by screening for actin stress fiber association in mammalian fibroblasts. The Plant Journal 48 (3):367-379. doi: 10.1111/j.1365-313X.2006.02883.x

Alsheikh MK, Svensson JT, Randall SK (2005) Phosphorylation regulated ion-binding is a property shared by the acidic subclass dehydrins. Plant, Cell & Environment 28 (9):1114-1122. doi:doi:10.1111/j.1365-3040.2005.01348.x

Atkinson J, Clarke MW, Warnica JM, Boddington KF, Graether SP (2016) Structure of an Intrinsically Disordered Stress Protein Alone and Bound to a Membrane Surface. Biophysical journal 111 (3):480-491. doi:10.1016/j.bpj.2016.07.001

Badek B, Napiórkowska B, Masny A, Korbin M (2014) Changes In The Expression Of Three Cold-Regulated Genes In 'Elsanta' And 'Selvik' Strawberry (Fragaria × Ananassa) Plants Exposed To Freezing. 22 (2):53. doi:https://doi.org/10.2478/johr-2014-0022

Banerjee A, Roychoudhury A (2016) Group II late embryogenesis abundant (LEA) proteins: structural and functional aspects in plant abiotic stress. Plant Growth Regulation 79 (1):1-17. doi:10.1007/s10725-015-0113-3

Boyer JS (1982) Plant productivity and environment. Science 218 (4571):443-448. doi:10.1126/science.218.4571.443

Bremer A, Kent B, Hauss T, Thalhammer A, Yepuri NR, Darwish TA, Garvey CJ, Bryant G, Hincha DK (2017) Intrinsically Disordered Stress Protein COR15A Resides at the Membrane Surface during Dehydration. Biophysical journal 113 (3):572-579. doi:10.1016/j.bpj.2017.06.027

Castresana C, de Carvalho F, Gheysen G, Habets M, Inze D, Van Montagu M (1990) Tissue-specific and pathogen-induced regulation of a Nicotiana plumbaginifolia beta-1,3-glucanase gene. The Plant cell 2 (12):1131-1143. doi:10.1105/tpc.2.12.1131

Charfeddine S, Charfeddine M, Saïdi MN, Jbir R, Bouzid RG (2017) Potato dehydrins present high intrinsic disorder and are differentially expressed under ABA and abiotic stresses. Plant Cell, Tissue and Organ Culture (PCTOC) 128 (2):423-435. doi:10.1007/s11240-016-1120-4

Chinnusamy V, Zhu J, Zhu JK (2007) Cold stress regulation of gene expression in plants. Trends in plant science 12 (10):444-451. doi:10.1016/j.tplants.2007.07.002

Chung HJ, Ferl RJ (1999) Arabidopsis alcohol dehydrogenase expression in both shoots and roots is conditioned by root growth environment. Plant physiology 121 (2):429-436

Close TJ(1996) Dehydrins: Emergence of a biochemical role of a family of plant dehydration proteins. Physiologia Plantarum 97 (4):795-803. doi:doi:10.1111/j.1399-3054.1996.tb00546.x

Close TJ (1997) Dehydrins: A commonalty in the response of plants to dehydration and low temperature. Physiologia Plantarum 100 (2):291-296. doi:doi:10.1111/j.1399-3054.1997.tb04785.x

Cuevas-Velazquez CL, Saab-Rincon G, Reyes JL, Covarrubias AA (2016) The Unstructured N-terminal Region of Arabidopsis Group 4 Late Embryogenesis Abundant (LEA) Proteins Is Required for Folding and for Chaperone-like Activity under Water Deficit. The Journal of biological chemistry 291 (20):10893-10903. doi:10.1074/jbc.M116.720318

Darrow G (1966) The Strawberry. History, breeding, and physiology. Holt, Rinehart and Winston, New York

Davik J, Daugaard H, Svensson B (2000) Strawberry production in the Nordic countries. Advances in Strawberry Research 19:13-18

Davik J, Koehler G, From B, Torp T, Rohloff J, Eidem P, Wilson RC, Sonsteby A, Randall SK, Alsheikh M (2013) Dehydrin, alcohol dehydrogenase, and central metabolite levels are associated with cold tolerance in diploid strawberry (Fragaria spp.). Planta 237 (1):265-277. doi:10.1007/s00425-012-1771-2

Ding Y, Li H, Zhang X, Xie Q, Gong Z, Yang S (2015) OST1 kinase modulates freezing tolerance by enhancing ICE1 stability in Arabidopsis. Developmental cell 32 (3):278-289. doi:10.1016/j.devcel.2014.12.023

Egawa C, Kobayashi F, Ishibashi M, Nakamura T, Nakamura C, Takumi S (2006) Differential regulation of transcript accumulation and alternative splicing of a DREB2 homolog under abiotic stress conditions in common wheat. Genes & genetic systems 81 (2):77-91

Eriksson S, Eremina N, Barth A, Danielsson J, Harryson P (2016) Membrane-Induced Folding of the Plant Stress Dehydrin Lti30. Plant physiology 171 (2):932-943. doi:10.1104/pp.15.01531

Eriksson SK, Kutzer M, Procek J, Grobner G, Harryson P (2011) Tunable membrane binding of the intrinsically disordered dehydrin Lti30, a cold-induced plant stress protein. The Plant cell 23 (6):2391-2404. doi:10.1105/tpc.111.085183

Fennoy SL, Nong T, Bailey-Serres J (1998) Transcriptional and post-transcriptional processes regulate gene expression in oxygen-deprived roots of maize. The Plant journal : for cell and molecular biology 15 (6):727-735. doi:10.1046/j.1365-313X.1998.00249.x

Floris M, Mahgoub H, Lanet E, Robaglia C, Menand B (2009) Post-transcriptional regulation of gene expression in plants during abiotic stress. International journal of molecular sciences 10 (7):3168-3185. doi:10.3390/ijms10073168

Gao F, Zhou Y, Zhu W, Li X, Fan L, Zhang G (2009) Proteomic analysis of cold stress-responsive proteins in Thellungiella rosette leaves. Planta 230 (5):1033-1046. doi:10.1007/s00425-009-1003-6

Guo W, Ward RW, Thomashow MF (1992) Characterization of a Cold-Regulated Wheat Gene Related to Arabidopsis cor47. Plant physiology 100 (2):915-922

Hahn M, Walbot V (1989) Effects of cold-treatment on protein synthesis and mRNA levels in rice leaves. Plant physiology 91 (3):930-938

Hajela RK, Horvath DP, Gilmour SJ, Thomashow MF (1990) Molecular Cloning and Expression of cor (Cold-Regulated) Genes in Arabidopsis thaliana. Plant physiology 93 (3):1246-1252

Hanin M, Brini F, Ebel C, Toda Y, Takeda S, Masmoudi K (2011) Plant dehydrins and stress tolerance: versatile proteins for complex mechanisms. Plant signaling & behavior 6 (10):1503-1509. doi:10.4161/psb.6.10.17088

Heidarvand L, Maali Amiri R (2010) What happens in plant molecular responses to cold stress? Acta Physiologiae Plantarum 32 (3):419-431. doi:10.1007/s11738-009-0451-8

Hernandez-Sanchez IE, Maruri-Lopez I, Graether SP, Jimenez-Bremont JF (2017) In vivo evidence for homo- and heterodimeric interactions of Arabidopsis thaliana dehydrins AtCOR47, AtERD10, and AtRAB18. Scientific reports 7 (1):17036. doi:10.1038/s41598-017-15986-2

Houde M, Dallaire S, N'Dong D, Sarhan F (2004) Overexpression of the acidic dehydrin WCOR410 improves freezing tolerance in transgenic strawberry leaves. Plant biotechnology journal 2 (5):381-387. doi:10.1111/j.1467-7652.2004.00082.x

Hughes SL, Schart V, Malcolmson J, Hogarth KA, Martynowicz DM, Tralman-Baker E, Patel SN, Graether SP (2013) The importance of size and disorder in the cryoprotective effects of dehydrins. Plant physiology 163 (3):1376-1386. doi:10.1104/pp.113.226803

Imamura T, Higuchi A, Takahashi H (2013) Dehydrins are highly expressed in overwintering buds and enhance drought and freezing tolerance in Gentiana triflora. Plant science : an international journal of experimental plant biology 213:55-66. doi:10.1016/j.plantsci.2013.08.012

Jensen LJ, Jensen TS, de Lichtenberg U, Brunak S, Bork P (2006) Co-evolution of transcriptional and post-translational cell-cycle regulation. Nature 443 (7111):594-597. doi:10.1038/nature05186

Jiang B, Shi Y, Zhang X, Xin X, Qi L, Guo H, Li J, Yang S (2017) PIF3 is a negative regulator of the CBF pathway and freezing tolerance in Arabidopsis. Proceedings of the National Academy of Sciences of the United States of America 114 (32):E6695-e6702. doi:10.1073/pnas.1706226114

Kaplan RS, Pedersen PL (1985) Determination of microgram quantities of protein in the presence of milligram levels of lipid with amido black 10B. Analytical biochemistry 150 (1):97-104

Koehler G, Randall S, Wilson R, Winge P, Rohloff J, Alsheikh M (2010) Molecular cold responses for two strawberry cultivars: comparison of proteomic and microarray analysis. In: XXVIII International Horticultural Congress on Science and Horticulture for People (IHC2010): International Symposium on 929. pp 73-79

Koehler G, Rohloff J, Wilson RC, Kopka J, Erban A, Winge P, Bones AM, Davik J, Alsheikh MK, Randall SK (2015) Integrative "omic" analysis reveals distinctive cold responses in leaves and roots of strawberry, Fragaria x ananassa 'Korona'. Frontiers in plant science 6:826. doi:10.3389/fpls.2015.00826

Koehler G, Weisel T, Randall S (2007) Transcript expression analysis indicates distinct roles for dehydrin subclasses. Current Topics in Phytochemistry 8:73-83

Koehler G, Wilson RC, Goodpaster JV, Sonsteby A, Lai X, Witzmann FA, You JS, Rohloff J, Randall SK, Alsheikh M (2012) Proteomic study of low-temperature responses in strawberry cultivars (Fragaria x ananassa) that differ in cold tolerance. Plant physiology 159 (4):1787-1805. doi:10.1104/pp.112.198267

Kosova K, Vitamvas P, Prasil IT (2011) Expression of dehydrins in wheat and barley under different temperatures. Plant science : an international journal of experimental plant biology 180 (1):46-52. doi:10.1016/j.plantsci.2010.07.003

Koussounadis A, Langdon SP, Um IH, Harrison DJ, Smith VA (2015) Relationship between differentially expressed mRNA and mRNA-protein correlations in a xenograft model system. Scientific reports 5:10775. doi:10.1038/srep10775

Kovacs D, Kalmar E, Torok Z, Tompa P (2008) Chaperone Activity of ERD10 and ERD14, Two Disordered Stress-Related Plant Proteins. Plant physiology 147:381-390. doi 10.1104/pp.108.118208

Kreps JA, Wu Y, Chang HS, Zhu T, Wang X, Harper JF (2002) Transcriptome changes for Arabidopsis in response to salt, osmotic, and cold stress. Plant physiology 130 (4):2129-2141. doi:10.1104/pp.008532

Laemmli UK (1970) Cleavage of structural proteins during the assembly of the head of bacteriophage T4. Nature 227 (5259):680-685

Legrand S, Marque G, Blassiau C, Bluteau A, Canoy AS, Fontaine V, Jaminon O, Bahrman N, Mautord J, Morin J, Petit A, Baranger A, Riviere N, Wilmer J, Delbreil B, Lejeune-Henaut I (2013) Combining gene expression and genetic analyses to identify candidate genes involved in cold responses in pea. Journal of plant physiology 170 (13):1148-1157. doi:10.1016/j.jplph.2013.03.014

Liu Y, Wang L, Zhang T, Yang X, Li D (2017) Functional characterization of KS-type dehydrin ZmDHN13 and its related conserved domains under oxidative stress. Scientific reports 7 (1):7361. doi:10.1038/s41598-017-07852-y

Maier T, Guell M, Serrano L (2009) Correlation of mRNA and protein in complex biological samples. FEBS letters 583 (24):3966-3973. doi:10.1016/j.febslet.2009.10.036

Mazzucotelli E, Mastrangelo AM, Crosatti C, Guerra D, Stanca AM, Cattivelli L (2008) Abiotic stress response in plants: when post-transcriptional and post-translational regulations control transcription. Plant Science 174 (4):420-431

Miura K, Furumoto T (2013) Cold signaling and cold response in plants. International journal of molecular sciences 14 (3):5312-5337. doi:10.3390/ijms14035312

Ner-Gaon H, Halachmi R, Savaldi-Goldstein S, Rubin E, Ophir R, Fluhr R (2004) Intron retention is a major phenomenon in alternative splicing in Arabidopsis. The Plant journal : for cell and molecular biology 39 (6):877-885. doi:10.1111/j.1365-313X.2004.02172.x

Novillo F, Alonso JM, Ecker JR, Salinas J (2004) CBF2/DREB1C is a negative regulator of CBF1/DREB1B and CBF3/DREB1A expression and plays a central role in stress tolerance in Arabidopsis. Proceedings of the National Academy of Sciences of the United States of America 101 (11):3985-3990. doi:10.1073/pnas.0303029101

Osuagwu, NU. (2014) Molecular characterization of novel proteins associated with low temperature stress tolerance in diploid strawberry (*Fragaria vesca*). Hedmark Univeristy College Masters Thesis.

Ohnishi T, Takanashi H, Mogi M, Takahashi H, Kikuchi S, Yano K, Okamoto T, Fujita M, Kurata N, Tsutsumi N (2011) Distinct gene expression profiles in egg and synergid cells of rice as revealed by cell type-specific microarrays. Plant physiology 155 (2):881-891. doi:10.1104/pp.110.167502

Parihar P, Singh S, Singh R, Singh VP, Prasad SM (2015) Effect of salinity stress on plants and its tolerance strategies: a review. Environmental science and pollution research international 22 (6):4056-4075. doi:10.1007/s11356-014-3739-1

Peleg Z, Blumwald E (2011) Hormone balance and abiotic stress tolerance in crop plants. Current opinion in plant biology 14 (3):290-295. doi:10.1016/j.pbi.2011.02.001

Pradet-Balade B, Boulme F, Beug H, Mullner EW, Garcia-Sanz JA (2001) Translation control: bridging the gap between genomics and proteomics? Trends in biochemical sciences 26 (4):225-229

Rajam M, Chandola N, Goud PS, Singh D, Kashyap V, Choudhary M, Sihachakr D (2007) Thaumatin gene confers resistance to fungal pathogens as well as tolerance to abiotic stresses in transgenic tobacco plants. Biologia Plantarum 51 (1):135-141

Robison J, Arora N, Yamasaki Y, Saito M, Boone J, Blacklock B, Randall S (2017) Glycine max and Glycine soja are capable of cold acclimation. Journal of Agronomy and Crop Science 203 (6):553-561

Rohde P, Hincha DK, Heyer AG (2004) Heterosis in the freezing tolerance of crosses between two Arabidopsis thaliana accessions (Columbia-0 and C24) that show differences in non-acclimated and acclimated freezing tolerance. The Plant journal : for cell and molecular biology 38 (5):790-799. doi:10.1111/j.1365-313X.2004.02080.x

Rohloff J, Kopka J, Erban A, Winge P, Wilson RC, Bones AM, Davik J, Randall SK, Alsheikh MK (2012) Metabolite profiling reveals novel multi-level cold responses in the diploid model Fragaria vesca (woodland strawberry). Phytochemistry 77:99-109. doi:10.1016/j.phytochem.2012.01.024

Romagnoli S, Maddaloni M, Livini C, Motto M (1990) Relationship between gene expression and hybrid vigor in primary root tips of young maize (Zea mays L.) plantlets. TAG Theoretical and applied genetics Theoretische und angewandte Genetik 80 (6):769-775. doi:10.1007/bf00224190

Rorat T (2006) Plant dehydrins--tissue location, structure and function. Cellular & molecular biology letters 11 (4):536-556. doi:10.2478/s11658-006-0044-0

Schulz E, Tohge T, Zuther E, Fernie AR, Hincha DK (2016) Flavonoids are determinants of freezing tolerance and cold acclimation in Arabidopsis thaliana. Scientific reports 6:34027. doi:10.1038/srep34027

Shen Y, Wu X, Liu D, Song S, Liu D, Wang H (2016) Cold-dependent alternative splicing of a Jumonji C domain-containing gene MtJMJC5 in Medicago truncatula. Biochemical and biophysical research communications 474 (2):271-276. doi:10.1016/j.bbrc.2016.04.062

Singh VP, Prasad SM, Munne-Bosch S, Muller M (2017) Editorial: Phytohormones and the Regulation of Stress Tolerance in Plants: Current Status and Future Directions. Frontiers in plant science 8:1871. doi:10.3389/fpls.2017.01871

Song R, Messing J (2003) Gene expression of a gene family in maize based on noncollinear haplotypes. Proceedings of the National Academy of Sciences of the United States of America 100 (15):9055-9060. doi:10.1073/pnas.1032999100

Thomashow MF (2010) Molecular basis of plant cold acclimation: insights gained from studying the CBF cold response pathway. Plant physiology 154 (2):571-577. doi:10.1104/pp.110.161794

Thompson CE, Fernandes CL, de Souza ON, de Freitas LB, Salzano FM (2010) Evaluation of the impact of functional diversification on Poaceae, Brassicaceae, Fabaceae, and Pinaceae alcohol dehydrogenase enzymes. Journal of molecular modeling 16 (5):919-928. doi:10.1007/s00894-009-0576-0

Vaseva, II, Anders I, Feller U (2014) Identification and expression of different dehydrin subclasses involved in the drought response of Trifolium repens. Journal of plant physiology 171 (3-4):213-224. doi:10.1016/j.jplph.2013.07.013

Wang W, Vinocur B, Altman A (2003) Plant responses to drought, salinity and extreme temperatures: towards genetic engineering for stress tolerance. Planta 218 (1):1-14. doi:10.1007/s00425-003-1105-5

Wang W, Vinocur B, Shoseyov O, Altman A (2004) Role of plant heat-shock proteins and molecular chaperones in the abiotic stress response. Trends in plant science 9 (5):244-252. doi:10.1016/j.tplants.2004.03.006

Wang Y, Xu H, Zhu H, Tao Y, Zhang G, Zhang L, Zhang C, Zhang Z, Ma Z (2014) Classification and expression diversification of wheat dehydrin genes. Plant science : an international journal of experimental plant biology 214:113-120. doi:10.1016/j.plantsci.2013.10.005

Xie C, Zhang R, Qu Y, Miao Z, Zhang Y, Shen X, Wang T, Dong J (2012) Overexpression of MtCAS31 enhances drought tolerance in transgenic Arabidopsis by reducing stomatal density. The New phytologist 195 (1):124-135. doi:10.1111/j.1469-8137.2012.04136.x

Yan SP, Zhang QY, Tang ZC, Su WA, Sun WN (2006) Comparative proteomic analysis provides new insights into chilling stress responses in rice. Molecular & cellular proteomics : MCP 5 (3):484-496. doi:10.1074/mcp.M500251-MCP200

Yang W, Zhang L, Lv H, Li H, Zhang Y, Xu Y, Yu J (2015) The K-segments of wheat dehydrin WZY2 are essential for its protective functions under temperature stress. Frontiers in plant science 6:406. doi:10.3389/fpls.2015.00406

Zhou MQ, Shen C, Wu LH, Tang KX, Lin J (2011) CBF-dependent signaling pathway: a key responder to low temperature stress in plants. Critical reviews in biotechnology 31 (2):186-192. doi:10.3109/07388551.2010.505910

# VITA

**Zach Deitch**

**Education**

**Indiana University – Purdue University (IUPUI), Indianapolis Indiana**

August 2016 - August 2018

Masters of Science: Biology (Plant Biology)

**University of Colorado, Boulder, Colorado** August 2011 – May 2014

Bachelor of Arts, Major: Ecology and Evolutionary Biology

**Experience**

**Research Assistant – Master's thesis project**

Title: Cold Response Biomarker Identification in Strawberry Defense Date: May 24, 2018

IUPUI Biology Department, Indianapolis, IN August 2016 – May 2016

Principal Investigator: Stephen Randall

*- Developed a high-throughput method for protein assays and western blotting.*

*- Investigated potential biomarkers in octoploid strawberry.*

*- Investigated transcript and protein accumulation for two dehydrins in diploid strawberry, focusing on discerning transcriptional versus post-transcriptional regulation of the COR47 dehydrin.*

- Wrote papers, protocols, reports, and presented data to peers and teachers
- Presenter at Indiana Academy of Science (2017 & 2018)
  - Cold Response Biomarker Identification in Diploid Strawberry – 2017
  - Cold Regulation of the Dehydrins in Diploid Strawberry - 2018
- Poster presenter at ASPB MW 2017
  - Cold Response Biomarker Identification in Diploid Strawberry
- Laboratory Skills – Western blotting, primer design, RT-PCR, RT-qPCR, protein assays
- Designed, carried out experiments, managed time, collaborated as well as working independently
- Troubleshot multiple methods when dealing with strawberry DNA/RNA/protein

**Professional Experience**

**Quality Assurance/ Software Tester**

Epic – Verona, WI September 2014 - November 2015

*Tested software for a healthcare software company. Ensured workflows and standards of the industry were kept and that the software upheld world-class expectations.*

- Testing world class software for bugs and errors
- Ensured customers that government requirements could be met with quality
- Used Excel test plans to organize and perform testing procedures daily
- Developed critical and analytical skills to assess how a piece of code could be tested efficiently and fully

**The Nature Conservancy**

Invasive Species Intern – Indianapolis, IN May 2013 – August 2013

- Prepared draft assessments of 100+ potential invasive plants species
- Field analysis of oak and hickory forest burn plot regeneration
- GIS mapping of invasive plant distribution by county in Indiana
- Literature reviews and document editing

**Tropical Ecology and Conservation Study Abroad**

Biological Research Station – Monteverde, Costa Rica August 2012 – November 2012

- Environmental conservation and ecology research
- Collection and laboratory analysis of native anoles, epiphytes, and plant adaptation by elevation
- Painted leaf cutter ants to see if resource availability affected trail recruitment
- Independent study of hawk moth pollination in relation to corolla length of flowers

**Leadership**

Eagle Scout

Secretary of the Biology Graduate Organization - IUPUI (August 2017 – June 2018)

Mentor and contact reference for study abroad program - CU Boulder (2012 - 2014)